

SYNTHESIS, CHARACTERIZATION AND ELECTRICAL PROPERTIES OF
DIAZOPHENYLENE AND DIAZODIPHENYLENE BRIDGED Co, Ni, Cu, Ce, AND
Er PHTHALOCYANINE POLYMERS

A THESIS SUBMITTED TO
THE GRADUATE SCHOOL OF NATURAL AND APPLIED SCIENCES
OF
MIDDLE EAST TECHNICAL UNIVERSITY

BY

CEMİL ALKAN

IN PARTIAL FULFILLMENT OF THE REQUIREMENTS
FOR
THE DEGREE OF DOCTOR OF PHILOSOPHY
IN
POLYMER SCIENCE AND TECHNOLOGY

SEPTEMBER 2004

Approval of the Graduate School of Natural and Applied Sciences

Prof. Dr. Canan Özgen
Director

I certify that this thesis satisfies all the requirements as a thesis for the degree of Doctor of Philosophy.

Prof. Dr. Ali Usanmaz
Head of Department

This is to certify that we have read this thesis and that in our opinion it is fully adequate, in scope and quality, as a thesis for the degree of Doctor of Philosophy.

Prof. Dr. Güngör Gündüz
Co-Supervisor

Prof. Dr. Leyla Aras
Supervisor

Examining Committee Members

Prof. Dr. Ahmet Önal (METU, CHEM) _____

Prof. Dr. Leyla Aras (METU, CHEM) _____

Prof. Dr. Ali Güner (HACETTEPE UNV., CHEM) _____

Prof. Dr. Ülkü Yılmaz (METU, CHE) _____

Prof. Dr. Idris Mecidoğlu (METU, CHEM) _____

I hereby declare that all information in this document has been obtained and presented in accordance with academic rules and ethical conduct. I also declare that, as required by these rules and conduct, I have fully cited and referenced all material and results that are original to this work.

Name, Last Name : Cemil Alkan

Signature:

ABSTRACT

SYNTHESIS, CHARACTERIZATION, AND ELECTRICAL PROPERTIES OF DIAZOPHENYLENE AND DIAZODIPHENYLENE BRIDGED Co, Ni, Cu, Ce, AND Er PHTHALOCYANINE POLYMERS

Alkan, Cemil

M. Sc., Department of Polymer Science and Technology

Supervisor: Prof.Dr. Leyla Aras

Co- Supervisor: Prof.Dr. Güngör Gündüz

September 2004, 112 pages

In this research, diazophenylene and diazodiphenylene bridged metal-phthalocyanine polymers were produced from diazonium salt of diaminophenylene/bensidin and pre-synthesized tetraamino metal phthalocyanines. Tetraamino metal phthalocyanine complexes of Co, Ni, Cu, Ce, and Er were obtained by reducing tetranitro metal phthalocyanine complexes synthesized from 3-nitrophthalic anhydride, urea, metal salt, and ammonium molybdate catalyst.

Complexes and polymers were characterized by Fourier Transform Infrared Radiation (FTIR) and UV-Visible spectroscopies. X-Ray analysis showed that there were short range orientations in the polymers.

Thermal analysis of the complexes and the polymers were done by differential scanning calorimetry and thermal gravimetric analysis at a heating rate of $10^{\circ}\text{Cmin}^{-1}$ under nitrogen atmosphere. Ash analysis was performed to determine the metal content of the polymers.

Viscosity and ebullioscopy measurements of the soluble part of the polymers were carried out in THF at 25°C . Scanning electron microscopy were used for morphology investigations of the polymers.

Four probe conductivity measurements showed that electrical conductivity of the polymers increased according to the metallic conductivity of the metal at the center of the phthalocyanine units. When doped with iodine, the polymer samples showed 10^4 fold increase in their conductivities. Current-Voltage (I-V) measurements showed that the polymers were optically sensitive and semiconductors. Electrochemical analysis of the soluble part of the polymers were determined in tributylamine perchlorite+dichloromethane mixture utilizing cyclic voltammetry (CV).

Keywords: Phthalocyanine polymers, electrical conductivity, current voltage characteristic, cyclic voltammetry

ÖZ

DİAZOFENİLEN VE DİAZODİFENİLEN KÖPRÜLÜ Co, Ni, Cu, Ce VE Er FİTALOSİN POLİMERLERİNİN SENTEZ, KAREKTERİZASYON VE ELEKTRİKSEL ÖZELLİKLERİ

Alkan, Cemil

Doktora, Polimer Bilimi ve Teknolojisi

Tez Yöneticisi: Leyla Aras, Prof.Dr.

Ortak Tez Yöneticisi: Güngör Gündüz, Prof.Dr.

Eylül 2004, 112 sayfa

Bu çalışmada diazofenilen ve diazodifenilen köprülü fitalosin polimerleri diaminofenilen ve bensidinin diazonyum tuzlarından ve daha evvel sentezlenmiş metal tetraamino metal-fitalosin kompleksinden hazırlandı. Co, Ni, Cu, Ce, ve Er'un tetraamino fitalosin kompleksleri 3-nitro fitalik anhidrit, üre, metal tuzu ve amonyum molibdat katalizörden elde edilen tetranitro metal fitalosin komplekslerinin indirgenmesiyle elde edildi.

Kompleks ve polimerlerin karakterizasyonu Fourier Dönüşümlü Kızılötesi Işıma (FTIR) ve mor ötesi-görünür bölge spektroskopisi yöntemleriyle yapıldı. X-Ray analizleri sonucunda polimerlerde küçük çapta oriyantasyon olduğu görüldü.

Kompleks ve polimerlerin ısısız analizleri diferansiyel taramalı kalorimetre (DSC) ve termal gravimetrik analiz (TGA) cihazları ile 10°C.dakika⁻¹ ısıtma hızında yapıldı. Polimerdeki metal miktarı kül analizi ile tayin edildi.

Viskosite ve ebuliyoskopi ölçümleri tetrahidro furan çözücünde 25°C'de gerçekleştirildi. Polimerlerin morfoloji analizi taramalı elektron mikroskobu ile yapıldı.

Dört proflu elektriksel iletkenlik ölçümleri polimerlerin elektriksel iletkenliğinin fitalosin kompleksinde bulunan metallerin elektriksel iletkenliğine göre arttığı gösterdi. Iyot buharı ile doplanan örneklerde iletkenliğin 10⁴ kat arttığı saptandı. Akım-Voltaj ölçümleri elde edilen polimerlerin ışığa duyarlı ve yarı iletken özellikte olduğunu gösterdi. Çözünen kısmın elektrokimyasal özelliği tributilamine perklorit+diklorometan karışımında dönüşümlü voltametre (CV) ile incelendi.

Anahtar sözcükler: Fitalosin polimeri, elektriksel iletkenlik, akım-voltaj karakteri, dönüşümlü voltametre

To my family

ACKNOWLEDGEMENTS

I would like to express my sincere appreciation and gratitude to my supervisor Prof. Dr. Leyla Aras for her invaluable suggestions and support throughout this study. I also wish to express my special thanks to my co-supervisor Prof. Dr. Güngör Gündüz for his encouragement, and valued guidance.

I would like to thank also members of thesis supervising committee Prof. Dr. Ülkü Yılmaz and Prof. Dr. İdris Mecidođlu for their cooperation. I would like to extend my sincere thanks to Prof. Dr. Rařit Turan for his help in using voltage-current measurements.

I am thankful to Cengiz Tan from Metallurgical and Materials Engineering for his helps about SEM, and also to Yılser Gldođan from Hacettepe University, Chemical Engineering Department for her help in TGA measurements.

I want to thank to my wife for her encouragement and great patience. She was always with me.

I wish to express my sincere thanks to Arzu Bykyađcı, Gler elik, and Gkhan Kıdıl for their friendship and help. I am also very grateful to Atilla Cihaner, Gliz Otabatmaz akmak, Seha Tirkeř and Ali ırpan for their assistance, suggestions, friendships, and helps during this study. I would like to thank to all the post lab mates for their help and friendship.

TABLE OF CONTENTS

PLAGIARISM.....	iii
ABSTRACT.....	iv
ÖZ.....	vi
ACKNOWLEDGEMENTS.....	ix
TABLE OF CONTENTS.....	x
LIST OF TABLE.....	xv
LIST OF FIGURES.....	xvi
CHAPTER	
1. INTRODUCTION.....	1
1.1 Phthalocyanines: Complexes and Polymers.....	1
1.2. Synthesis of Phthalocyanines in Macromolecular Phases.....	5
1.2.1. Phthalocyanines as Part of the Polymer Chain or Network: Type I.....	5
1.2.1.1. Polymeric Phthalocyanines by Polycyclotetramerization of Tetracarbonitriles.....	6
1.2.1.2. Polymeric Phthalocyanines by Polycondensation Reactions of Low Molecular Weight Phthalocyanines.....	7
1.2.2. Polymeric Cofacial Stacked Phthalocyanines, Type II.....	8
1.2.3. Binding of Phthalocyanines to Macromolecular Carriers by Covalent Bonds, Type III.....	10
1.2.3.1. Synthesis of Phthalocyanines at Macromolecular Carriers.....	11
1.2.3.2. Covalent Binding of Phthalocyanines.....	11
1.2.3.3. Polymerization of Vinyl-Substituted Phthalocyanines.....	12

1.2.4. Binding of Phthalocyanines to Macromolecular Carriers by Coordinative or Ionic Bonds, Type IV.....	13
1.2.4.1. Binding by Coordinative Bonds.....	13
1.2.4.2. Binding By Ionic Bonds.....	13
1.2.5. Physical Incorporation into a Macromolecular Matrix, Type V.....	14
1.3. Properties of Phthalocyanines in Macromolecular Phases.....	15
1.3.1. Electrical Conductivity and Photoconductivity.....	15
1.3.1.1. Electrical Conductivity in Polymers.....	17
1.3.2. Electrochemical Charge-Discharge Behavior of Phthalocyanine Thin Film Electrodes.....	19
1.3.3. Photooxidation of Various Substrates.....	20
1.3.4. X-Ray Powder Diffraction Spectroscopy.....	21
1.3.4.1. XRD of Polymers.....	22
1.4. Industrial Applications of Phthalocyanines.....	24
1.4.1. Traditional Applications.....	24
1.4.2. High Technology Applications.....	25
1.5. Aim of the study.....	27
2. EXPERIMENTAL	29
2.1. Chemicals.....	29
2.2. Instrumentation	29
2.2.1 Fourier Transform Radiation Spectroscopy.....	30
2.2.2 UV-Visible Spectroscopy.....	30

2.2.3. X-Ray Powder Diffraction Spectroscopy.....	30
2.2.4 Ash Analysis.....	31
2.2.5 Differential Scanning Calorimetry.....	31
2.2.6 Thermal Gravimetric Analysis.....	31
2.2.7 Scanning Electron Microscopy.....	32
2.2.8 Dilute Solution Viscosimetry.....	32
2.2.9 Boiling Point Elevation (Ebullioscopy).....	33
2.2.10 Conductivity Measurement.....	34
2.2.11 Cyclic Voltammetry	35
2.2.12 Current Voltage (I-V) Characteristics.....	36
2.3 Synthesis of Materials.....	38
2.3.1. Synthesis of Tetranitro Cu-phthalocyanine.....	38
2.3.2 Reduction of tetranitro Cu-phthalocyanine of Tetraamino Cu- phthalocyanine.....	39
2.3.3. Synthesis of Diazophenylene Bridged Cu-phthalocyanine.....	40
2.3.4. Synthesis of Diazodiphenylene Bridged Cu-phthalocyanine Polymer...	42
3. RESULTS AND DISCUSSION.....	44
3.1 Spectroscopic Analysis.....	44

3.1.1 FTIR Spectroscopy.....	44
3.1.2 UV-Visible Spectroscopy.....	48
3.1.3 X-Ray Diffraction Spectroscopy.....	51
3.2 Thermal Analysis.....	53
3.2.1 Ash Analysis.....	53
3.2.2 Differential Scanning Calorimetry.....	54
3.2.2.1 Complexes.....	54
3.2.2.2 Polymers.....	54
3.2.3 Thermal Gravimetric Analysis.....	56
3.3 Molecular Weight Analysis.....	58
3.3.1 Ebullioscopy.....	58
3.3.2 Viscometry.....	59
3.4 Scanning Electron Microscopy.....	60
3.5 Electrical Properties.....	61
3.5.1 Conductivity.....	61
3.5.2 Cyclic Voltammetry (CV).....	71
3.5.3 I-V Characteristics of Polymers.....	73
4. CONCLUSIONS.....	79
REFERENCES.....	82
APPENDICES.....	88
A. FTIR spectra of tetraamino metal-phthalocyanine complexes, diazophenylene bridged metal-phthalocyanine polymers and diazodiphenylene bridged metal-phthalocyanine polymers.....	88

B. X-Ray Diffraction spectra of tetraamino metal-phthalocyanine complexes, diazophenylene bridged metal-phthalocyanine polymers and diazodiphenylene bridged metal-phthalocyanine polymers.....	97
C. DSC thermograms of tetraamino metal-phthalocyanine complexes, diazophenylene bridged metal-phthalocyanine polymers and diazodiphenylene bridged metal-phthalocyanine polymers.....	101
D. TGA thermograms of tetraamino metal-phthalocyanine complexes, diazophenylene bridged metal-phthalocyanine polymers and diazodiphenylene bridged metal-phthalocyanine polymers.....	106
E. Cyclic Voltammograms of tetraamino metal-phthalocyanine complexes, diazophenylene bridged metal-phthalocyanine polymers and diazodiphenylene bridged metal-phthalocyanine polymers.....	109
VITA.....	112

LIST OF TABLES

TABLE

3.1	Theoretical and experimental values of metal amounts present in the polymer.....	53
3.2	Melting temperatures of tetraamino metal-phthalocyanine complexes....	54
3.3	Degradation temperatures of polymers in°C.....	56
3.4	Number average molecular weights (in gmol^{-1}) of complexes and soluble parts of polymers determined by boiling point elevation technique (ebullioscopy).....	59
3.5	Intrinsic viscosity $[\eta]$ of soluble parts of polymers determined by dilute solution viscosimetry.....	60
3.6	Intrinsic conductivities of complexes (in Scm^{-1}).....	62
3.7	Intrinsic conductivities of polymers (in Scm^{-1}).....	62
3.8	Oxidation reduction potentials of polymers obtained from soluble parts of the polymers.....	72

LIST OF FIGURES

FIGURES

1.1	Schematic representations of a porphyrin and phthalocyanine complexes a) Porphyrin, b) PcH ₂ , c) PcM, d) 1,2-NcH ₂ e) 2,3-NcH ₂	1
1.2	Binding of phthalocyanine complexes to a polymer by ionic bonds.....	14
2.1	Schematic representation of a four probe conductivity measuring device.	35
2.2	The circuit for I-V measurements.....	37
2.3	Basic current-voltage relationships for different kinds of materials: A is a material which obeys ohms law, B is a material showing semiconductivity behaviour, C is a material illustrating filament lamp behaviour, and D is a material representing thermistor behaviour.....	38
2.4	Synthesis of tetranitro Cu-phthalocyanines.....	39
2.5	Reduction of tetranitro Cu-phthalocyanine complexes to tetraamino metal-phthalocyanines.....	40
2.6	Structure of diazophenylene bridged Cu-phthalocyanine polymer	41
2.7	Structure of diazodiphenylene bridged Cu-Phthalocyanine polymer.....	43
3.1	FTIR spectrum for tetranitro Cu-phthalocyanine complexes.....	45
3.2	FTIR spectrum of tetraamino Cu-phthalocyanine complexes.....	46
3.3	FTIR spectrum of 1,4-diazophenylene bridged Cu-phthalocyanine polymers.....	46
3.4	FTIR spectrum of diazodiphenylene bridged Cu-phthalocyanine polymers.....	47
3.5	UV-Visible spectra of tetranitro metal-phthalocyanine complex recorded in THF.....	49

3.6	UV-Visible spectra of tetraamino metal-phthalocyanine complex recorded in THF	49
3.7	UV-Visible spectra of diazophenylene bridged metal-phthalocyanine polymers recorded in THF	50
3.8	UV-Visible spectra of diazophenylene bridged metal-phthalocyanine polymer recorded in THF	50
3.9	X-Ray powder diffraction spectrum of tetraamino Cu-phthalocyanine complex.....	51
3.10	X-Ray powder diffraction spectrum of diazophenylene bridged Cu-phthalocyanine polymer.....	52
3.11	X-Ray powder diffraction spectrum of diazodiphenylene bridged Cu-phthalocyanine polymer.....	52
3.12	DSC thermograms for diazophenylene bridged Cu-phthalocyanine polymer.....	55
3.13	DSC thermograms for diazodiphenylene bridged Cu-phthalocyanine polymer.....	55
3.14	TGA graph for diazophenylene bridged Cu-phthalocyanine polymer.....	57
3.15	TGA graph for diazodiphenylene bridged Cu-phthalocyanine polymer...	57
3.16	General appearances from diazophenylene bridge phthalocyanine polymer (diazophenylene bridged Co-phthalocyanine) (a) and diazodiphenylene bridged polymer (diazodiphenylene bridged Ni-phthalocyanine) (b)	61
3.17	Power law dependency of diazophenylene bridged Co/Ni/Cu/Ce/Er phthalocyanine polymers on metallic conductivity.....	63

3.18	Power law dependency of diazodiphenylene bridged Co/Ni/Cu/Ce/Er phthalocyanine polymers on metallic conductivity.....	64
3.19	Linear dependency of diazophenylene bridged Co/Ni/Cu/Ce/Er phthalocyanine polymers on covalent radius.....	65
3.20	Linear dependency of diazodiphenylene bridged Co/Ni/Cu/Ce/Er phthalocyanine polymers on covalent radius.....	65
3.21	Effect of iodine doping on conductivity of diazophenylene bridged Co-phthalocyanine polymer.....	66
3.22	Effect of iodine doping on conductivity of diazodiphenylene bridged Co-phthalocyanine polymer.....	67
3.23	Effect of iodine doping on conductivity of diazophenylene bridged Ni-phthalocyanine polymer.....	67
3.24	Effect of iodine doping on conductivity of diazodiphenylene bridged Ni-phthalocyanine polymer.....	68
3.25	Effect of iodine doping on conductivity of diazophenylene bridged Cu-phthalocyanine polymer.....	68
3.26	Effect of iodine doping on conductivity of diazodiphenylene bridged Cu-phthalocyanine polymer.....	69
3.27	Effect of iodine doping on conductivity of diazophenylene bridged Ce-phthalocyanine polymer.....	69
3.28	Effect of iodine doping on conductivity of diazodiphenylene bridged Ce-phthalocyanine polymer.....	70
3.29	Effect of iodine doping on conductivity of diazophenylene bridged Er-phthalocyanine polymer.....	70

3.30	Effect of iodine doping on conductivity of diazodiphenylene bridged Er-phthalocyanine polymer.....	71
3.31	I-V characteristic of diazophenylene bridged Co-phthalocyanine polymer.....	74
3.32	I-V characteristic of diazodiphenylene bridged Co-phthalocyanine polymer.....	74
3.33	I-V characteristic of diazophenylene bridged Ni-phthalocyanine polymer.....	75
3.34	I-V characteristic of diazodiphenylene bridged Ni-phthalocyanine polymer.....	75
3.35	I-V characteristic of diazophenylene bridged Cu-phthalocyanine polymer.....	76
3.36	I-V characteristic of diazodiphenylene bridged Cu-phthalocyanine polymer.....	76
3.37	I-V characteristic of diazophenylene bridged Ce-phthalocyanine polymer.....	77
3.38	I-V characteristic of diazodiphenylene bridged Ce-phthalocyanine polymer.....	77
3.39	I-V characteristic of diazophenylene bridged Er-phthalocyanine polymer.....	78
3.40	I-V Characteristic of diazodiphenylene bridged Er-phthalocyanine Polymer.....	78
A.1	FTIR spectrum of tetranitro Co-phthalocyanine complex.....	88
A.2	FTIR spectrum of tetranitro Ni-phthalocyanine complex.....	89
A.3	FTIR spectrum tetranitro Ce-phthalocyanine complex.....	89

A.4	FTIR spectrum of tetranitro Er-phthalocyanine complex.....	90
A.5	FTIR spectrum of tetraamino Co-phthalocyanine complex	90
A.6	FTIR spectrum of tetraamino Ni-phthalocyanine complex.....	91
A.7	FTIR spectrum for tetraamino Cu-phthalocyanine complex.....	91
A.8	FTIR spectrum for tetraamino Ce-phthalocyanine complex.....	92
A.9	FTIR spectrum for tetraamino Er-phthalocyanine complex.....	92
A.10	FTIR spectrum of diazophenylene bridged Co-phthalocyanine polymer.....	93
A.11	FTIR spectrum of diazophenylene bridged Ni-phthalocyanine polymer.....	93
A.12	FTIR spectrum of diazophenylene bridged Ce-phthalocyanine polymer.....	94
A.13	FTIR spectrum of diazophenylene bridged Er-phthalocyanine polymer.....	94
A.14	FTIR spectrum for diazodiphenylene bridged Co-phthalocyanine polymer.....	95
A.15	FTIR Spectrum for diazodiphenylene bridged Ni-phthalocyanine polymer.....	95
A.16	FTIR Spectrum for diazodiphenylene bridged Ce-phthalocyanine Polymer.....	96
A.17	FTIR Spectrum for diazodiphenylene bridged Er-phthalocyanine Polymer.....	96
B.1	X-Ray diffraction spectrum of tetraamino Co-phthalocyanine complex	97

B.2	X-Ray diffraction spectrum of tetraamino Ni-phthalocyanine complex	97
B.3	X-Ray diffraction spectrum of tetraamino Cu-phthalocyanine complex	98
B.4	X-Ray diffraction spectrum of diazophenylene bridged Co-phthalocyanine polymer	98
B.5	X-Ray diffraction spectrum of diazophenylene bridged Ni-phthalocyanine polymer.....	98
B.6	X-Ray diffraction spectrum of diazophenylene bridged Ce-phthalocyanine polymer.....	99
B.7	X-Ray diffraction spectrum of diazophenylene bridged Er-phthalocyanine polymer.....	99
B.8	X-Ray diffraction spectrum of diazodiphenylene bridged Co-phthalocyanine polymer.....	99
B.9	X-Ray diffraction spectrum of diazodiphenylene bridged Ni-phthalocyanine polymer.....	100
B.10	X-Ray diffraction spectrum of diazodiphenylene bridged Ce-phthalocyanine polymer.....	100
B.11	X-Ray diffraction spectrum of diazodiphenylene bridged Er-phthalocyanine polymer.....	100
C.1	DSC thermogram of tetranitro Co-phthalocyanine complex.....	101
C.2	DSC thermogram of tetranitro Ni-phthalocyanine complex.....	101
C.3	DSC thermogram of tetranitro Ce-phthalocyanine complex.....	101
C.4	DSC thermogram of tetranitro Er-phthalocyanine complex.....	101
C.5	DSC thermogram of tetraamino Co-phthalocyanine complex.....	101

C.6	DSC thermogram of tetraamino Ni-phthalocyanine complex	102
C.7	DSC thermogram of tetraamino Cu-phthalocyanine complex	102
C.8	DSC thermogram of tetraamino Ce-phthalocyanine complex	103
C.9	DSC thermogram of tetraamino Er-phthalocyanine complex	103
C.10	DSC thermogram of diazophenylene bridged Co-phthalocyanine polymer.....	103
C.11	DSC thermogram of diazodiphenylene bridged Co-phthalocyanine polymer.....	103
C.12	DSC thermogram of diazophenylene bridged Ni-phthalocyanine polymer.....	104
C.13	DSC thermogram of diazodiphenylene bridged Ni-phthalocyanine polymer.....	104
C.14	DSC thermogram of diazophenylene bridged Cu-phthalocyanine polymer.....	104
C.15	DSC thermogram of diazodiphenylene bridged Cu-phthalocyanine polymer.....	104
C.16	DSC thermogram of diazophenylene bridged Ce-phthalocyanine polymer.....	105
C.17	DSC thermogram of diazodiphenylene bridged Ce-phthalocyanine polymer.....	105
C.18	DSC thermogram of diazophenylene bridged Er-phthalocyanine polymer.....	105
C.19	DSC thermogram of diazodiphenylene bridged Er-phthalocyanine polymer.....	105

D.1	TGA thermogram of diazophenylene bridged Co-phthalocyanine polymers.....	106
D.2	TGA thermogram of diazodiphenylene bridged Co-phthalocyanine polymers.....	106
D.3	TGA thermogram of diazophenylene bridged Ni-phthalocyanine polymers.....	107
D.4	TGA thermogram of diazodiphenylene bridged Ni-phthalocyanine polymers.....	107
D.5	TGA thermogram of diazophenylene bridged Cu-phthalocyanine polymers.....	107
D.6	TGA thermogram of diazodiphenylene bridged Cu-phthalocyanine polymers.....	107
D.7	TGA thermogram of diazophenylene bridged Ce-phthalocyanine polymers.....	108
D.8	TGA thermogram of diazodiphenylene bridged Ce-phthalocyanine polymers.....	108
D.9	TGA thermogram of diazophenylene bridged Ce-phthalocyanine polymers.....	108
D.10	TGA thermogram of diazodiphenylene bridged Er-phthalocyanine polymers.....	108
E.1	CV of soluble part of diazophenylene bridged Co-phthalocyanine polymer.....	109
E.2	CV of soluble part of diazodiphenylene bridged Co-phthalocyanine polymer.....	109
E.3	CV of soluble part of diazophenylene bridged Ni-phthalocyanine polymer.....	109

E.4	CV of soluble part of diazodiphenylene bridged Ni-phthalocyanine polymer.....	109
E.5	CV of soluble part of diazophenylene bridged Cu-phthalocyanine polymer.....	110
E.6	CV of soluble part of diazodiphenylene bridged Cu-phthalocyanine polymer.....	110
E.7	CV of soluble part of diazophenylene bridged Ce-phthalocyanine polymer.....	110
E.8	CV of soluble part of diazodiphenylene bridged Ce-phthalocyanine polymer.....	110
E.9	CV of soluble part of diazophenylene bridged Er-phthalocyanine polymer.....	111
E.10	CV of soluble part of diazodiphenylene bridged Er-phthalocyanine polymer.....	111

CHAPTER 1

INTRODUCTION

1.1 Phthalocyanines: Complexes and Polymers

Phthalocyanine (Pc) is a planar 18π electron heterocyclic aromatic system derived from porphyrin. The more systematic name is tetraazatetrabenzo porphyrine. The annulation of further benzene units leads to the naphthalocyanines (Nc) 1,2-NcH₂ and 2,3-NcH₂, respectively as seen in Figure 1.1.

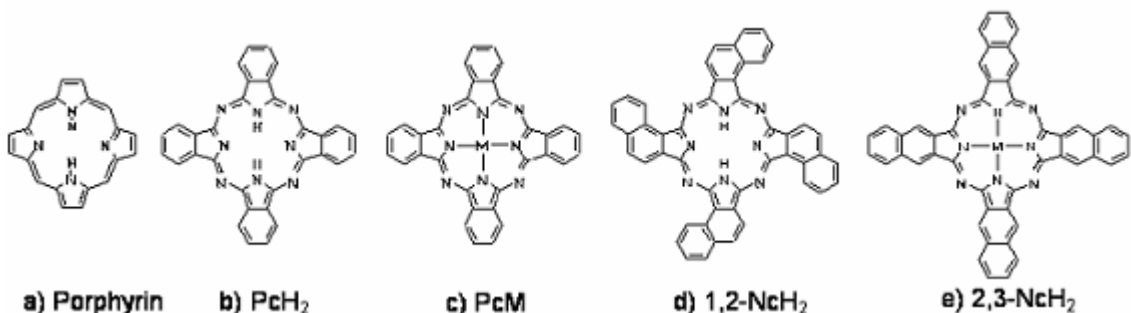


Figure 1.1: Schematic representations of a porphyrin and phthalocyanine complexes a) Porphyrin, b) PcH₂, c) PcM, d) 1,2-NcH₂ e) 2,3-NcH₂

A large variety of complexes of the planar macrocycle Pc⁻² and its derivatives have been described in the literature [1-3]. Main group metals (e. g. Si, Ge) as well as numerous transition metals like Fe, Co or Ni serve as central units.

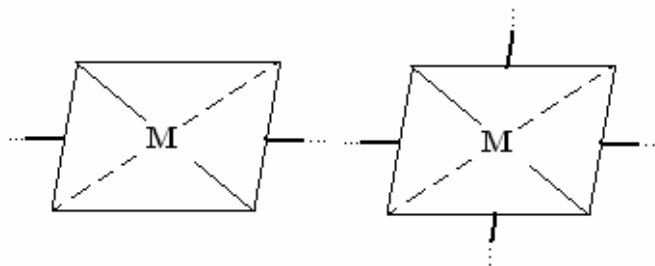
Low molecular weight porphyrin-type compounds such as phthalocyanines and the structurally related macrocycles, naphthalocyanines and porphyrins (e. g. 5,10,15,30-tetraphenylporphyrin) are interesting as materials with various conventional and new unconventional properties.

Variation of substituents at the ligand and of the metal ion in the core of the ligand is the prerequisite for constructing new materials. The production of phthalocyanines for the use of dyes and pigments (absorption at 660-730 nm with $\epsilon 10^5 \text{ L mol}^{-1} \text{ cm}^{-1}$) is around 80000 tons per year. Applications were also realized as a catalyst e.g., the oxidation of sulfur compounds in gasoline fractions in the petroleum industry (MEROX process), as photoconductors in xerographic double layers of laser printers and copy machines, as photosensitizers in the photodynamic therapy of cancer, and as active materials in writable disks. Other fascinating properties with potential applications are coming out from the use of phthalocyanines as sensors, as molecular organic semiconductors in organic photovoltaic cells and as active electron transfer compounds in catalysis, photochemistry and photoelectrochemistry.

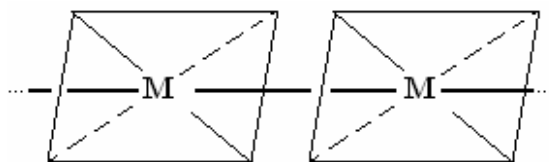
The combination of a phthalocyanine with a macromolecule or the incorporation of a phthalocyanine into a macromolecular matrix is another powerful tool for designing new materials with special properties [4,5]. The combination of a metal ion, a ligand and the chemical environment (such as a macromolecule) determines the chemical and physical behavior. The reversible binding of oxygen is the consequence of the combination Fe(II)/porphyrin-derivative/ macromolecule. Other exciting examples in nature are realized in catalytic active systems, electron-transfer chains and photosynthesis. The preparative chemistry gives way for the synthesis of various combinations of phthalocyanines with macromolecules. These functionalized

macromolecules are part of the field of macromolecular metal complexes which means the combination of a metal cluster, metal ion, metal complex or metal chelate with a macromolecule.

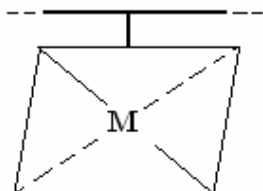
Type I combination: The ligand phthalocyanine is part of a polymer network or chain. In general, these polymers are insoluble in organic solvents, but films or coatings on suitable carriers can be prepared. The polymers exhibit good thermal stability, high electrical conductivity and good catalytic or electrochemical activity [6-10].



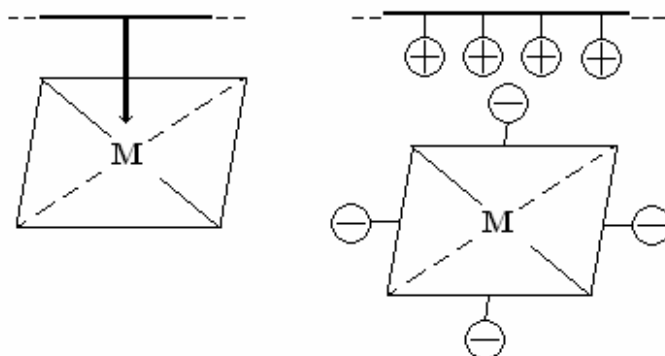
Type II combination: In this case, the metal ion in the core of the phthalocyanine ligand is part of a polymer chain. The stacking of the phthalocyanines results in high electrical conductivity of the polymers [11-14].



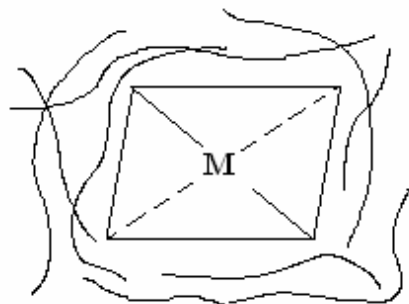
Type III combination: Phthalocyanines are covalently bound via the ligand to an organic or inorganic macromolecule. Characteristic properties of these materials are electron or photoelectron transfer, catalytic or photocatalytic activity [15-16].



Type IV combination: The interaction of a phthalocyanine occurs coordinatively between the metal of a phthalocyanine and a polymer donor ligand or electrostatically between a charged phthalocyanine and a charged polymer chain. The materials are mainly investigated for their activity in catalysis or photocatalysis [17].



Type V Combination: The simplest combination deals with physical incorporation into the matrix of an organic or inorganic macromolecule. These materials are of interest as dye stuffs, photoconductors, active electrode coatings in photoelectrochemistry and catalysts.



1.2. Synthesis of Phthalocyanines in Macromolecular Phases

1.2.1. Phthalocyanines as part of the Polymer Chain or Network: Type 1

Phthalocyanines contain four benzene rings at equivalent positions (Figure 1 b) and of the same reactivity. Therefore, the connection of phthalocyanine rings with each other by alternate benzene rings leads the polymers of Type I existing in a two dimensional structure in an ideal case. Two possibilities exist for preparing phthalocyanines covalently connected via the ligand. The well-known synthesis of low molecular weight phthalocyanines starts from 1,2-benzenedicarbonitriles (phthalonitrile) or 1,2-benzenedicarboxylic acid derivatives (phthalic acid anhydride). These compounds are monofunctional in phthalocyanine synthesis because the cyclotetramerization results in the formation of low molecular weight compounds. On using bifunctional reagents, such as aromatic tetracarbonitriles or tetracarboxylic acid derivatives in the synthesis, polymeric phthalocyanine by polycyclotetramerization are obtained.

The second possibility utilizes tetra or disubstituted low-molecular weight-phthalocyanine derivatives. By reacting with other bifunctional or higher functional compounds (or by self-condensation), polymeric phthalocyanines are prepared.

1.2.1.1. Polymeric Phthalocyanines by Polycyclotetramerization of Tetracarbonitriles

Compared to low molecular weight phthalocyanines, only relatively few reports describe the synthesis and properties of polymeric phthalocyanines [18-19]. For polycyclotetramerization, bifunctional monomers based on tetracarbonitriles, such as 1,2,4,5-tetracyanobenzene [20-21], various oxyarylenedioxy-, and alkylenedioxy-bridged diphthalonitriles [22], and other nitriles or tetracarboxylic acid derivatives, such as 1,2,4,5-benzenetetracarboxylic acid dianhydride are employed mainly in the presence of metal salts or metals in bulk at higher temperatures [23-24]. The polymers exhibit good thermal stability under an inert gas atmosphere up to $\approx 500^{\circ}\text{C}$ and under oxidative conditions up to $\approx 350^{\circ}\text{C}$.

Low molecular weight phthalocyanines can be purified depending on either being unsubstituted or containing suitable substituents by sublimation or liquid chromatography. Common instrumental techniques are employed for their analytical characterization. In contrast, polymeric phthalocyanines are not soluble in organic solvents (sometimes only partially soluble in concentrated sulfuric acid) and are not vaporizable.

For a complete characterization of the polymers, the following points must be considered: structural uniformity, nature of end groups, metal content and degree of polymerization (molecular weight).

1.2.1.2. Polymeric Phthalocyanines by Polycondensation Reactions of Low Molecular Weight Phthalocyanines

This route for the preparation of polymeric phthalocyanines exhibits the advantage that well-characterized low-molecular weight phthalocyanines are applied for polycondensation reactions. In general, tetrafunctional phthalocyanines, such as the tetraamines and tetracarboxylic acid derivatives are used as starting materials. Due to the high functionality (>2), network formation easily occurs, and the insoluble polymers obtained are difficult to characterize (degree of network formation, molecular weight, end groups). Therefore, often no detailed structure determination was carried out. The polymers were mainly investigated with respect to their thermal stability [25].

Heating of 2,9,16,23-tetracarboxyphthalocyanines at 350-400°C gives insoluble polymers containing phthalocyanines under elimination of CO₂ [26].

2,9,16,23 Tetraaminophthalocyanines were employed in the synthesis of polyimides and as curing agents for epoxy. (Metals: Cu(II), Co(II), Ni(II), Zn(II)) and pyromellitic dianhydride or benzophenone tetracarboxylic dianhydride, respectively, were stirred in dimethylsulfoxide (DMSO) at 25-70°C to give the corresponding polyamide-acids [27-28]. These precursors are soluble, and films can be cast. Fairly flexible, tough films of the corresponding polyimides were then obtained by heating to

300°C. Another procedure utilizes the cocondensation of tetraamine in the presence of various aromatic diamines and the above mentioned tetracarboxylic acid dianhydrides. Solutions of the polyamide acid copolymers can be used to fabricate films or fibers. The polyamide copolymers obtained in the second step of the reaction are insoluble. Excellent thermal stabilities up to 500°C in air and 600°C under vacuum are reported.

A series of functional Fe(III) and Co(II) phthalocyanines and their polymers as models for catalase, peroxidase, oxidase, and oxygenase were synthesized. Copolymers containing Fe(III) and Cd(II) phthalocyanines were obtained by polycondensation of phthalocyanine dicarboxylic acid dichlorides with terephthalic acid dichloride and phthalic diols. Green or blue colored fibers could be obtained by melt spinning of the copolyesters containing below 1 mole% of the metal complex. Disubstituted phthalocyanine carboxylic acids were prepared by statistical synthesis from a pyromellithic acid derivative and a phthalic acid derivative which is difficult to conduct using a specifically disubstituted phthalocyanine isomer as the bifunctional monomer for a polycondensation [29].

1.2.2. Polymeric Cofacial Stacked Phthalocyanines, Type II

Stacked arrangements in the face orientation of macrocyclic metal complexes are realised by connecting the metal ions in the core with different bivalent atoms or groups [30]. The interest in the materials is connected with their properties: electrical conduction, photoconduction, non-linear optical and electroluminescent behaviour. The solubility of these polymers which is important for the preparation of thin film devices by coating is improved by introducing bulky groups into the ligand. The degree of

polymerization of macrocycles can be up to around 200. A mathematical model for the number of isomers in tetrasubstituted cofacial stacked polymeric phthalocyanines was developed. The polymers are subdivided into four main groups.

Group A: covalent-covalent bonds in μ -oxo-bridged polymers are realised with tetravalent Si, Ge, and Sn. Reactions are carried out by polycondensation of dihydroxy-metal macrocycles (Metal: $\text{Si}(\text{OH})_2$, $\text{Ge}(\text{OH})_2$, $\text{Sn}(\text{OH})_2$, either in high boiling solvent (the HO-groups can be activated by better leaving groups, such as CF_3COO^-) or in the solid state (under topochemical control). Vapor deposition of monomer $\text{Si}(\text{OH})_2\text{Pc}$ or $(\text{Si}(\text{O})\text{Pc})_n$ on the surface can result in oligomers with the stack axis perpendicular and polymers with the stack axis parallel to the substrate surface.

Group B: Covalent coordinative bonds between macrocycles in polymers are possible with trivalent Al, Ga, Cr and fluoro as the bridging group by vapor deposition or trivalent Co, Fe, etc. and $-\text{CN}$, $-\text{SCN}$, $-\text{N}_3$ as the bridging group for example by the Na-ligand splitting.

Group C: Coordinative/coordinative bonds are obtained with metal ions in the macrocycles having an oxidation state of +2 which are able to react in solution with stoichiometric amounts of bifunctional donors to give polymers.

Group D: Phthalocyanines substituted with long chain substituents in peripheric positions can form liquid crystalline discotic phases (metallomesogenes). Polymerization of liquid crystalline phthalocyanines with polymerizable substituents leads to supramolecular structures with fixed columnar orientation.

The reaction of dihydroxy-metal macrocycles with alcohols, phenols and carboxylic acids was described by Wöhrle et al [31]. Reactions of (M: Si(OH)₂, Ge(OH)₂) with monovalent alcohols, phenols and carboxylic acids result in the corresponding alkoxides, aroxides and carboxides. Polymers were prepared using analogies bivalent comonomers such as ethylene glycole/hydroquinone and adipic acid. The mechanism of the reactions with alcohols and phenols is described as nucleophilic substitution at the metal atom for silonium and germonium ions. Disadvantage point is that all the polymers are insoluble in organic solvents.

Some reactions of phthalocyanines of silicone, germanium, and tin under alkaline conditions was investigated by Myakov et. al [32].

1.2.3. Binding of Phthalocyanines to Macromolecular Carriers by Covalent Bonds, Type III

The covalent binding of phthalocyanines to a linear organic polymer combines the properties of the polymer carrier, such as its solubility, thermal and mechanical behaviour, with those of chelate. Principally, the properties of the bonded phthalocyanines are preserved but in addition influenced by the polymer environment, e.g. the polarity or charge of the polymer. On the other hand, covalent immobilization onto a crosslinked macromolecule, either organic or inorganic, results in materials which can be employed as heterogeneous catalysts. The covalent bond is distinguished from coordinative or ionic bonds by its long term stability. Various possibilities exist for realizing a covalent bond between macromolecule and phthalocyanine:

A: Synthesis of phthalocyanine directly at a modified polymer

B: Polymer-analogous reactions between polymer and phthalocyanine

C: Polymerization reactions of vinyl-substituted phthalocyanines

1.2.3.1. Synthesis of Phthalocyanines at Macromolecular Carriers

The first step toward the synthesis of phthalocyanines at a polymer carrier is the immobilization of an aromatic o-dinitrile. In the second step, the conversion of the covalently polymer-bound dinitrile to polymer bound phthalocyanines using a dissolved low molecular weight o-nitrile is carried out. The bonded chelates may be cleaved to obtain a low molecular weight phthalocyanine containing one reactive functional group only (unsymmetrically substituted phthalocyanine). Only few papers are known dealing with this method to prepare covalently bound phthalocyanines at crosslinked divinylbenzene-styrene copolymers [33] and at poly(organophosphazenes) [34].

1.2.3.2. Covalent Binding of Phthalocyanines

A general route that allows the binding of different phthalocyanines at linear polymers was described in the literature [35].

Substituted phthalocyanines contain nucleophilic amino groups of similar reactivity. Therefore, an identical synthetic procedure can be applied to conduct the covalent binding to a polymer with reactive sites. Besides the binding of one kind of porphyrin, the addition of different porphyrines to the reaction mixture allows the fixation of two or three different porphyrines at a polymer system in a one step

procedure. Mainly, a method was selected where a dilute solution of the polymer is added dropwise to a diluted solution of the porphyrines. If the reaction of poly(4-chloro methylstyrene) is carried out in the presence of excess triethylamine, covalent binding of the porphyrine and a quaternization reaction occur simultaneously. Uncharged water soluble polymers containing phthalocyanine moieties are obtained by reaction of poly[(N-vinylpyrrolidone)-co-(methacrylic acid)] with low molecular weight substituted phthalocyanines. Residual carboxylic acid groups were converted to methyl esters [35]. The phthalocyanine content in the polymers was determined by means of quantitative Visible spectroscopy and metal analysis. The polymers were prepared as containing phthalocyanine moieties up to ≈ 10 wt.-%.

1.2.3.3. Polymerization of Vinyl-Substituted Phthalocyanines

Covalently polymer-bound macrocyclic compounds were also prepared by homo- and copolymerization of phthalocyanine type monomers containing polymerizable groups. Suitable substituted phthalocyanines were investigated in detail [36-39]. In order to avoid crosslinking, mainly monosubstituted acryloyloxy-, methacryloyloxy- and acrylamido-substituted phthalocyanines were studied for polymerization reactions in solution. In contrast the thermal bulk polymerization of octasubstituted phthalocyanines, such as their octaacryloyloxy and octamethacryloyloxy derivatives, in the presence of 2,2'-azobisisobutyronitrile (AIBN) resulted in insoluble products due to crosslinking. The radical copolymerization of analogously tetrasubstituted phthalocyanines using a large excess of N-vinylcarbazole led to soluble non-crosslinked copolymers.

1.2.4. Binding of Phthalocyanines to Macromolecular Carriers by Coordinative or Ionic Bonds, Type IV

1.2.4.1. Binding by Coordinative Bonds

The donor properties of suitable nitrogen containing macromolecular ligands are used in a Lewis Base/Lewis Acid interaction with cobalt or iron in the core of porphyrin-type compounds to achieve coordinative binding. Some years ago, the coordinative binding of cobalt phthalocyanines with R=-COOH or R=-SO₃H was examined using polymer ligands such as poly(ethyleneimine), poly(vinylamine), amino group-modified poly(acrylamide) or modified silica gel. The materials were investigated toward their efficiency as catalysts in oxidation reactions [40].

1.2.4.2. Binding By Ionic Bonds

Electrostatic binding occurs easily by ionic interaction between easily charged macromolecular carriers and phthalocyanines.

Positively charged polymers such as ionenes $[-N^+(CH_3)_2-(CH_2)_x-N^+(CH_3)_2-(CH_2)_2-(CH_2)_y-]_n$, form stoichiometric complexes on interacting with tetrasulfonated phthalocyanine in a composition of $N^+/CoPc(SO_3^-)_4$ 4/1 [41] as shown in Figure 1.1. The tendency of phthalocyanines to aggregate in water strongly depends on the hydrophilic character of the latices based on copolymers of styrene, quaternized p-aminomethylstyrene and divinylbenzene

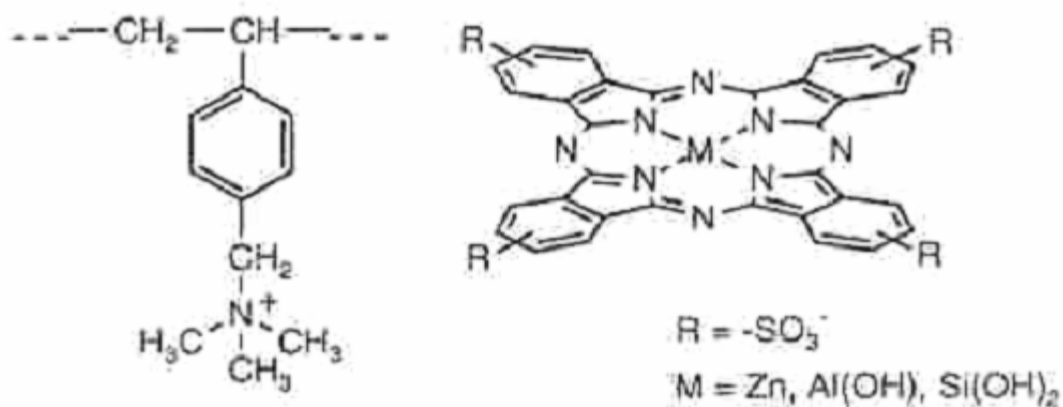


Figure 1.2 Binding of phthalocyanine complexes to a polymer by ionic bonds.

1.2.5. Physical Incorporation into a Macromolecular Matrix, Type V

For the preparation of thin films of phthalocyanines, physical vapor deposition is a common technique which can be applied to unsubstituted and a few substituted macrocycles. Thin films prepared from these compounds are interesting for photovoltaic and photoelectrochemical devices. The combination of phthalocyanines with polymers now offers the advantage of preparing more flexible films of higher mechanical stability. In addition, polar polymers can improve the activity in devices with phthalocyanine type compounds as active parts. Polymers of different polarity and coordination ability, such as polystyrene, poly(acrylonitrile), poly(1-vinylcarbazole), poly(4-vinylpyrine) or poly(vinylidene fluoride), were used [42].

1.3. Properties of Phthalocyanines in Macromolecular Phases

Nature has developed the ability to organize biopolymers with various kinds of metal ions, metal complexes and metal clusters for different processes of catalysis, photocatalysis, electron transport and binding of small molecules. Spatial organization is the fundamental pre-requisite for activity and selectivity in several processes. It is presumptuous to suggest that artificial systems designed by chemists will be able to obtain the complexity of natural ones. But recent results show that artificial macromolecular metal complexes approach partially natural functionalities. In addition, new properties are developed not occurring in natural systems.

Essentially important to the properties is the availability of π -electrons of the macrocyclic ring system and d-electrons of the central metal ion in the core of the ligand for electron transfer. Secondly, under irradiation with visible light, electron or energy transfer from the excited state can occur. It will be shown that the processes of electron transfer induced with or without irradiation and photo-induced energy transfer occurs efficiently in various combinations of phthalocyanines and macromolecules.

1.3.1. Electrical Conductivity and Photoconductivity

By careful design of low-molecular weight and especially polymeric phthalocyanines, the specific electrical conductivity covers several orders of magnitude. Low-molecular weight phthalocyanines are aromatic systems and can be described in the solid state as van der Waals bonded narrow-band molecular organic semiconductors with weak interactions between the molecules (distance > 0.378 nm in the direction of

the stack axis of the planar macrocycles). Therefore, the weak intermolecular electronic interactions between low molecular phthalocyanines (R = H) result in low intrinsic specific electrical conductivities in the order of $10^{-11} - 10^{-15} \text{ Scm}^{-1}$ dependent on the modification and the central metal ion in general. Several strategies were developed to enhance the electrical conductivity of phthalocyanines. By doping low molecular weight phthalocyanines, e.g., with iodine from the gas phase or from solution, partial oxidation to radical cations occurs. The molecules are perfectly orientated in stacks along the direction of the stack axis. NiPc(I₃)_{0,33} exhibits metallic conductivity up to 700 Scm^{-1} . Polymeric cofacially stacked phthalocyanines with covalent/covalent bonds in the main chain have the advantage of stable permanent stacking [31].

Another possibility to enhance the electrical conductivity are the enlargement of the conjugated π -electron system in the two-dimensional plane of polymeric phthalocyanines. Also compressed powders exhibit conductivities in the order of $10^{-3} - 10^{-7} \text{ S cm}^{-1}$ and the conductivity increases to 10^{-2} - 10^{-3} Scm^{-1} for thin films.

Anodically electropolymerized films of nickel(II)tetraaminophthalocyanine show high metallic-like conductivity of 3 Scm^{-1} because the aromatic π -system is part of the conducting pathways of the polyamine-type structure. In contrast, the anodically polymerized films of tetrapyrrolylethyleneoxyphthalocyanine are less conducting, since an isolating alkylene bridge exists between both parts [43].

Low molecular weight phthalocyanines absorb in the visible region, therefore photoconducting behavior is observed under irradiation. Photoconduction of phthalocyanines finds broad technical application in bilayer devices of laser printers and laser copy machines.

The macromolecular orientation-photoconductivity relationships of several kinds of phthalocyanine polymer oriented thin films was studied by Chen et. al [44].

1.3.1.1. Electrical Conductivity of Polymers

Polymers are generally plastic materials having excellent dielectric property both at high voltages and high frequencies. In spite of this, there has been scientific interest for many years in the possibility to produce electrically conducting polymers due to the ease and low cost of their preparation and fabrication, as compared to metals, especially in films and fibers. Conducting polymers promise a future in a wide range of applications. Such applications include rechargeable batteries, photovoltaic devices, solar cells, electronic circuitry such as resistors, capacitors, diodes, switching and memory devices, electromagnetic interference shielding.

The magnitude of electrical conductivity is represented in terms of specific conductivity σ (S.cm^{-1}) or its reciprocal, specific resistivity, ($\Omega.\text{cm}$). The specific conductivity represents the electrical current that flows across the unit area (cm^2) of electrode under the unit external electric field (1 V/cm) applied to the sample.

Generally, solids with conductivities of less than $10^{-12} \text{ S.cm}^{-1}$ are insulators. Solids with metallic properties in electrical conduction show conductivities higher than 10^2 S.cm^{-1} . Solids with electrical conductivities ranging from 10^{-5} to 10^2 S.cm^{-1} are semiconductors. Solids whose conductivities lie in the range of 10^{-12} - $10^{-5} \text{ S.cm}^{-1}$ at room temperature are neither good insulators nor good semiconductors and in some cases they are called semiinsulators. It should be noted that it is the temperature dependence of

electrical conductivity instead of its magnitude that distinguishes the metals from semiconductors. While the conductivity decreases with an increase in temperature for metals, the temperature dependence of the electrical conductivity, σ , for semiconductors follows equation

$$\sigma = \sigma_0 \cdot \exp[-E_a/kT] \quad (1)$$

where, E_a is the activation energy of conduction, k is the Boltzmann constant (eV/K), σ_0 is conductivity at zero Kelvin, and T is absolute temperature in Kelvin.

Molecular structures that permit a maximum of electron orbital overlap between neighbouring molecules favor high carrier mobilities and concentrations. By this way conductivity increases. For intrinsic conductivity, their carrier concentration decreases exponentially with increasing band gap, since conjugated polymers have relatively large band gaps, the concentration of free carriers is very low at normal temperatures. Therefore, even though conjugated polymers have backbone structures suited to conduction (i. e., high carrier mobilities), the low carrier concentration results in negligible conductivity.

The doping of conjugated polymers generates high conductivities primarily by increasing the carrier concentration. This is accomplished by oxidation or reduction with electron acceptors or donors, respectively. For example, the polymer is oxidized by the acceptor's removal of an electron, thereby producing a radical cation (or hole) on the chain. If the hole can overcome the Coulombic binding energy to the acceptor anion with thermal energy or at high dopant concentrations, via screening of the Coulombic charge of the anions, it moves through the polymer and contributes to conductivity.

Doping is accomplished by chemical methods of direct exposure of a charge transfer agent in the gas or solution phase to the conjugated polymer, or by electrochemical oxidation and reduction. For example, oxidation (p-doping) is accomplished by exposing the polymer to iodine vapors, whereas reduction (n-doping) involving treatment is performed with sodium naphthalenide.

1.3.2. Electrochemical Charge-Discharge Behavior of Phthalocyanines

Phthalocyanines dissolved in organic solvents can be reduced or oxidized [44]. This results in new transitions in the UV/Vis spectra which means color change. The property is studied on thin films of phthalocyanines on conducting electrodes in contact with weak aqueous acidic electrolytes. The limit is the beginning of hydrogen formation in the cathodic region. However, the reduction potential of phthalocyanine thin film electrodes is shifted to the anodic direction depending on the electron-attracting properties of substituents at the ligand. Octacyanophthalocyanine containing electron attracting cyano groups is reversibly reduced/reoxidized at $\approx +200$ mV vs. Normal Hydrogen Electrode (NHE) in contact with 1 N acidic solution.

Octacyanophthalocyanine was embedded in different polymers with the goal of enhancing the mechanical stability and flexibility of the films and maintaining the outstanding electrochemical properties at the same time. In addition, the influence of the polymer environment can be studied. Intensely green-colored and smooth films of octacyanophthalocyanine in poly(N-vinylcarbazole), a polyimide and poly(vinylidene fluoride) were prepared by casting from dimethyl formamide (DMA) solutions on to gold or Indium-Tin oxide (ITO)-substrates. The films with a thickness of

≈300 nm contain octacyanophthalocyanine and the polymer in a 1:1 ratio by weight. According to UV-Vis spectra, octacyanophthalocyanine in polyimide is partially monomolecularly dissolved, whereas, especially in poly(vinylidene fluoride), small particles exist giving conducting pathways through the film. The cyclic voltammogram of a film of octacyanophthalocyanine in poly(vinylidene fluoride) in contact with an acidic electrolyte exhibits two reductions at $E_{\text{red}}^{\text{I}} = 287 \text{ mV}$, $E_{\text{red}}^{\text{II}} = 208 \text{ mV}$ and two reoxidations at $E_{\text{ox}}^{\text{I}} = 305 \text{ mV}$, $E_{\text{ox}}^{\text{II}} = 217 \text{ mV}$ with high reversibility and electrochemical stability.

1.3.3. Photooxidation of Various Substrates

It is now interesting to consider oxidations carried out under additional irradiation. Phthalocyanines like porphyrins can be active photosensitizers. Reactions from the excited states of these photosensitizers obtained by irradiation with visible light using an artificial light source or, especially, solar radiation is of increasing interest for chemical energy conversion, decomposition of toxic compounds in the environment and synthesis of fine chemicals. Up to now, water detoxification using TO_2 , being active only in the UV region, has been investigated in detail. Investigations of photosensitizers absorbing in the visible region of solar light are only rarely known, Phthalocyanines with metal ions of open d-electron configuration such as Co(II) , Fe(II) are active as catalysts but not as photosensitizers. They exhibit a life time of the excited triplet state too short for reactions from the excited state due to metal-ligand interactions. In contrast, phthalocyanines with metal ions of closed d-electron configuration, such as Zn(II) , Al(III)OH or Si(IV)(OH)_2 , in the core of the ligand are characterized by a good

combination of long triplet lifetimes and high quantum yields of the excited triplet state obtained via the excited singlet state.

Photooxidations were also investigated in the presence of some macromolecular photosensitizers. In general, no good photoeffects were found using aggregated phthalocyanines or conjugated polymeric phthalocyanines dispersed on carriers SiO₂, charcoal or tetraaminophthalocyanine bonded polysiloxane.

1.3.4. X-Ray Powder Diffraction Spectroscopy

X-rays are electromagnetic radiation of wavelength about 1 Å (10⁻¹⁰ m), which is about the same size as an atom. They occur in that portion of the electromagnetic spectrum between gamma-rays and the ultraviolet. The discovery of X-rays in 1895 enabled scientists to probe crystalline structure at the atomic level. X-ray diffraction (XRD) has been in use in two main areas, for the fingerprint characterization of crystalline materials and the determination of their structure. Each crystalline solid has its unique characteristic X-ray powder pattern which may be used as a "fingerprint" for its identification. Once the material has been identified, X-ray crystallography may be used to determine its structure, i.e. how the atoms pack together in the crystalline state and what the interatomic distances and angles are. X-ray diffraction is one of the most important characterization tools used in solid state chemistry and materials science. We can determine the size and the shape of the unit cell for any compound most easily using the diffraction of x-rays.

1.3.4.1. XRD of Polymers:

Four main features of XRD are of importance to polymer analysis:

- 1) Indexing of Crystal Structures
- 2) Microstructure
- 3) Degree of Crystallinity
- 4) Orientation

1) Indexing of Crystal Structures: The main difference between inorganic complexes and polymers is that polymer crystals cannot be formed in perfect crystals. Also, polymer crystals tend to be of low symmetry, orthorhombic or lower symmetry, due to the asymmetry in bonding of the crystalline lattice, i.e. the c-axis is bonded by covalent bonds and the a and b axis are bonded by van der Waals interactions or hydrogen bonds. Additionally, the unit cell form factor tends to be fairly complicated in polymer crystals.

2) Microstructure: With a monochromatic incident beam the diffraction pattern from a single crystal is a sequence of spots where the Bragg condition is met for certain orientations of crystals.

Polymer crystals are on the order of 100\AA in thickness. Broadening of the diffraction lines due to small crystallite size becomes a dominant effect and the breadth of the diffraction lines can be used to measure the thickness of lamellar crystals.

3) Degree of Crystallinity: Polymers are never 100% crystalline since the stereochemistry is never perfect, chains contain defects such as branches, and crystallization is highly rate dependent in polymers due to the high viscosity and low transport rates in polymer melts. A primary use of XRD in polymers is determination of the degree of crystallinity.

The determination of the degree of crystallinity implies use of a two-phase model, i.e. the sample is composed of crystals and amorphous and no regions of semi-crystalline organization. The alternative to the two-phase model is a paracrystalline model which was popular in the early days of polymer science. There are limits to the two-phase model, particularly for fairly disorganized polymer crystalline systems such as polyacrylonitrile (PAN). Most polymer systems are amenable to the two-phase model but one should keep in mind that the 2-phase model ignores interfacial zones where the density may differ from that of the amorphous.

The integrated XRD intensity measures the volume fraction crystallinity. Other techniques such as density gradient columns measure a mass fraction crystallinity.

4) Orientation: There are a number of techniques for the quantification of orientation from diffraction data. The Wulff net is useful if single crystals are studied and it is desired to determine the orientation with respect to the diffraction such as in orientation of semi-conductor samples for cleavage. In most polymer applications it is desired to determine the distributions of orientation for a polycrystalline sample with respect to processing directions such as the direction of extrusion, the cross direction and the sample normal direction.

1.4. Industrial Applications of Phthalocyanines [45-46]

Phthalocyanines are the second most important class of colorant, and copper phthalocyanine is the single largest volume colorant sold. Traditional uses of phthalocyanines are as blue and green colorants as blue and green pigments for automotive paints and printing inks and as blue/cyan dyes for textiles and paper. Phthalocyanines have also found extensive use in many of the modern high technologies, e. g. as cyan dyes for ink jet printing, in electrophotography as charge generation materials for laser printers and as colorants for cyan toners. In the visible region, phthalocyanines are limited to blue, cyan and green colours. However their absorption may be extended into the near infrared and by suitable chemical engineering it is possible to fingerprint the 700-1000 nm region. The properties and effects of these infrared-absorbing phthalocyanines are diverse and cover many important hi-tech applications, including photodynamic therapy, optical data storage, reverse saturable absorbers and solar screens.

1.4.1. Traditional Applications

Although many metal derivatives of phthalocyanine have been made (all are blue to green in colour), the copper derivative is by far the most important. It is extremely stable and gives clean, bright cyan colours. Other metal phthalocyanines are less stable and/or are greener and duller, usually owing to the Soret band absorption tailing into the visible region. Therefore the emphasis in literature is on copper phthalocyanines. Copper phthalocyanines are used both as pigments and as dyes.

1.4.2. High Technology Applications

Ink Jet Printing: Being the only true primary printing technology, ink jet printing is rapidly becoming the dominant printing technology. Indeed, it is hard to imagine anything simpler than merely squirting coloured water on to a substrate.

Ink Jet Printing has made tremendous strides over the last decade, with the advances made in colorant and ink technology playing a major role. Because of their unique set of properties, copper phthalocyanine dyes are the cyan dyes of choice for virtually all ink jet printers.

The early or first generation ink jet printers that appeared in the late 1980s had to use normal ink dyes but they were purified to a much higher standard for ink jet use. The cyan dye chosen at that time, and still used widely in today's ink jet printers, was CI Direct Blue 199 (Na neutralised tetrasulfonated Cu-phthalocyanine). This dye has very good all-round properties but, being a very water-soluble dye under most conditions, displays poor water fastness on plain paper.

Research by Avecia produced a dye having much better, although still not perfect, water fastness. This dye used the principle of differential solubility. Most ink jet inks are alkaline (pH 7.5-10) whereas most paper surfaces are slightly acidic to neutral (pH 4.5-7.0). The carboxy group has the correct pK_a to exist in the water soluble ionised form in the ink but is converted to the free acid water insoluble form on the paper.

Electrophotography: Electrophotography, the use of light and electricity to produce an image, is another important technology. It is probably more familiar as

photocopying and laser printing. Phthalocyanines are again key chemicals in both the image formation process on the photoconductor and in producing the visible image on the substrate.

The best material to generate the latent image in laser printers is titanoyloxy phthalocyanine type IV polymorph. It has excellent compatibility with the semiconductor infrared lasers and an extremely fast photoinduced discharge speed. The toners used to produce the image in colour photocopiers and laser printers use pigments. Not surprisingly, the cyan toner is based on the copper phthalocyanine pigment CI Pigment Blue 15.

Photodynamic Therapy of Cancer: One of the most prominent new applications of phthalocyanine derivatives is their application in medicine as photosensitisers for photodynamic therapy of cancer diseases [47-49]. This modality is based on the so-called photodynamic effect-generation of singlet oxygen ($^1\text{O}_2$) as a result of interaction of photoexcited molecules of photosensitizer with common triplet oxygen. A photosensitizer is capable of selective localization in tumours is administered by intravenous injection of its solution, preferably aqueous, 1-48 h prior to light treatment. Formed under light, preferably laser excitation, singlet oxygen is a powerful oxidant leading to necrosis of tumour tissue. The various aspects of photodynamic therapy, including the development and study of photosensitizers, are described in detail in numerous reviews.

Electrochromic Materials and Devices: Since the first report of multicolor electrochromism of thin films of lutetium bis(phthalocyanine) in 1970, numerous metal phthalocyanines have been investigated for their electrochromic properties. Solid state

electrochromism has been observed in phthalocyanine compounds of more than 30 metals, predominantly, among the sandwich-type diphthalocyanine (bisphthalocyanine) of the lanthanide and actinide rare earths and the related Group III elements lanthanide, yttrium and scandium [50].

Other Applications: Blue and Green Phthalocyanine pigments are the colorants used primarily in colour filters for liquid crystal displays, and hexadecafluoro copper phthalocyanine is one of the leading electron transport materials for organic semiconductors. Phthalocyanines have potential to find some new applications [51-55].

1.5. Aim of the Study

Phthalocyanine polymers are still attracting materials for a wide range of applications. Also their application areas are broadening day by day. Reaching better qualifications for phthalocyanine complexes or polymers requires scientific investigations of phthalocyanines with different metal or functional groups.

To the best of our knowledge, diazo-bridged phthalocyanines have never been investigated and diazo linkage may increase conjugation in the systems because of the unbonded electrons in the nitrogen. Increasing conjugation in a polymeric system may affect the electronic properties and result in a material with better properties.

As a result, synthesis of diazobridged phthalocyanine polymers were aimed to get improved electrical properties.

Most of the azo polymers that have been reported in the literature may be broadly classified into three groups: -polymers formed by the modification of existing polymers, -addition polymers, which have azo structures appended to the polymer backbone and are obtained from azo compound carrying olefinic groups, and -polymers that have azo group as an integral part of the main chain which represents the polymer type synthesized in this work.

The synthesized polymer have been further characterized for their electrical properties, thermal properties and morphology in the scope of the aim of this research.

CHAPTER 2

EXPERIMENTAL

2.1. Chemicals

CuCl (Riedel de Haen), NiSO₄·6H₂O (J. T. Baker), CoSO₄·7H₂O (J. T. Baker), CeSO₄·4H₂O (Merck), ErCl₃ (Aldrich), Urea (Merck), 3-nitrophthalic acid (Across), ammonium molybdate (Sigma), 1,4-Dinitrobenzene (Merck), Bensidin (Riedel de Haen), Methanol (J. T. Baker), SnCl₂ (Merck), NaNO₂ (Merck), CH₃COONa (Merck) are available and analytical grade. Acetic anhydride, HCl (Merck) Methanol (J. T. Baker), Tetrahydrofuran (THF)(Merck) and Nitrobenzene(Merck), were all commercially available and used without further purification. 3-nitrophthalic anhydride (Merck) was synthesized from 3-nitrophthalic acid according to literature [56].

2.2. Instrumentation

Mixing of reactants before complex preparation and reduction of dinitrophenyl and tetranitro metal-phthalocyanine complexes were performed in Heidolph VV micro rotovapor. Nüve FN 400 oven was operated to supply 180°C constant temperature for 5

hours during the synthesis of tetranitro metal-phthalocyanine compounds. Complexes and polymers were dried under vacuum in a Şimşek Labor teknik vacuum incubator till constant weight. Ash test were performed in a high temperature oven.

2.2.1 Fourier Transform Infrared Spectroscopy (FTIR)

FTIR is a useful method for the characterization of conducting polymers because it does not require polymers to be soluble. It is primarily used for the detection of the functional groups, but analysis of the spectra in the lower frequency finger print region can give evidence of degree of polymerization, the extent of mislinking within the polymer and the effect of substituents on the electronic properties of the polymer backbone. In this work, FTIR spectra of the polymers were recorded on a Nicolet 510 FT-spectrophotometer.

2.2.2 Ultraviolet (UV)-Visible Spectroscopy

A Shimadzu UV-1601 model spectrophotometer was employed in determination of UV-Visible spectra of polymers.

2.2.3 X-Ray Powder Diffraction Spectroscopy

X-Ray diffraction spectroscopy measurements were made by Rigaku Geigerflex X-Ray Powder Diffractometer. This is a general purpose diffractometer which can be used to characterize powders and polycrystalline materials.

2.2.4 Ash Analysis

Ash analysis were performed in a high temperature oven. The temperature was increased to 800°C in 2 hours and maintained at that temperature. Metals in the core of the phthalocyanine units were assumed to be converted to metal oxides at maximum oxidation states, so that theoretical values could be calculated and these values were compared to the theoretical values. Theoretical and experimental metal weight percentages were calculated according to the following equations;

$$\% \text{ Metal (experimental)} = \left\{ [W_{\text{ash}} - ((W_{\text{ash}}/MW_{\text{metal oxide}}) \times n_{\text{O}} \times 16.00)] / W_{\text{sample}} \right\} \times 100 \quad (2)$$

$$\% \text{ Metal (theoretical)} = (MW_{\text{metal}}/MW_{\text{repeat unit}}) \times 100 \quad (3)$$

where W: weight, MW: molecular weight, n_{O} : number of oxygen atoms in the complex.

2.3.5. Differential Scanning Calorimetry (DSC)

Thermal analysis of complexes and polymers were done by DSC 910S of TA Instruments differential scanning calorimetry. A constant heating rate of 10°C/min was used during DSC measurements.

2.2.6 Thermal Gravimetric Analysis (TGA)

Thermal Gravimetric Analysis of the polymers were performed by Setaram Labsys instrument in an isothermal nitrogen atmosphere with a heating rate of

10°Cmin⁻¹ between 20-500°C. A Thermogravimetric Analyser measures weight changes in materials with regard to temperature. This allows for the effective quantitative analysis of thermal reactions that are accompanied by mass changes. Examples include: evaporation, decomposition, gas absorption and dehydration. Changes can be measured over a temperature range of ambient to 900°C.

2.2.7. Scanning Electron Microscopy

Scanning electron micrographs of polymer samples was taken by JEOL model JSM 6400 scanning electron microscope at 20 kV with varying levels of magnification.

2.2.8. Dilute Solution Viscosimetry

Viscosity measurements were performed by Ubbelohde viscometers in THF solvent at 25°C, then the time is measured with a stopwatch.

The intrinsic viscosity is a hypothetical construct [57]. As viscosity varies with concentration, the intrinsic viscosity is the hypothetical viscosity at a hypothetical “zero concentration”. The intrinsic viscosity is an important number, because it is the one that will tell the molecular weight, momentarily.

Molecular weight of the polymer which is called as viscosity average molecular weight for polymers can be calculated by a simple equation called as Mark Houwink relationship.

$$[\eta] = k M^a \quad (4)$$

M is viscosity average molecular weight, k and a are Mark Houwink constants. There is a specific set of Mark Houwink constants for every polymer solvent combination. This means that it is not possible to determine molecular weight of a polymer just invented because of not having Mark Houwink constants available. But it still can give a qualitative idea of whether the molecular weight is high or low. Sometimes this is the only way to decide that what it is obtained is indeed a polymer.

2.2.9. Boiling Point Elevation (Ebullioscopy) [58-61]

One consequence of Raoult's law is that the boiling point of a solution made of a liquid solvent and a nonvolatile solute is greater than the boiling point of the pure solvent. The boiling point of a liquid is defined as the temperature at which the vapor pressure of that liquid equals the atmospheric pressure. For a solution, the vapor pressure of the solvent is lower at any given temperature. Therefore, a higher temperature is required to boil the solution than the pure solvent. If we represent the difference in boiling points between the pure solvent and a solution as ΔT_b , we can calculate molecular weight from the following formula.

$$\Delta T_b = iK_b m \quad (5)$$

where m is molality (molality is used for concentration because it is temperature independent). The term K_b is boiling point elevation constant that depends on the particular solvent being used. The term i in the above equation is called the van't Hoff factor and represents the number of dissociated moles of particles per mole of solute.

The van't Hoff factor is 1 for all non-electrolyte solutes and equals the total number of ions released for electrolytes. .

The Beckmann thermometer is used for determination of temperature difference. It is one of the most versatile of the differential mercury thermometers, since it can be adjusted between -20°C to $+140^{\circ}\text{C}$ with a precision up to $+0.01^{\circ}\text{C}$. It can register temperature differences but not absolute values.

2.2.10. Conductivity Measurement

Among available conductivity techniques, four probe methods have several advantages for measuring electrical properties of conducting polymers. Four probe techniques eliminates errors caused by contact resistance and allows conductivity measurements over a broad range of applied currents[62-63].

There are three types of four probe conductivity techniques that can be employed in the study of conducting polymers: Van Der Pauw [64], four wire [65], and four point probe (Signatone) [66] and their use depends on the instrumentation available as well as sample quality and geometry. In this work signatone technique was operated.

Figure 2.1 shows the simplest form of a four point probe measurement setup. A row of pointed electrodes touches the surface of a polymer film taped or spin cast on an insulating substrate. A known current I is injected at the electrode 1 and is collected at the electrode 4, while the potential difference ΔV between contacts 2 and 3 is measured. Conductivity is calculated from the following equation:

$$\sigma = \ln 2 / (\pi R t) \quad (6)$$

where R is the resistance of the sample in ohms, and t is the thickness in cm.

Keithley 617 Programmable Electrometer were operated with four probe system during the conductivity measurements.

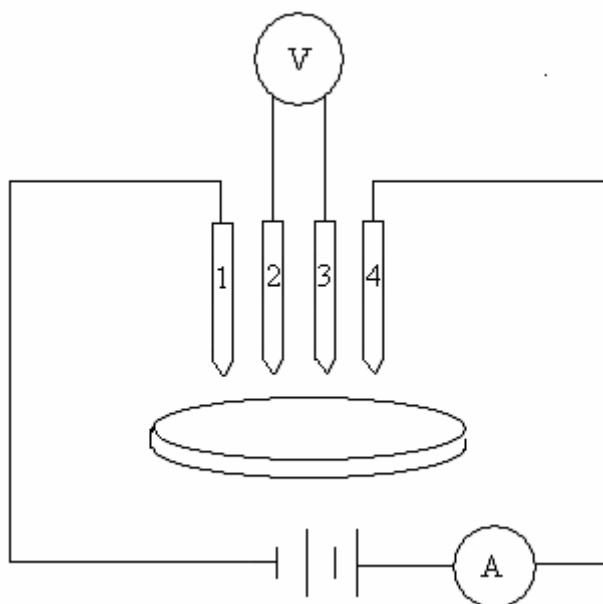


Figure 2.1 Schematic representation of a four probe conductivity measuring device

2.2.11. Cyclic Voltammetry [67-68]

Cyclic voltammetry method sweeps the potential of an electrode, immersed in an unstirred solution, and measuring the resulting current at the working electrode. Therefore, the obtained voltammogram is a display of current (vertical axis) versus

potential (horizontal axis). A simple potential wave form that is often used in electrochemical experiments is the linear wave form i.e., the potential is continuously changed as a linear function of time. The rate of change of potential with time is referred to as the scan rate (v).

The reducing and oxidizing strength of the working electrode is precisely controlled by the applied potential. Continuous deposition of the polymer onto the working electrode can be monitored by the increase in the polymer's anodic and cathodic peak currents, while the polymer redox properties are characterized by the magnitudes of its peak potentials.

CV measurements are carried out by a HEKA IEEE-488 potentiostat/galvanostat, utilizing a three-electrode configuration. Oxygen removal from the reaction medium is carried out by bubbling $\text{Ar}_{(g)}$ prior to electropolymerization, whereas maintaining the cell oxygen-free during an experiment is accomplished by passing $\text{Ar}_{(g)}$ over the solution. Pt-wire and Pt-coil were used as working and counter electrode, respectively. Saturated calomel electrode, SCE, was used as reference electrode. Measurements were made in a mixture of tributylamine perchlorate (TBAClO_4) and Dichloromethane (1:1 v/v) using NaClO_4 as supporting electrolyte at room temperature.

2.2.12. Current-Voltage (I-V) Characteristics

I-V measurement is a very useful technique to determine the material electrical properties. I-V shows the changes of materials properties when an electric field is applied. Electronic materials may show constant resistivity, capacitive resistivity or semiconductivity at a constant measurement condition. Figure 2.5 shows a basic I-V

measurement system used in this research. In addition, light was operated to determine optical sensitivity.

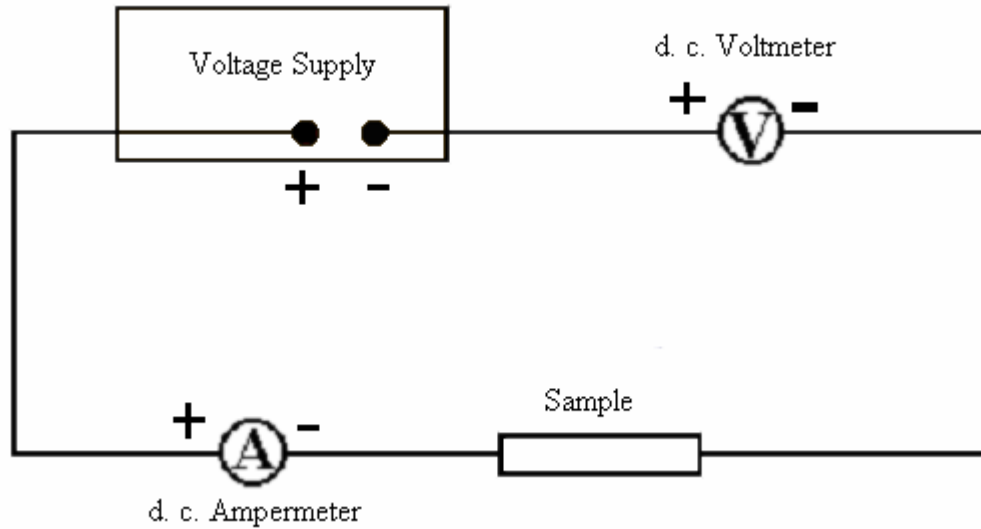


Figure 2.2 The circuit for I-V measurements

The system is connected in serial because high current for highly resistive material may damage the voltmeter. Figure 2.6 shows basic current-voltage relationships for different kinds of materials.

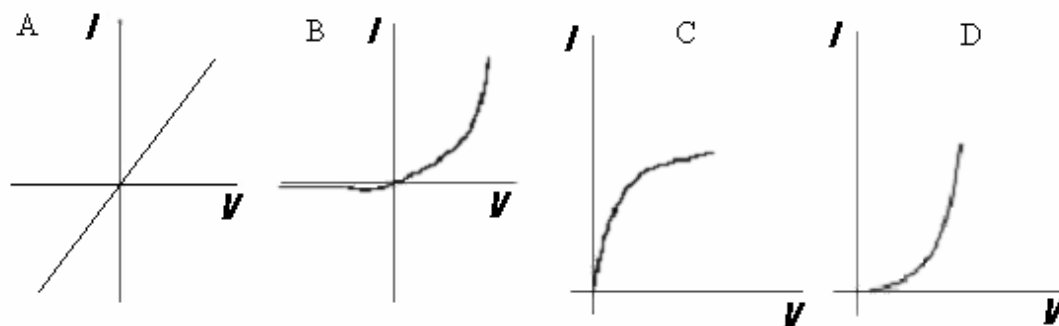


Figure 2.3 Basic current-voltage relationships for different kinds of materials: A is a material which obeys ohms law, B is a material showing semiconductivity behaviour, C is a material illustrating filament lamp behaviour, and D is a material representing thermistor behaviour

2.3. Synthesis of Materials

2.3.1. Synthesis of Tetranitro Metal-phthalocyanines [69-70]

5.54g (92 mmol) Urea, 3.28g (18 mmol) 3-nitrophthalic anhydride, 0.50 g (5 mmol) Copper (I) chloride and 75.0 mg of ammonium molybdate are pulverized and mixed with nitrobenzene to make the pasty solution for the synthesis of tetranitro Cu-phthalocyanine complex. After mixing, it is refluxed at 185°C for 5 hours. The reaction product is purified in three steps by methanol, 6 M HCl, and 20% w/w NaOH solution and each is followed by washing with hot water. Figure 2.7 shows the synthesis of tetranitro Cu-phthalocyanine. The yield of the reaction is higher than 90% for all of the metals used.

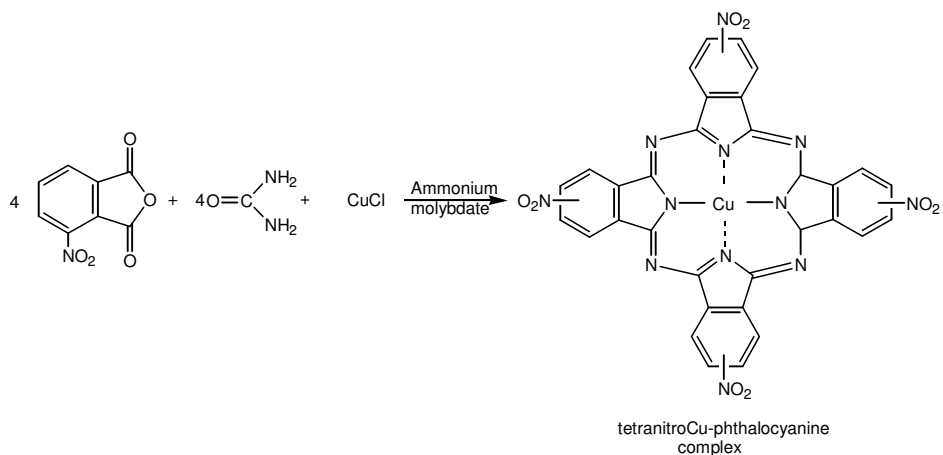


Figure 2.4 Synthesis of tetranitro Cu-phthalocyanines

For the synthesis of the other metals tetranitro phthalocyanine complexes same procedure was applied. Stoichiometric amount of $\text{NiSO}_4 \cdot 6\text{H}_2\text{O}$ for tetranitro Ni-phthalocyanine complex, $\text{CoSO}_4 \cdot 7\text{H}_2\text{O}$ for tetranitro Co-phthalocyanine, $\text{CeSO}_4 \cdot 4\text{H}_2\text{O}$ for tetranitro Ce-phthalocyanine, and ErCl_3 for tetranitro Er-phthalocyanine were used.

2.3.2. Reduction of Tetranitro Metal-phthalocyanine Complexes to Tetraamino Metal-phthalocyanine Complexes [71]

10 mL concentrated HCl is added in small portions to a mixture of 1.00 g of the nitro compound and 3.00 g of granulated Tin (II) chloride in a small flask fitted with a micro rotovapor. The flask is rotated well (to ensure thorough mixing) during the addition of the acid. Temperature is maintained at 100°C for 10 minutes to ensure complete dissociation of nitro compound. The reaction mixture is cooled thoroughly and and it is made alkaline with 20% NaOH. Tetraamino Cu-phthalocyanine is filtered and dried at 50°C in vacuum oven. The yield of the reduction process is about 50%.

Following scheme shows reduction of one of the isomers of tetranitro Cu-phthalocyanine complex to tetraamino metal-phthalocyanine complex

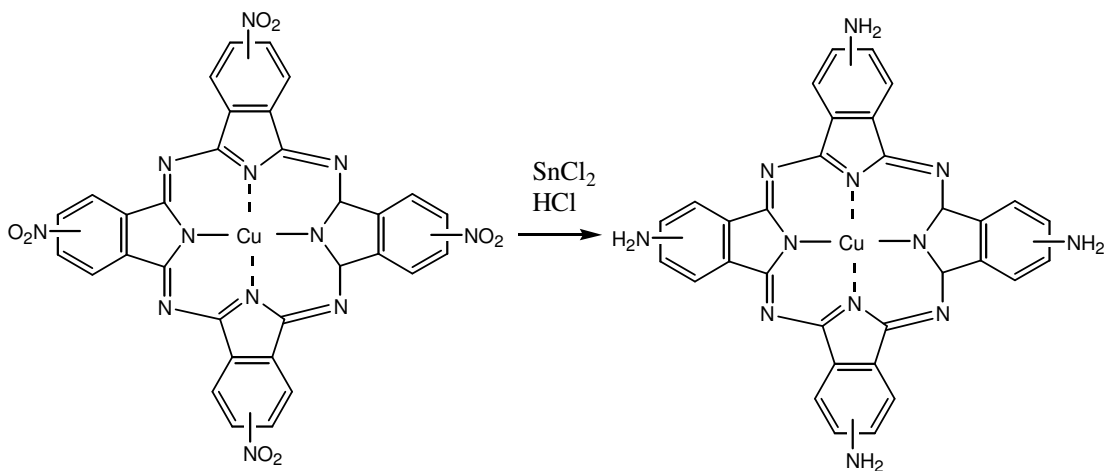


Figure 2.5 Reduction of tetranitro Cu-phthalocyanine complexes to tetraamino metal-phthalocyanines

Tetranitro Ni-phthalocyanine, tetranitro Co-phthalocyanine, tetranitro Ce-phthalocyanine, tetranitro Er-phthalocyanine complexes were also reduced by the same procedure.

2.3.3. Synthesis of Diazophenylene Bridged Metal-phthalocyanine Polymers

Diazophenylene bridged Cu-phthalocyanine polymer is synthesized from condensation of diazonium salt of diaminobenzene with tetraamino Metal-phthalocyanine in CH_3COONa solution.

Azo compounds are prepared by the interaction of a diazonium salt with an amine in the presence of sodium acetate [72].

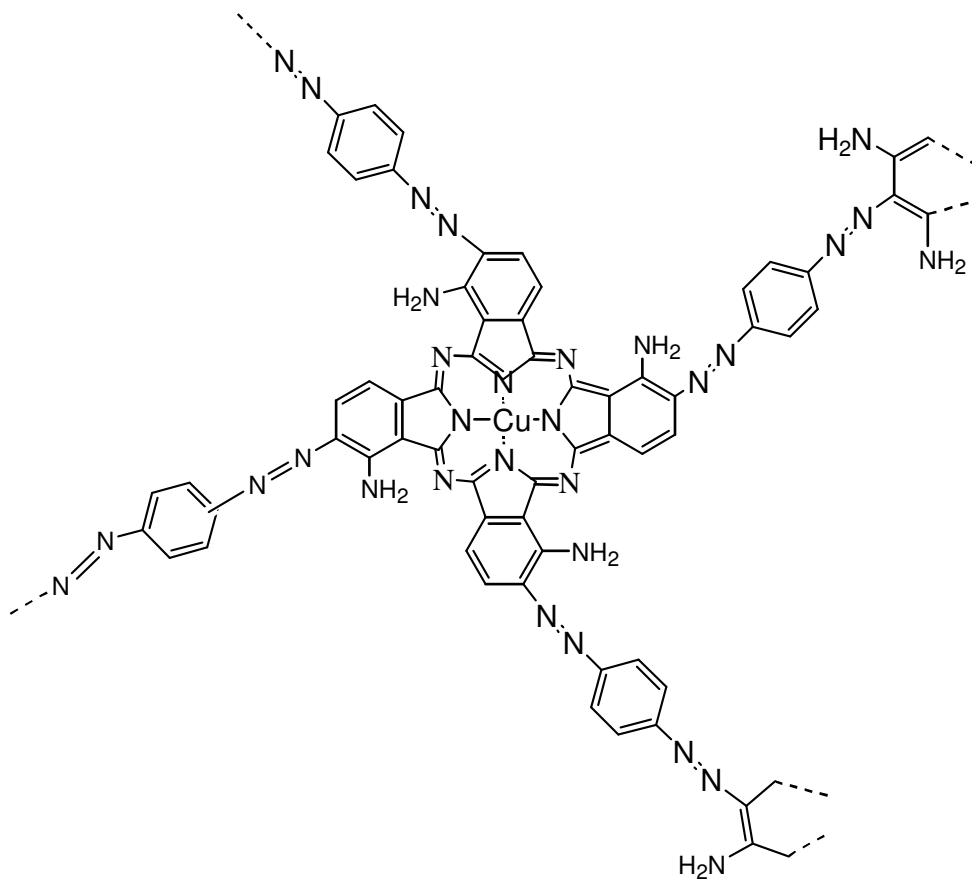


Figure 2.6 Structure of Diazophenylene Bridged Cu-phthalocyanine Polymer Structure

Preparation of diazonium salt is based on Piccard's study [72]. 0.54 g (5 mmol) of 1,4-diamino benzene is dissolved in a hot mixture of 2.40 mL concentrated HCl and 20 mL of water. Temperature is decreased to 0°C and the solution is tetraazotised by the addition of 0.70 g (10 mmol) of NaNO₂ in 5.00 mL of water within 1 minute. Tetraazo solution is left in ice for 5 minutes and then added to a suspension of 0.5 g of tetraamino Cu-phthalocyanine and 4.00 g of crystallized CH₃COONa in 50 mL of water. It is stirred

well and allowed to stand for 1 hour. Then resultant mixture is heated up to 80°C. Purification is made by hot water. The yield of this process is above 90%.

Other diazophenylene bridged polymers (Co, Ni, Ce, and Er) were synthesized by the same procedure.

2.3.4 Synthesis of Diazodiphenylene Bridged Cu-phthalocyanine Polymers

0.92 g (0.05 mmol) of bensidine is dissolved in a hot mixture of 2.40 mL concentrated HCl and 20 mL of water. Temperature is decreased up to 0°C and the solution is tetraazotised by the addition of 0.70 g (0.10 mmol) of NaNO₂ in 5.00 mL of water within 1 minute. Tetraazo solution is left in ice for 5 minutes and then added to a suspension of 0.50 g of tetraamino Cu-phthalocyanine and 4.00 g of crystallized NaCH₃COO in 50 mL of water. The mixture is stirred well and allowed to stand for 1 hour at room temperature. Then the resultant mixture is heated up to 80°C. Purification process is the same with the synthesis of diazophenylene bridged Cu-phthalocyanine polymer. Thus produced polymer is dried under vacuum at room temperature. The yield of the polymerization reaction is above 90%.

Other diazodiphenylene bridged polymers (Co, Ni, Ce, and Er) were synthesized by the same procedure.

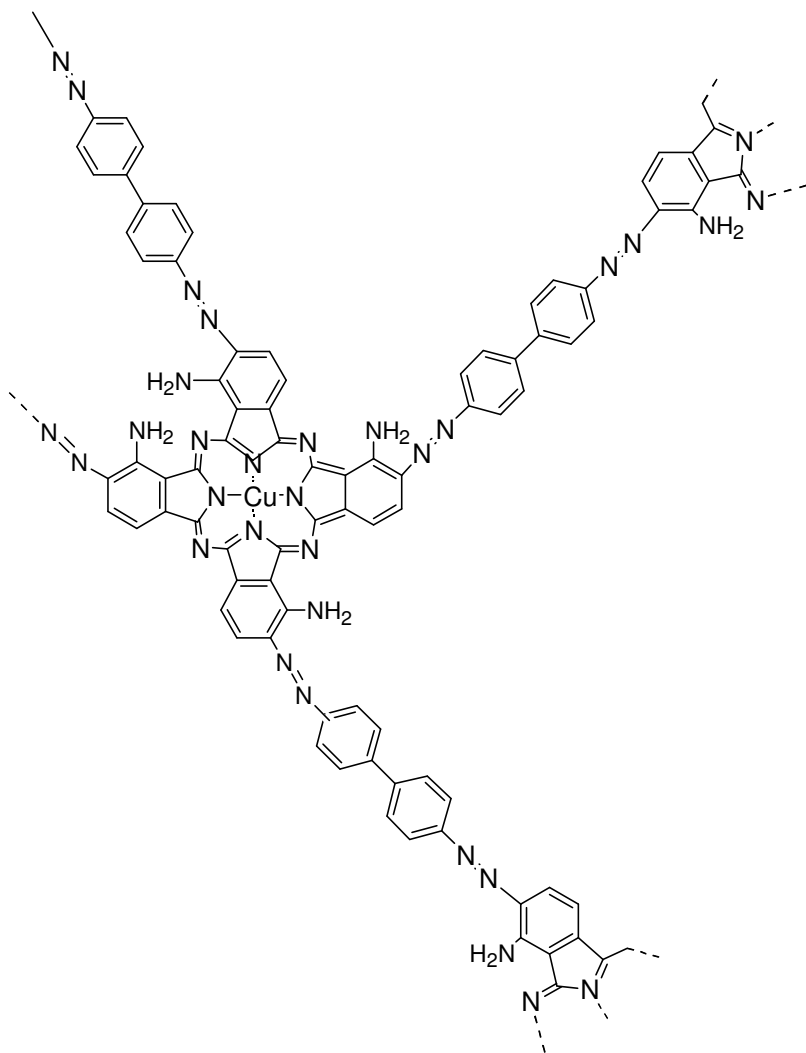


Figure 2.7 Structure of Diazodiphenylene Bridged Cu-Phthalocyanine Polymer Structure.

CHAPTER 3

RESULTS AND DISCUSSION

Diazodiphenylene and diazodiphenylene bridged metal (Co/Ni/Cu/Ce/Er)-phthalocyanine polymers are found to be partially soluble in THF and dichloromethane. Both the soluble and the insoluble parts of the polymer have the same structure.

3.1 Spectroscopic Analysis

3.1.1 FTIR Spectroscopy

The synthesis and the chemical structures of tetranitro metal-phthalocyanine complexes, tetraamino metal-phthalocyanine complexes, and diazophenylene and diazodiphenylene bridged metal-phthalocyanine polymers are confirmed by FTIR spectra [3,20,73-76] taken in KBr. The tetranitro metal-phthalocyanine complexes have characteristic NO₂ peaks at 1340 cm⁻¹ and 1540 cm⁻¹ as illustrated in Figure 3.1. The characteristic nitro peaks in tetranitro metal-phthalocyanine complexes disappear after reduction and the band at 3540 cm⁻¹ as shown in Figure 3.2 results from the stretching vibration of the NH₂ group in tetraamino metal-phthalocyanine complexes. The

characteristic bands for phthalocyanine groups in tetranitro metal-phthalocyanine complexes, tetraamino metal-phthalocyanine complexes, and diazophenylene and diazodiphenylene bridged phthalocyanine polymers were at 3100 and 2900 cm^{-1} for aromatic C-H stretching, 1610 cm^{-1} for C=C conjugation and 1540, 1250, 1100, and 750 cm^{-1} as shown in Figures 3.1, 3.2, 3.3, and 3.4 respectively. The peaks at around 1405 cm^{-1} in Figures 3.3 and 3.4 were due to N=N bond in diazophenylene and diazodiphenylene bridged metal-phthalocyanine polymers. The characteristic bands of phenylene groups in polymers are observed at around 1620, 1480, and 820 cm^{-1} .

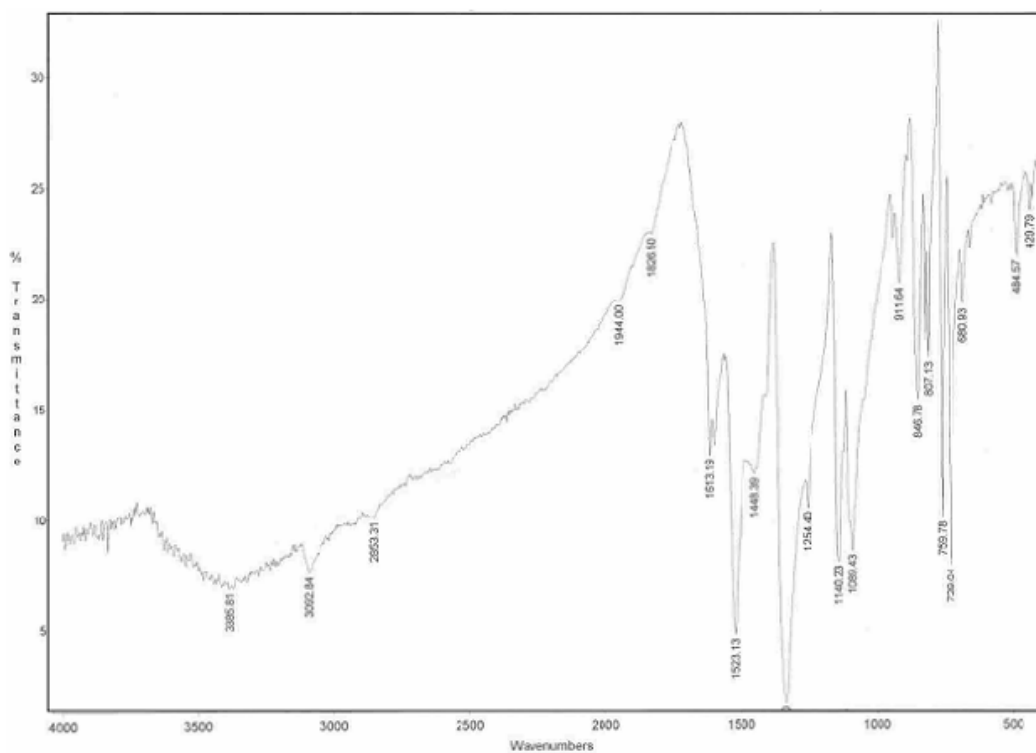


Figure 3.1 FTIR spectrum for tetranitro Cu-phthalocyanine complexes

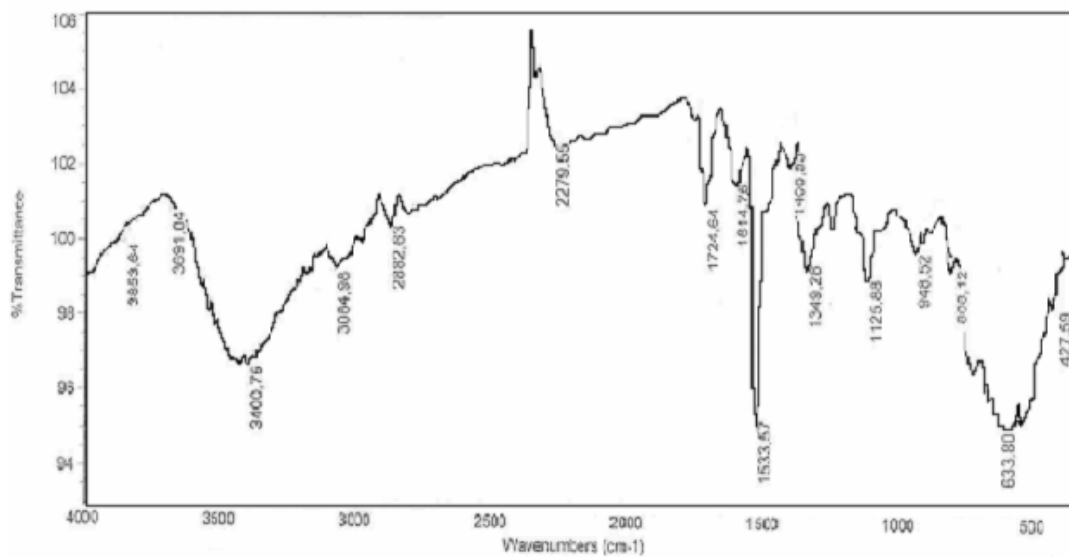


Figure 3.2 FTIR spectrum of tetraamino Cu-phthalocyanine complexes

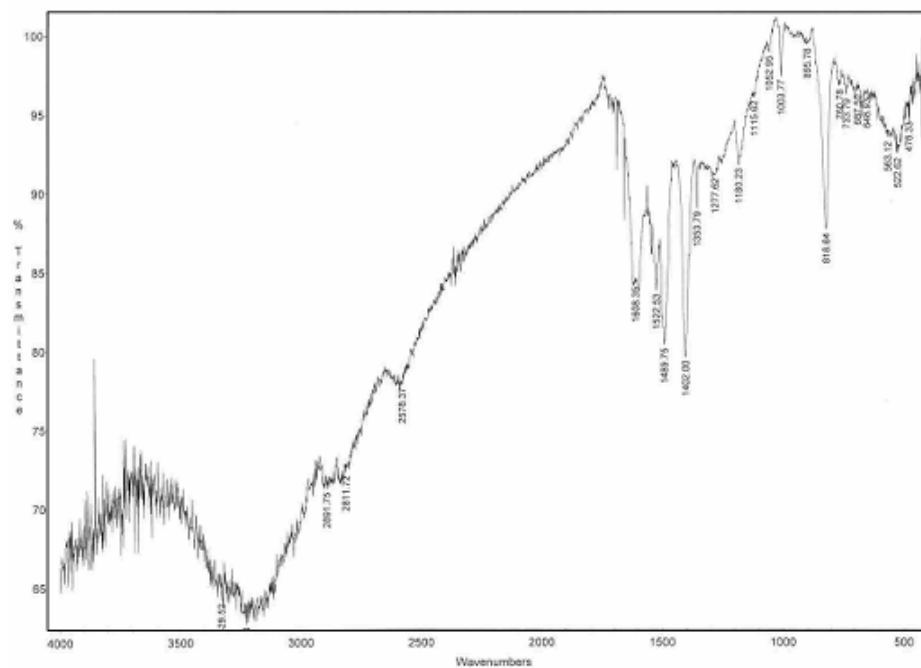


Figure 3.3 FTIR spectrum of 1,4-diazophenylene bridged Cu-phthalocyanine polymers

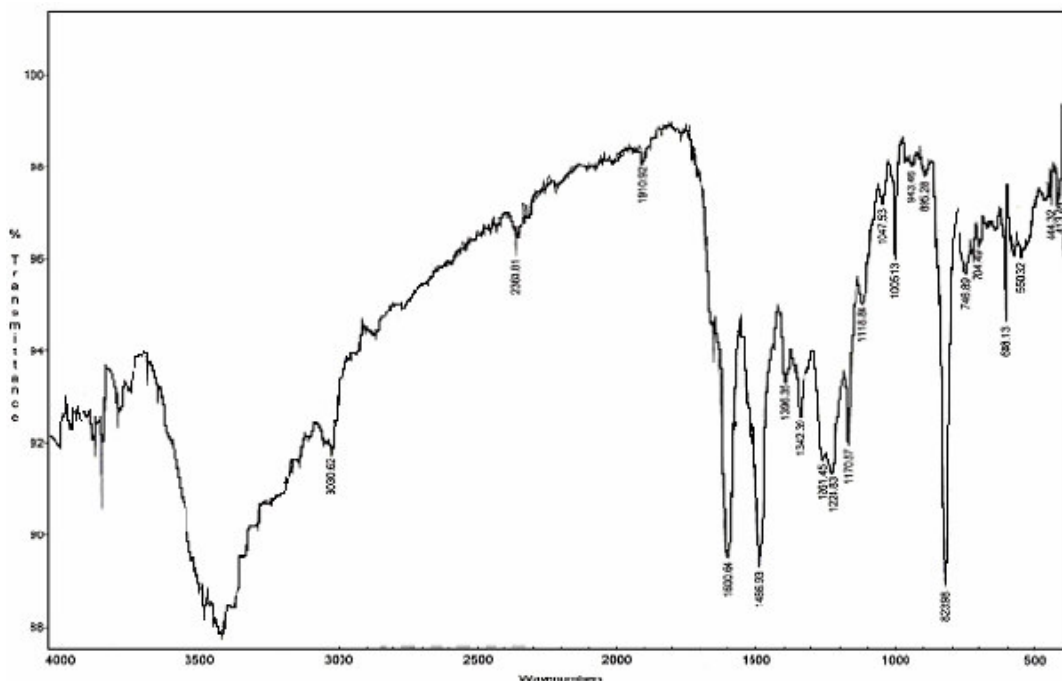


Figure 3.4 FTIR spectrum of diazodiphenylene bridged Cu-phthalocyanine polymers

The only difference between the FTIR spectrum of diazophenylene bridged polymers and diazodiphenylene bridged polymers is the relative intensity of the characteristic bands of phthalocyanine group to the characteristic bands of phenylene group. The characteristic bands of phenylene in diazodiphenylene bridged polymers are stronger than the bands in diazophenylene bridged polymers. The stronger bands in diazodiphenylene bridged polymers may be attributed to the difference in molar ratios of the phenylene and phthalocyanine units. Phenylene/phthalocyanine ratio of diazodiphenylene bridged polymer is approximately twice the ratio of the same peaks in diazophenylene bridged polymer (Figures 3.3, 3.4).

The FTIR spectra for tetranitro Co/Ni/Ce/Er phthalocyanines, tetraamino Co/Ni/Ce/Er phthalocyanines, diazophenylene bridged Co/Ni/Ce/Er phthalocyanine polymers, and diazodiphenylene bridged Co/Ni/Ce/Er phthalocyanine polymers are similar to tetranitro Cu-Phthalocyanine, tetraamino Cu-Phthalocyanine, diazophenylene bridged Cu-phthalocyanine, and diazodiphenylene bridged Cu-phthalocyanines respectively and, they are given in the Appendix A.

3.1.2. UV-Visible Spectroscopy

UV-Visible spectroscopy is one of the most versatile method for phthalocyanine characterization [76-77]. The simplest phthalocyanine unit is a 18π electron system giving electronic transitions in several different wavelengths. The most prominent bands is the one at around 650-700 nm. This peak is accepted as the evidence of phthalocyanine unit for such systems. If a phthalocyanine unit is amino functionalized, UV-visible spectroscopy produces a peak at 300 nm. Figure 3.5 to 3.8 show the UV-Visible spectra for tetranitro metal-phthalocyanine complexes, tetraamino metal-phthalocyanine complexes, and diazophenylene and diazodiphenylene bridged metal-phthalocyanine polymers respectively. The shoulder formation at 420 nm in polymers is the consequence of the stretching of N=N bonds as represented in Figure 3.7 and 3.8.

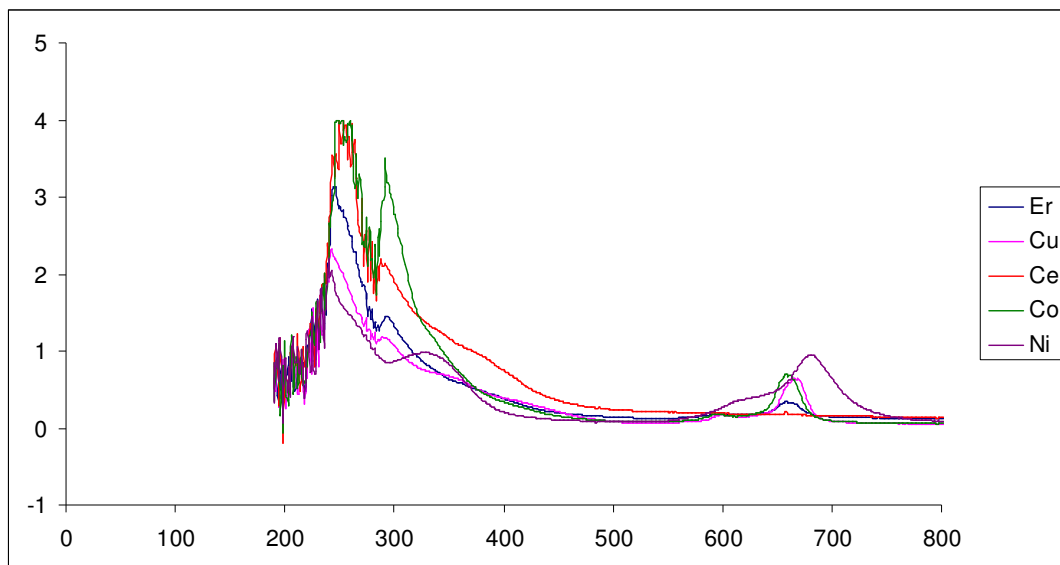


Figure 3.5 UV-Visible spectrum of tetranitro metal-phthalocyanine complexes recorded in THF

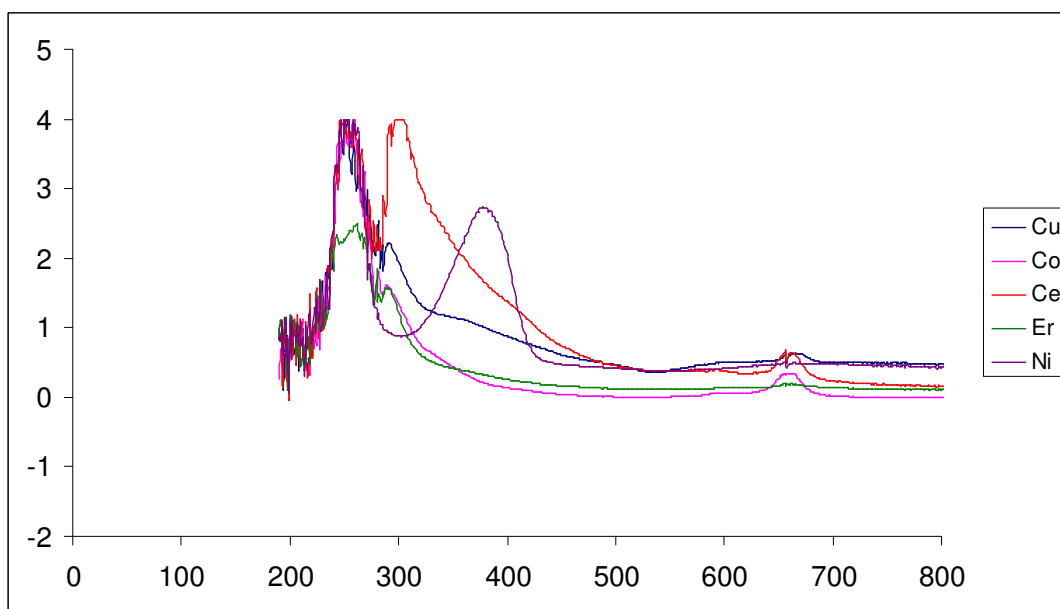


Figure 3.6 UV-Visible spectrum of tetraamino metal-phthalocyanine complexes recorded in THF

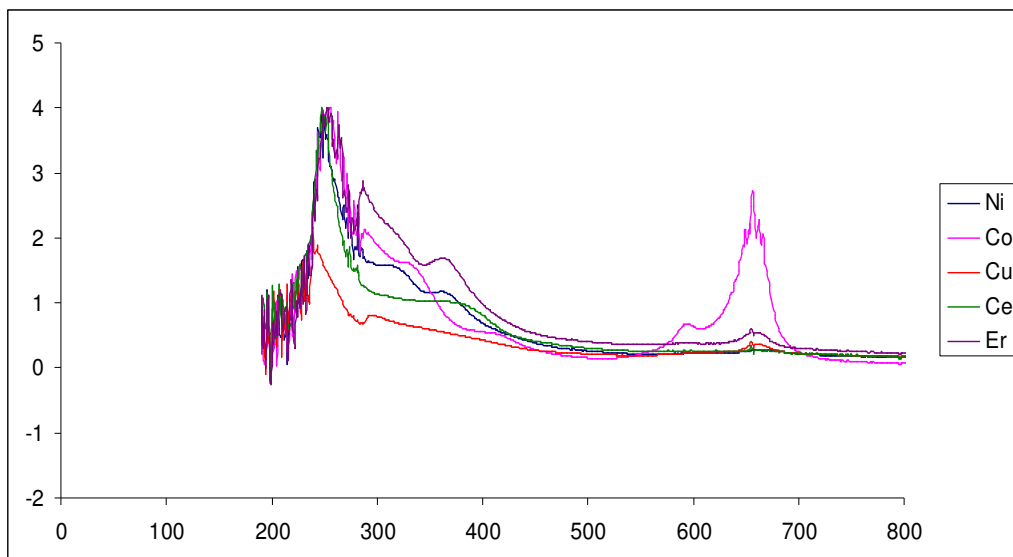


Figure 3.7 UV-Visible spectrum of diazophenylene bridged metal-phthalocyanine polymers recorded in THF

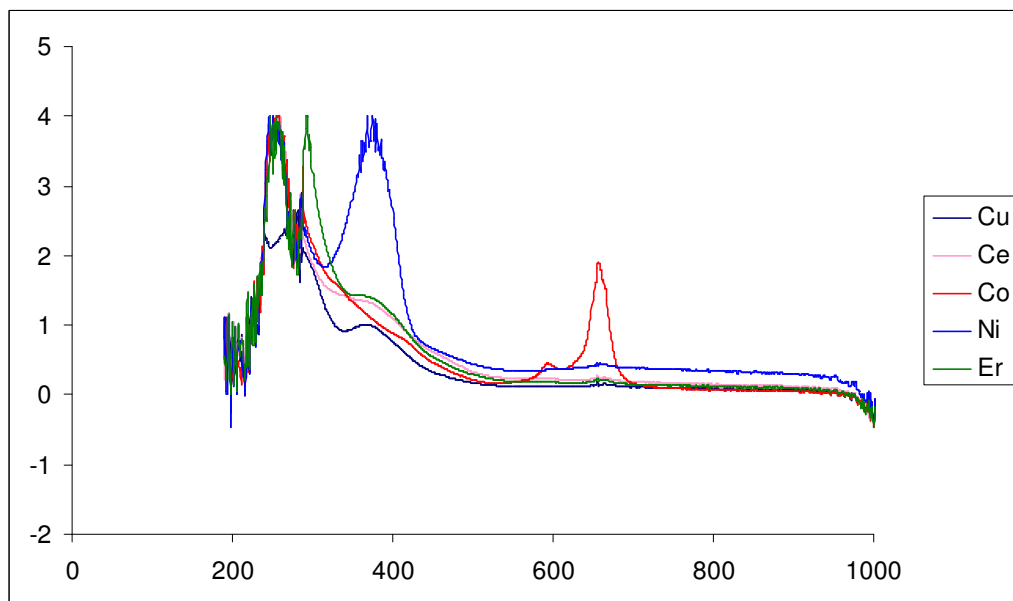


Figure 3.8 UV-Visible spectrum of diazodiphenylene bridged metal-phthalocyanine polymers recorded in THF

3.1.3 X-Ray Powder Diffraction Spectroscopy [78-81]

X-Ray spectra of polymers have been taken in 0-35° angles in 35 minutes. Diazophenylene and diazodiphenylene bridged metal phthalocyanine polymers are amorphous materials. The peaks observed are low in intensity and broad which is the result of short range ordering in the polymers. This short range ordering is observed at maximum in diazophenylene bridged Ce-phthalocyanine and diazodiphenylene bridged Ni-phthalocyanine polymers as shown in Appendix C. Figures 3.9 to 3.11 are X-ray spectra of tetra amino Cu-phthalocyanine, diazophenylene bridged metal-phthalocyanine and diazodiphenylene bridged metal-phthalocyanine polymers respectively.

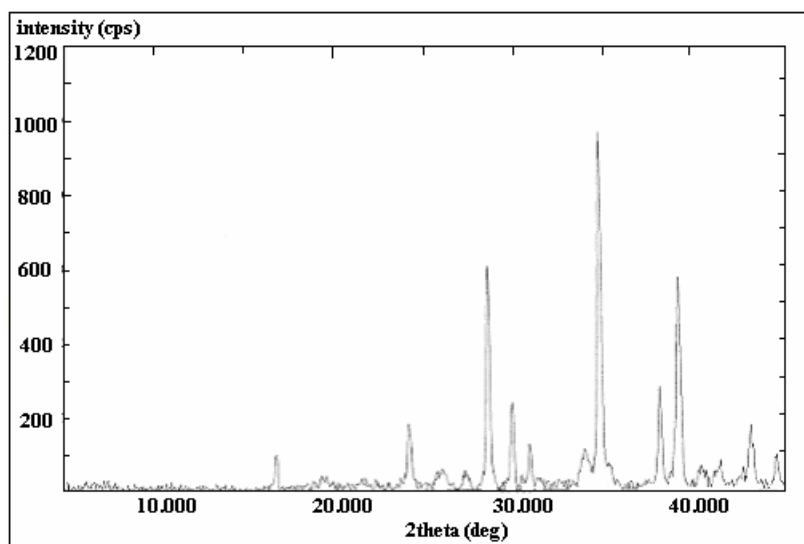


Figure 3.9 X-Ray powder diffraction spectrum of tetraamino Cu-phthalocyanine complex

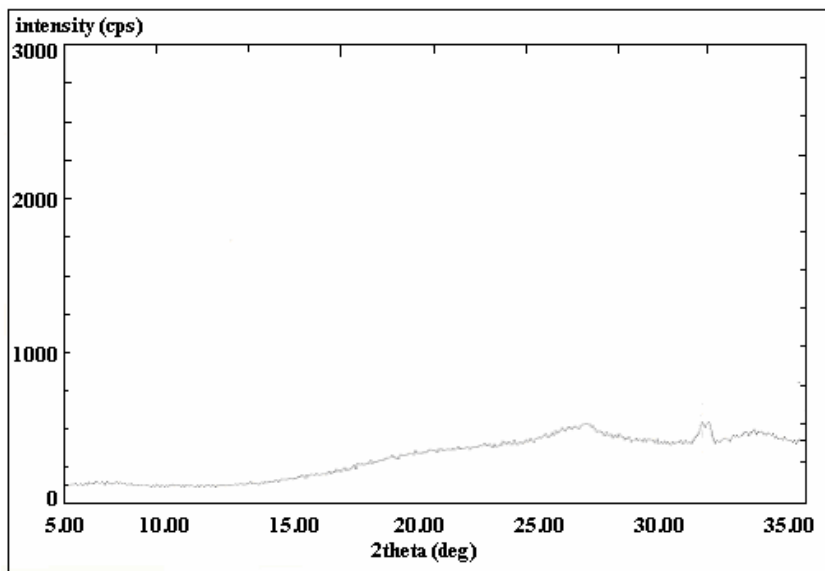


Figure 3.10 X-Ray powder diffraction spectrum of diazophenylene bridged Cu-phthalocyanine polymer

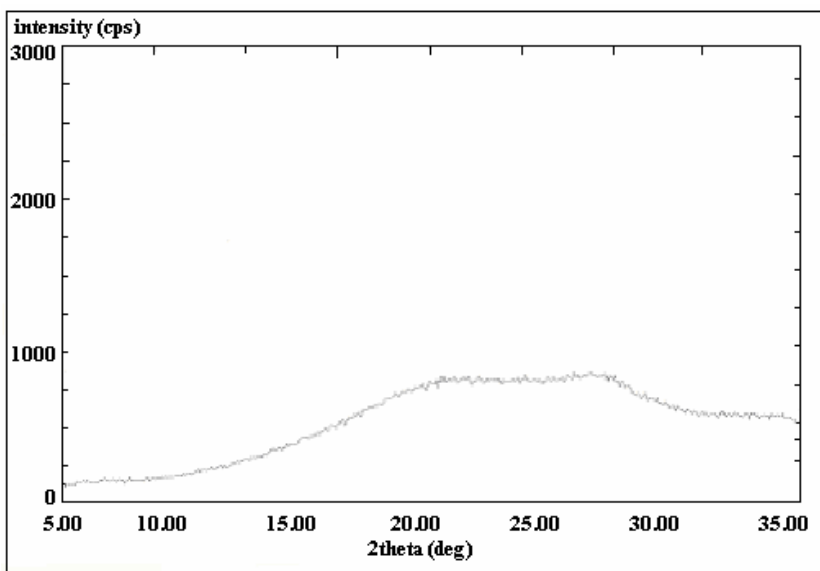


Figure 3.11 X-Ray powder diffraction spectrum of diazodiphenylene bridged Cu-phthalocyanine polymer

X-Ray spectra of diazophenylene bridged Co/Ni/Ce/Er and diazodiphenylene bridged Co/Ni/Ce/Er polymers are given in the Appendix B.

3.2 Thermal Analysis

3.2.1 Ash Analysis

The metal contents of the polymers were determined by ash analysis in which the temperature was increased stepwise. Metal oxides are formed at high temperatures. The weight percentages of metals in diazophenylene bridged metal-phthalocyanine and diazodiphenylene bridged metal-phthalocyanine polymers were calculated according to the equations given in the experimental parts (equation 2 and 3) and tabulated in Table 3.1.

Table 3.1 Theoretical and experimental values of metal amounts present in the polymers

	Diazophenylene bridged polymers		Diazodiphenylene bridged polymers	
	Exp.	Theo.	Exp.	Theo.
Co-phthalocyanine	7.81	7.09	6.54	6.06
Ni-phthalocyanine	7.66	6.59	6.93	5.62
Cu-phthalocyanine	7.21	6.62	8.79	5.66
Ce-phthalocyanine	15.71	14.41	14.34	12.46
Er-phthalocyanine	16.83	16.74	17.62	14.53

The experimental values of metal content was higher than the theoretical values. This can be explained by the aggregation of SnCl₂, SnCl₄, and NaCH₃O₂ salts. It is well known that ionic aggregation can easily occur in aqueous solutions of phthalocyanines.

3.2.2 Differential Scanning Calorimetry

3.2.2.1 Complexes

DSC thermograms of tetraamino metal-phthalocyanine complexes were investigated in two runs and the melting temperatures of phthalocyanine complexes were determined and tabulated in Table 3.2.

Table 3.2 Melting temperatures of tetraamino metal-phthalocyanine complexes

	Melting Temperature in °C
Tetraamino Co-phthalocyanine complex	256.03, 263.28
Tetraamino Ni-phthalocyanine complex	269.48
Tetraamino Cu-phthalocyanine complex	256.03
Tetraamino Ce-phthalocyanine complex	280.34
Tetraamino Er-phthalocyanine complex	285.02

3.2.2.2 Polymers

Diazophenylene and diazodiphenylene bridged metal-phthalocyanine polymers were thermosets due to the tetrafunctionality of the tetraamino metal-phthalocyanine complexes. Figures 3.12 and 3.13 show the DSC thermograms for diazophenylene and diazodiphenylene bridged Cu-phthalocyanine polymers respectively.

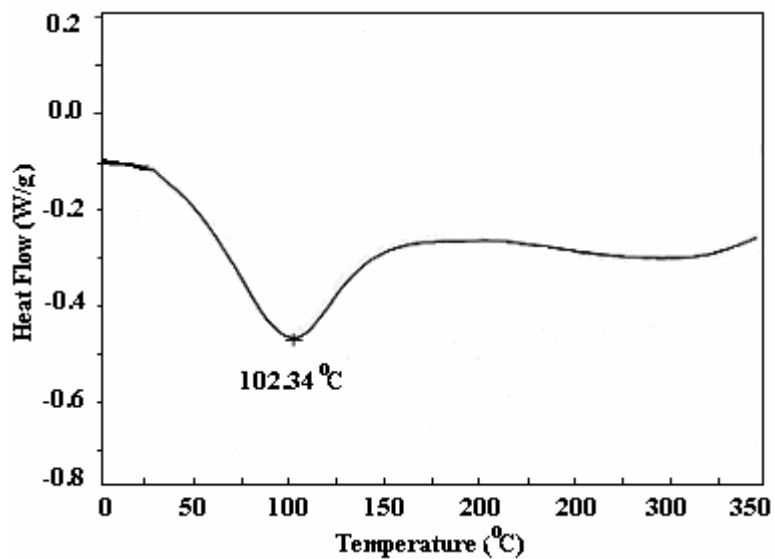


Figure 3.12 DSC thermogram for diazophenylene bridged Cu-phthalocyanine polymer

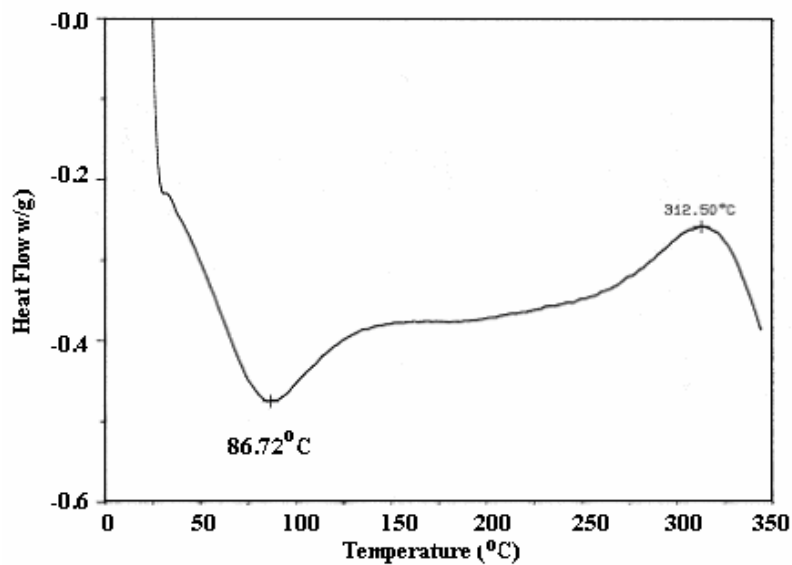


Figure 3.13 DSC thermogram for diazodiphenylene bridged Cu-phthalocyanine polymers

The degradation temperatures for polymers are given in Table 3.3.

Table 3.3 Degradation temperatures of polymers in °C

	Diazophenylene bridged polymers	Diazodiphenylene bridged polymers
Co-phthalocyanine	96.98	86.72
Ni- phthalocyanine	122.66	84.38
Cu- phthalocyanine	102.34	86.72
Ce- phthalocyanine	124.22	89.06
Er- phthalocyanine	110.16	99.22

It is obvious from Table 3.3 that diazodiphenylene bridged polymers degrades at lower temperatures i.e. phenyl group in diazophenylene bridged metal phthalocyanine polymers stabilize the polymers better than diphenylene unit.

3.2.3 Thermal Gravimetric Analysis

Thermal stability of the polymers were measured by thermogravimetric analysis (TGA). TGA was carried out under nitrogen at a heating rate of $10^{\circ}\text{Cmin}^{-1}$ and the TGA curves were used to determine the initial decomposition temperatures. It is appearant from the DSC results that diazodiphenylene bridged phthalocyanine polymers degraded at around 85°C and diazodiphenylene bridged phthalocyanine polymers degraded at around 110°C . Figures 3.14 and 3.15 represents the TGA thermograms for diazophenylene bridged Cu-phthalocyanine and diazodiphenylene bridged Cu-phthalocyanine polymers respectively.

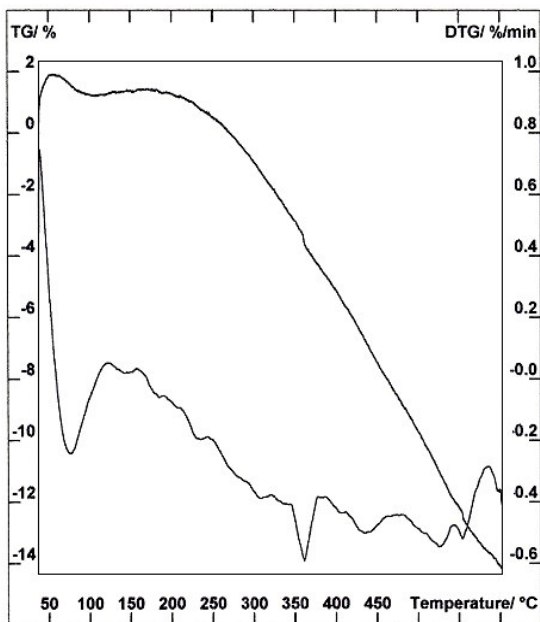


Figure 3.14 TGA graph for diazophenylene bridged Cu-phthalocyanine polymer

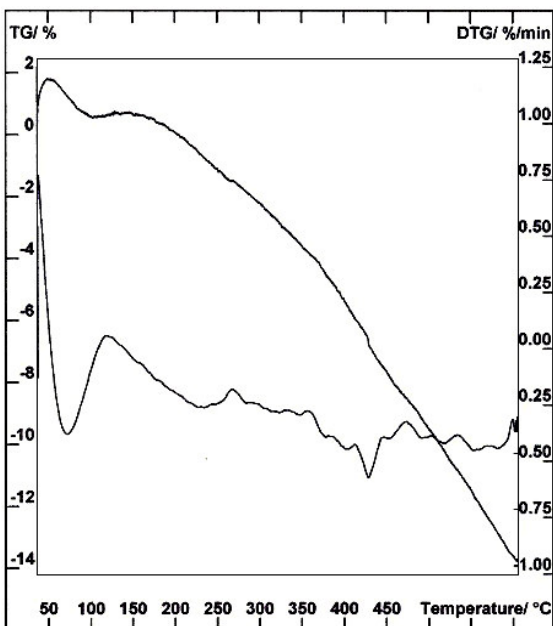


Figure 3.15 TGA graph for diazodiphenylene bridged Cu-phthalocyanine polymer

According to the DSC and TGA results, the degradations started at approximately the same temperatures and they are due to phenylene-nitrogen bond cleavage in the bridging point, since the first weight loss was considerably low for both diazophenylene and diazodiphenylene bridged metal-phthalocyanine polymers and this was considered to be the result of N₂ evolution.

Besides, the residual part after the first degradation is mainly heat resistant phthalocyanine units which are known as temperature resistant materials up to 600°C [81-84].

DSC and TGA thermograms of diazophenylene bridged Co/Ni/Ce/Er-phthalocyanine polymers and diazodiphenylene bridged Co/Ni/Ce/Er-phthalocyanine polymers are given in Appendix C and D respectively.

3.3 Molecular Weight Analysis

3.3.1 Ebullioscopy

Classical molecular weight determination methods known in polymer chemistry are very difficult to apply to phthalocyanine polymers [18]. This difficulty is due to the insolubility or very poor solubility of the polymers in organic solvents [1-3]. Determination of number average molecular weight of polymers by using colligative properties is very commonly used. In this study, ebullioscopic measurements were used for this purpose. THF was used as solvent and its ebullioscopic constant, K_b , was

determined by using azobenzol. Molecular weights of the complexes and the polymers are tabulated in Table 3.4.

Table 3.4 Number average molecular weights (in $\text{g}\cdot\text{mol}^{-1}$) of complexes and soluble parts of polymers determined by boiling point elevation technique (ebullioscopy)

	Complexes	Diazophenylene Bridged Polymers	Diazodiphenylene Bridged Polymers
Co-phthalocyanine	754	>30 000	Higher than detection limits
Ni-phthalocyanine	822	29 000	29 000
Cu-phthalocyanine	822	29 000	29 000
Ce-phthalocyanine	904	Higher than detection limits	Higher than detection limits
Er-phthalocyanine	924	Higher than detection limits	Higher than detection limits

The molecular weight analysis for tetraamino metal-phthalocyanine complexes is an easy task, since a considerable change in temperature can be observed. However in the cases such as diazophenylene bridged Co-phthalocyanine polymer and any of Ce and Er polymers this method did not give any useful results.

3.3.2 Viscometry

Basically, viscosity is based on the classical Huggins equation ($\eta_{sp}/c=[\eta]+K[\eta]^2c$) that expresses the specific viscosity of the polymer (η_{sp}) as a function of concentration (c) [57]. Solution viscosity measurements of the polymers are determined by Ubbelohde viscometer in THF solution at 25°C and their $[\eta]$ s are determined for the complexes and the polymers. The intrinsic viscosities of complexes

and polymers, $[\eta]$ s, were given in Table 3.5. It is well known that “k” and “a” parameters in Mark Houwink Sakurada relationship is dependent on solvent, temperature, and polymer type and there is a logarithmic relation between intrinsic viscosity and molecular weight i.e. an increase in intrinsic viscosity means a logarithmic increase in molecular weight. If “k” and “a” values are assumed to be similar for complex and polymers, their intrinsic viscosities can be compared to get an idea about their viscosity average molecular weights. $[\eta]$ s for the polymers were much larger than that of the complexes implying that complexes have been polymerized.

Also, when $[\eta]$ s were compared the molecular weight of the soluble part of the diazodiphenylene polymers were found to be higher than that of diazophenylene bridged polymers.

Table 3.5 Intrinsic viscosity $[\eta]$ of soluble parts of polymers determined by dilute solution viscosimetry

	Complexes	Diazophenylene Bridged Polymers	Diazodiphenylene Bridged Polymers
Co-phthalocyanine	0.0014	0.0054	0.0314
Ni-phthalocyanine	0.0165	0.0371	0.0709
Cu-phthalocyanine	0.0109	0.0324	0.1219
Ce-phthalocyanine	0.0237	0.0332	0.0316
Er-phthalocyanine	0.0163	0.0218	0.0855

3.4 Scanning Electron Microscopy

SEM micrographs for diazophenylene bridged Co-phthalocyanine polymer and diazodiphenylene bridged Ni-phthalocyanine polymer are given in Figure 3.12 and no phase separation was observed. Furthermore, there is not a significant difference between the SEM photographs of other samples.

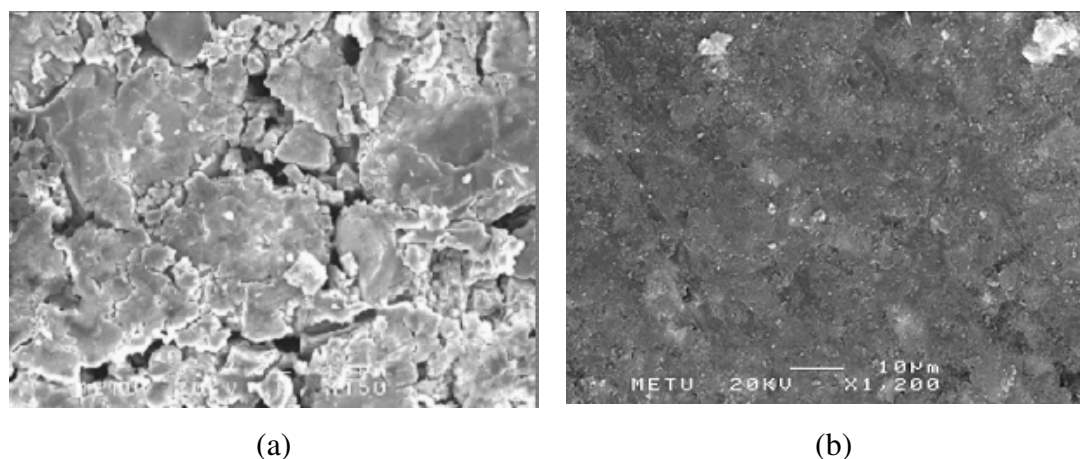


Figure 3.16 General appearances of diazophenylene bridge phthalocyanine polymer (diazophenylene bridged Co-phthalocyanine)(a) and diazodiphenylene bridged polymer (diazodiphenylene bridged Ni-phthalocyanine)(b)

3.5 Electrical Properties

3.5.1 Conductivity

Metal complexes and their polymeric derivatives have become of interest because of the possibility to yield organic conductors [85-86]. Conductivity measurements in this research were done by four probe conductivity measuring device.

Conductivities of complexes were tabulated in Table 3.6. Conductivity of the complexes increased in a similar manner as the metallic conductivity. Therefore, it is assumed that conductivity may be gained by metallic interactions. On the other hand, the metallic conductivities for Er and Ce metals were much lower yet their complexes were more conductive. This may be due to the sizes of these atoms.

Table 3.6 Intrinsic conductivities of complexes (in Scm^{-1})

Tetraamino complexes	Conductivity
^{27}Co -phthalocyanine	2.08×10^{-7}
^{28}Ni -phthalocyanine	1.17×10^{-7}
^{29}Cu -phthalocyanine	1.30×10^{-6}
^{58}Ce -phthalocyanine	3.34×10^{-5}
^{68}Er -phthalocyanine	1.34×10^{-4}

The conductivity of polymers is lower than the conductivity of complexes due to the easier orientation of phthalocyanine complexes than the polymers. X-Ray spectra (Figure 3.10-3.11) showed that there is only a short range orientation in the polymers and the mobility is fulfilled on the polymer chain due to the polymer backbones. Table 3.7 showed that the conductivities are higher in diazophenylene bridged polymers than in diazodiphenylene bridged polymers except the Co samples.

Table 3.7 Intrinsic conductivities of polymers (in Scm^{-1})

Tetraamino complexes	Diazophenylene bridged polymers	Diazodiphenylene bridged polymers
^{27}Co -phthalocyanine	2.10×10^{-7}	5.49×10^{-7}
^{28}Ni -phthalocyanine	1.21×10^{-7}	2.82×10^{-8}
^{29}Cu -phthalocyanine	6.80×10^{-6}	8.30×10^{-7}
^{58}Ce -phthalocyanine	2.40×10^{-9}	2.33×10^{-9}
^{68}Er -phthalocyanine	5.25×10^{-8}	7.70×10^{-9}

The conductivities of the diazophenylene and diazodiphenylene bridged polymers and the metallic conductivity were found to be power law dependent as shown in Figures 3.17 and 3.18 respectively except diazophenylene bridged Er-phthalocyanine polymer. The power law equation is $y = a + bx^n$ where $a=0$, $b=2 \times 10^{-17}$, and $n=1.9328$ for diazophenylene bridged phthalocyanine polymers and $a=0$, $b=1 \times 10^{-14}$, and $n=1.3473$ for diazodiphenylene bridged phthalocyanine polymers with regression factors of 0.9655 and 0.8360 respectively.

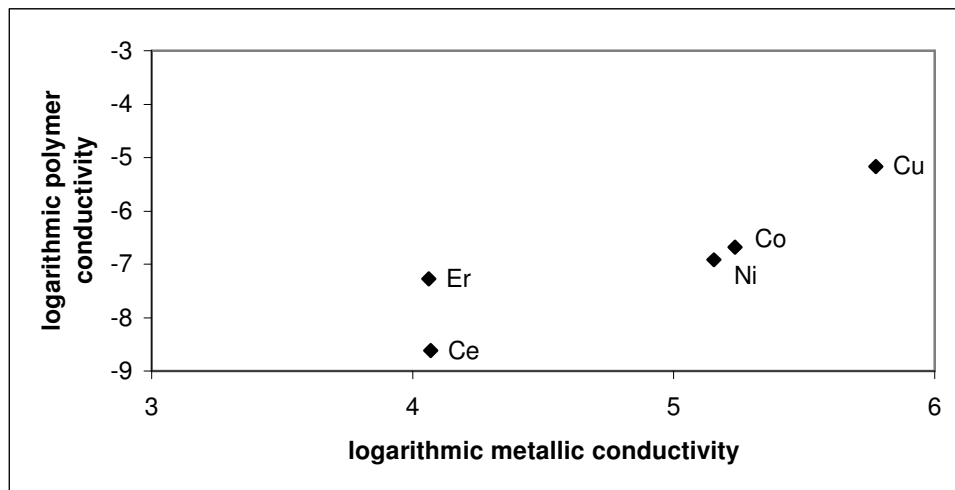


Figure 3.17 Power law dependency of diazophenylene bridged Co/Ni/Cu/Ce/Er phthalocyanine polymers on metallic conductivity

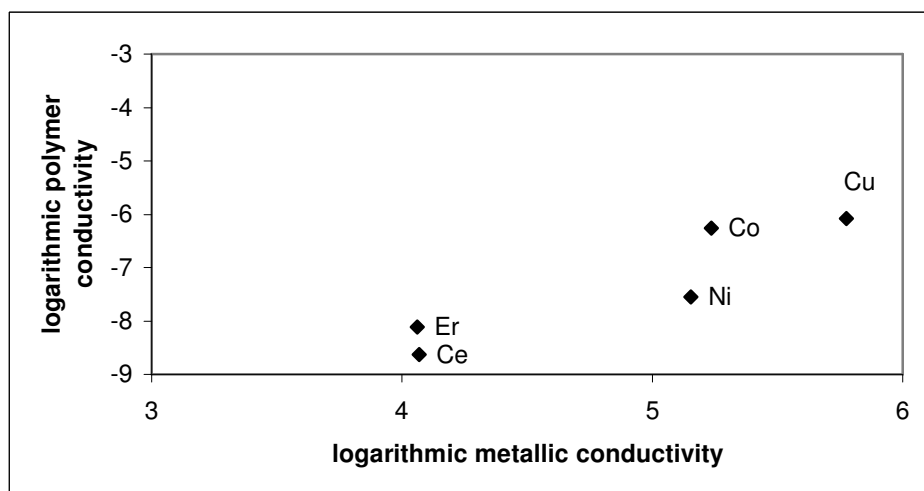


Figure 3.18 Power law dependency of diazodiphenylene bridged Co/Ni/Cu/Ce/Er phthalocyanine polymers on metallic conductivity

The conductivity results were also found to be dependent on covalent radius with the exception of Ce and Er polymers as shown in Figures 3.19 and 3.20. The

conductivity increases with a linear relation of $y=3\times 10^{-4}x-4\times 10^{-4}$ for diazophenylene bridged phthalocyanine polymers and $y=4\times 10^{-5}x-5\times 10^{-5}$ for diazodiphenylene bridged phthalocyanine polymers with regression factors of 0.7600 and 0.971 respectively.

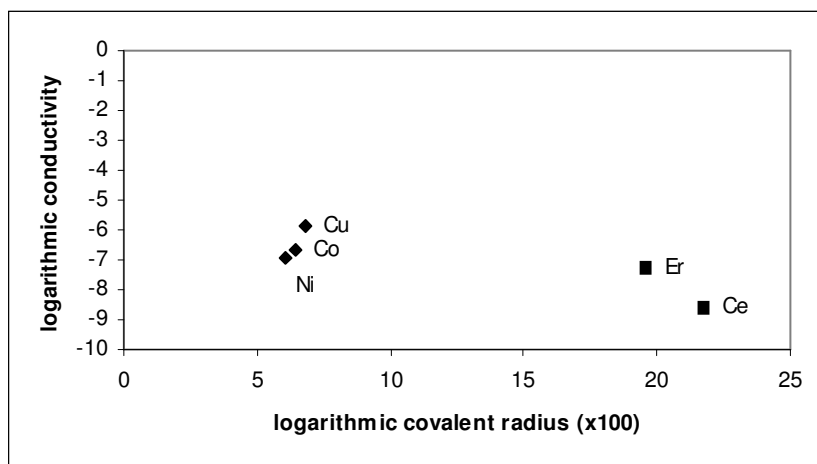


Figure 3.19 Linear dependency of diazophenylene bridged Co/Ni/Cu/Ce/Er phthalocyanine polymers on covalent radius

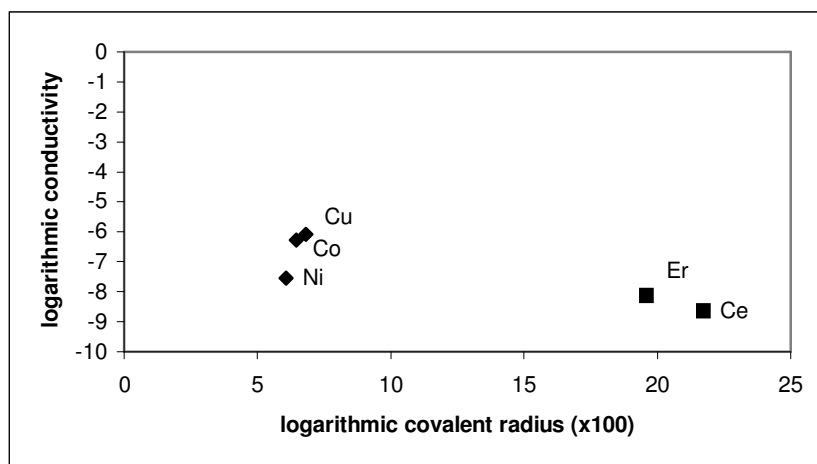


Figure 3.20 Linear dependency of diazodiphenylene bridged Co/Ni/Cu/Ce/Er phthalocyanine polymers on covalent radius

Conductivity is enhanced by suitable doping in electronic materials. By doping low molecular weight phthalocyanines with iodine from the gas phase or from solution, partial oxidation to radical cations occurs. Iodine doping is also effective in increasing the conductivity of diazophenylene and diazodiphenylene bridged polymers. Doping of polymer with iodine was achieved by the help of an U-tube and it is performed at 50°C in an oven. Iodine itself is a nonconductor. Yet, it increases the conductivity of conjugated systems by forming ions. When it is in excess amounts, it may form a nonconducting separate phase decreasing the conductivity. Figures 3.21 to 3.30 show the results of iodine doped conductivity of diazophenylene and diazodiphenylene bridged phthalocyanine polymers respectively. The increase in conductivity by iodine doping slows down after a critical concentration where iodine starts to form a separate phase and after that point the test is stopped.

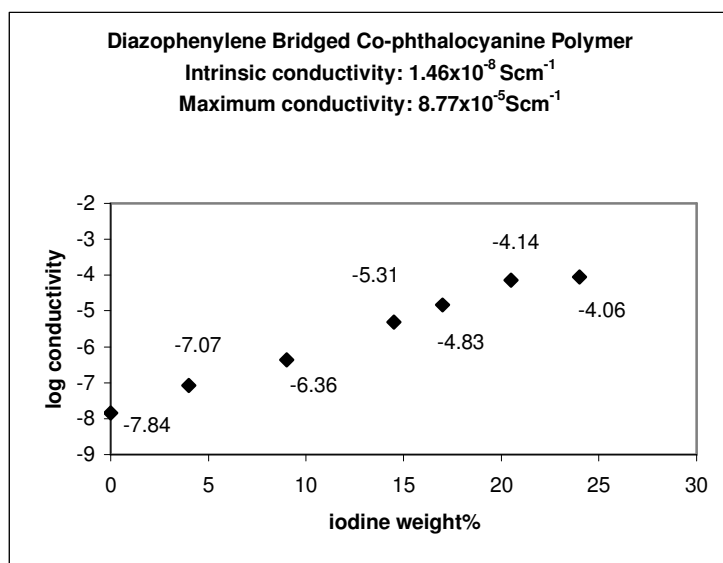


Figure 3.21 Effect of iodine doping on conductivity of diazophenylene bridged Co-phthalocyanine polymer

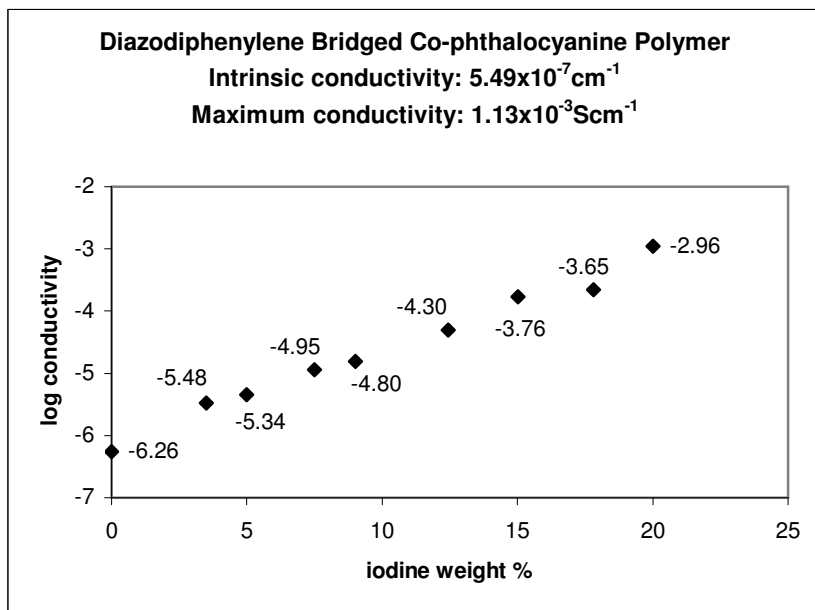


Figure 3.22 Effect of iodine doping on conductivity of diazodiphenylene bridged Co-phthalocyanine polymer

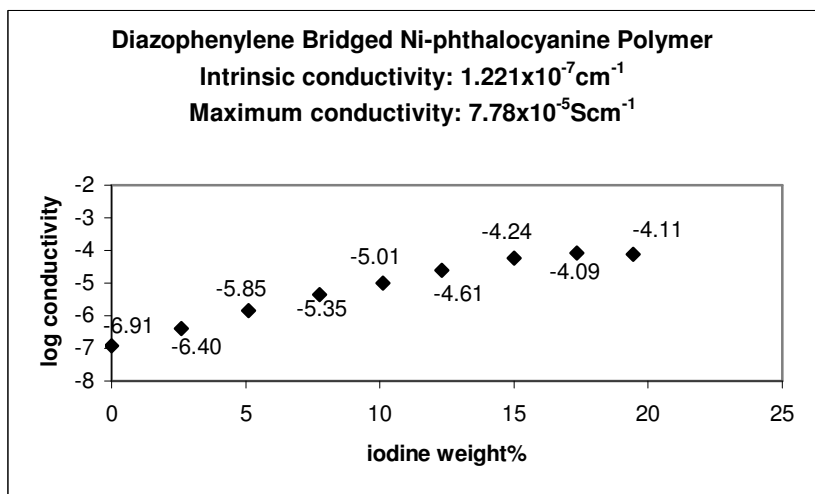


Figure 3.23 Effect of iodine doping on conductivity of diazophenylene bridged Ni-phthalocyanine polymer

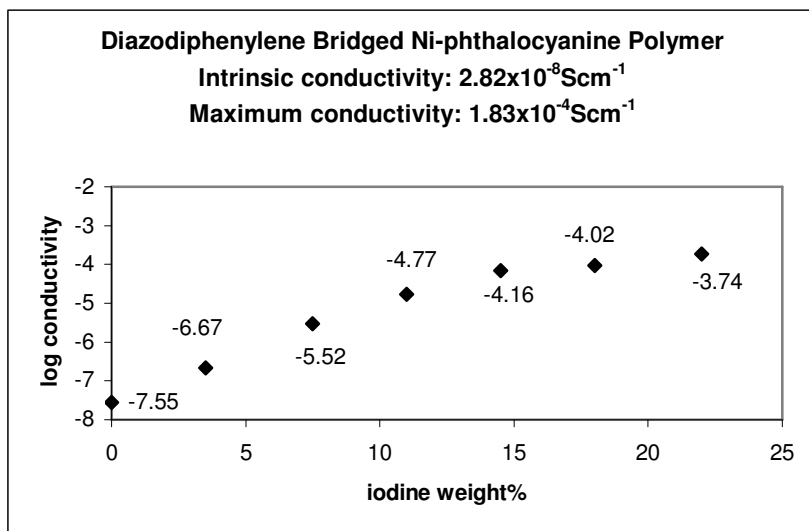


Figure 3.24 Effect of iodine doping on conductivity of diazodiphenylene bridged Ni-phthalocyanine polymer

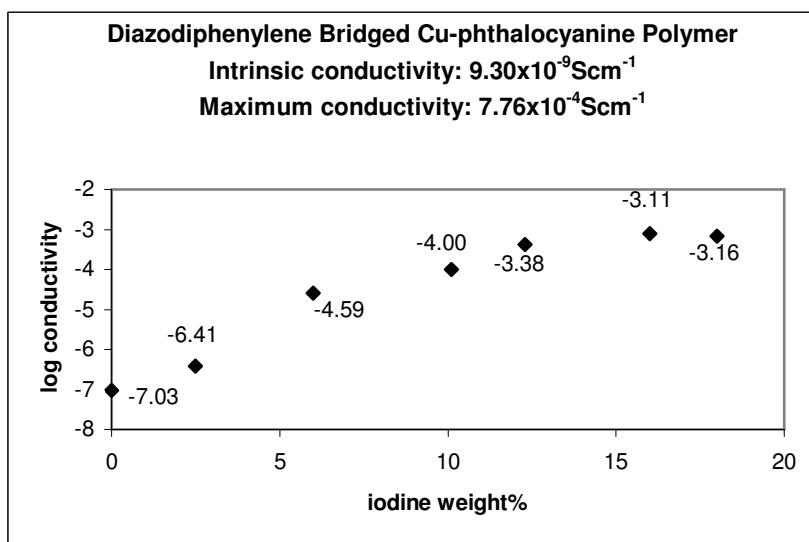


Figure 3.25 Effect of iodine doping on conductivity of diazodiphenylene bridged Cu-phthalocyanine polymer

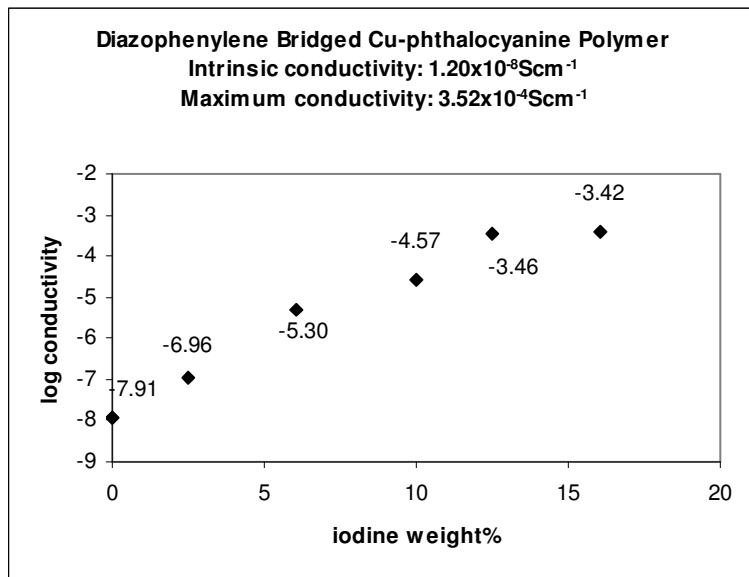


Figure 3.26 Effect of iodine doping on conductivity of diazodiphenylene bridged Cu-phthalocyanine polymer

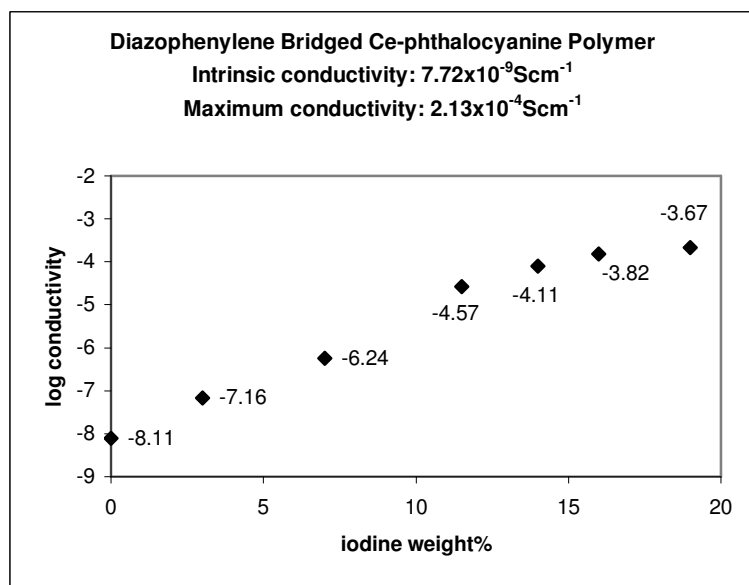


Figure 3.27 Effect of iodine doping on conductivity of diazophenylene bridged Ce-phthalocyanine polymer

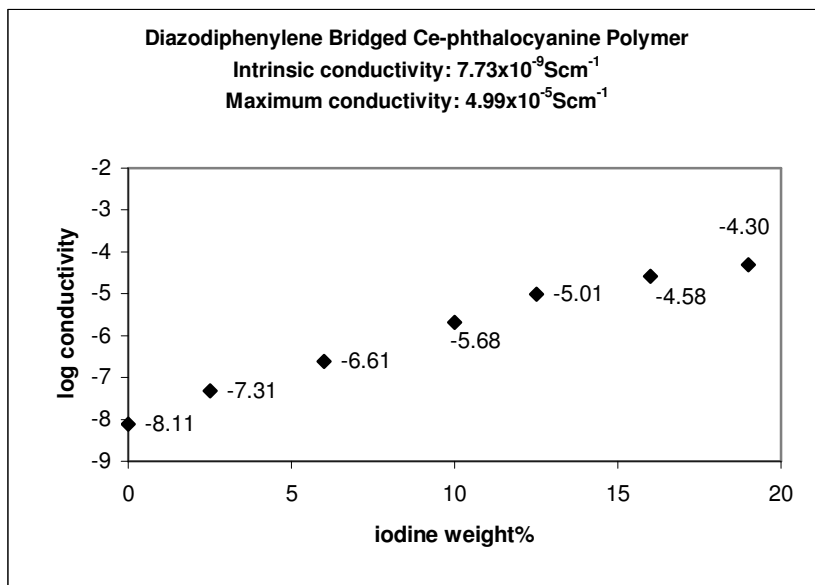


Figure 3.28 Effect of iodine doping on conductivity of diazodiphenylene bridged Ce-phthalocyanine polymer

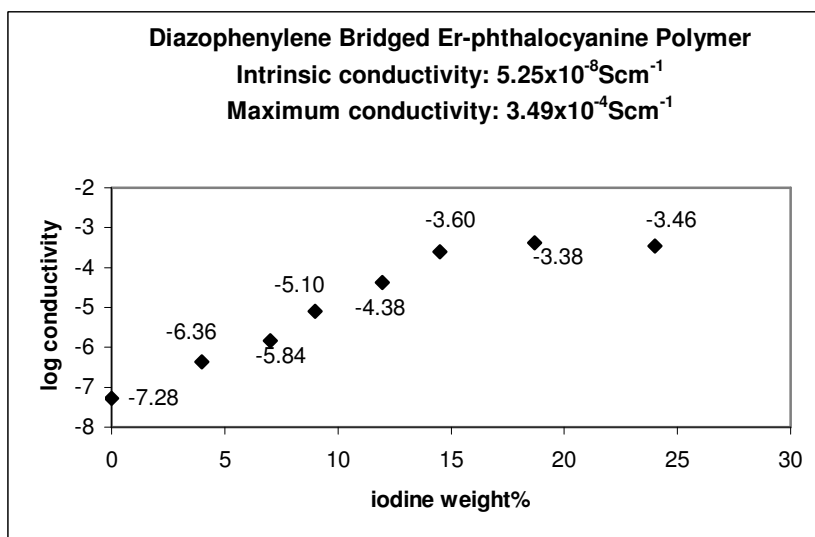


Figure 3.29 Effect of iodine doping on conductivity of diazophenylene bridged Er-phthalocyanine polymer

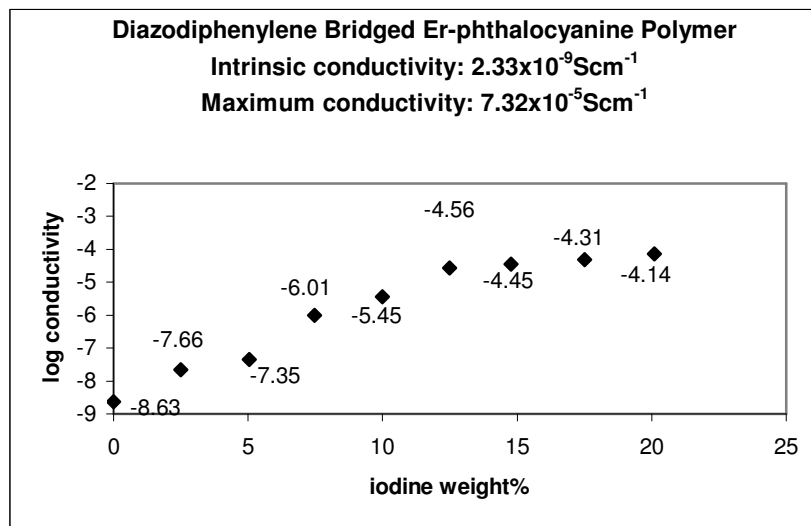


Figure 3.30 Effect of iodine doping on conductivity of diazodiphenylene bridged Er-phthalocyanine polymer

The maximum enhancement of conductivity by iodine doping was observed in diazophenylene bridged Co-phthalocyanine polymer with the conductivity value of $1.13 \times 10^{-3} \text{Scm}^{-1}$. The increase in the conductivity for diazophenylene and diazodiphenylene bridged polymers was about 10^4 fold. On the other hand the conductivity increased in the order of $\text{Cu} > \text{Er} > \text{Ce} > \text{Co} > \text{Ni}$ in diazophenylene bridged polymers and in the order of $\text{Co} > \text{Cu} > \text{Ni} > \text{Er} > \text{Ce}$ in diazodiphenylene bridged polymers.

3.5.2 Cyclic Voltammetry (CV)

Cyclic voltammetry (CV) was studied by several authors for preliminary oxidation reduction behaviour investigation of phthalocyanines. In this work, oxidation reduction behaviour for the polymer was investigated in dichloromethane. Table 3.8 illustrates the oxidation and reduction potentials determined in the soluble part of the

diazophenylene and diazodiphenylene bridged polymers, taken from Figures in Appendix E.

Table 3.8 Oxidation reduction potentials of polymers obtained from soluble parts of polymers

	Oxidation Potentials (in volts)	Reduction Potentials (in volts)
Diazophenylene bridged Co-phthalocyanine	-0.90, 0.20, 1.30	-0.90, 0.10, 1.20
Diazodiphenylene bridged Co-phthalocyanine	0.60, 0.75, 1.05, 1.3	0.35, 0.55, 0.70, 1.20
Diazophenylene bridged Ni-phthalocyanine	-0.80, 0.20	-0.85, 0.10, 0.40
Diazodiphenylene bridged Ni-phthalocyanine	0.58, 0.77, 1.04, 1.35	0.35, 0.54, 0.70
Diazophenylene bridged Cu-phthalocyanine	-0.80, -0.10, 1.40	-0.80, -0.20, 0.50
Diazodiphenylene bridged Cu-phthalocyanine	-0.90, -0.10, 0.60, 1.40	-0.90, -0.10, 0.50, 1.20
Diazophenylene bridged Ce-phthalocyanine	-0.90, 0.20, 1.30	-1.00, -0.10, 0.40
Diazodiphenylene bridged Ce-phthalocyanine	-0.90, -0.10, 0.25, 0.80, 1.15	-0.90, -0.10, 0.25, 0.45
Diazophenylene bridged Er-phthalocyanine	-0.90, -0.20, 0.60, 1.30	-0.90, -0.40, 0.50, 1.20
Diazodiphenylene bridged Er-phthalocyanine	0.60, 0.90, 1.04	0.40, 0.60

CV investigations showed that soluble parts of the polymers are electroactive. The CV of soluble parts of polymers were similar to CV of electrochemical synthesis of aniline in some cases. It is known that both NH₂ containing phthalocyanine and phenylene can electropolymerize when a suitable voltage is supplied [87].

CV of diazophenylene bridged Co/Ni/Ce/Er and diazodiphenylene bridged Co/Ni/Ce/Er polymers are given in Appendix E.

3.5.3 I-V Characteristics of Polymers

To determine the optical behaviour of diazophenylene and diazodiphenylene bridged polymers, current-voltage investigations were performed. In these investigations polymers were pressed at constant pressures ($\approx 5 \text{ lb/cm}^2$) and two probe current measurement was done as shown in Figure 1.6. Samples were scanned between -15 to $+15$ volts. The measurements were repeated both under day light and darkness.

I-V characteristics for diazophenylene and diazodiphenylene bridged polymers are given in Figures 3.31-3.40.

Basically, diazophenylene bridged polymers showed different slopes i.e. resistance values at positive and negative voltage regions. When measurements were done in daylight their voltage-current ratio (resistance) decreased i.e. they became more conductive. This showed that the current value of diazophenylene bridged polymers at the applied voltage were sensitive to light. The maximum change in voltage-current ratio (resistivity) was observed in Er polymer in which resistance decreased about 65%. I-V characteristics of diazophenylene bridged polymers is similar to semiconductor materials [88-94].

Diazodiphenylene bridged polymers represented a different character in negative and positive voltage regions as shown in Figures 3.32-3.36. The current measured at positive voltage values were higher than the currents at negative voltages which is the

property of semiconductor materials. On the other hand, the voltage-current ratio was not considerably different in negative and positive voltage values. In addition, the current of diazodiphenylene bridged polymers at the applied voltage were not as sensitive as diazophenylene bridged phthalocyanine polymers.

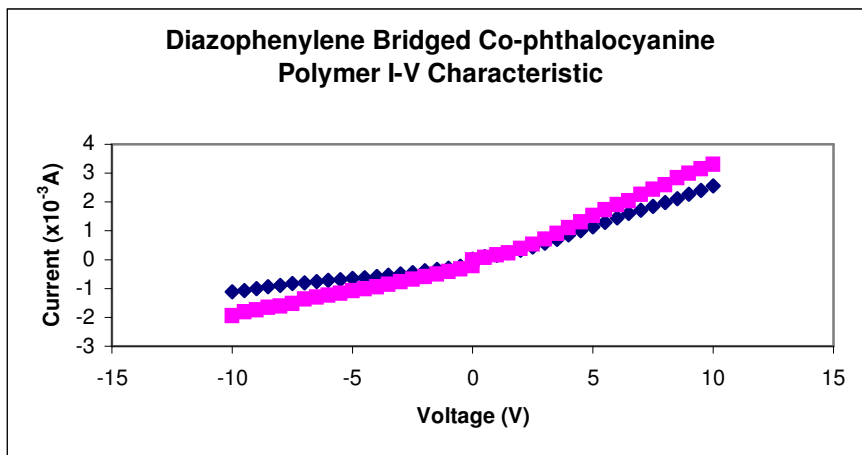


Figure 3.31 I-V characteristic of diazophenylene bridged Co-phthalocyanine polymer

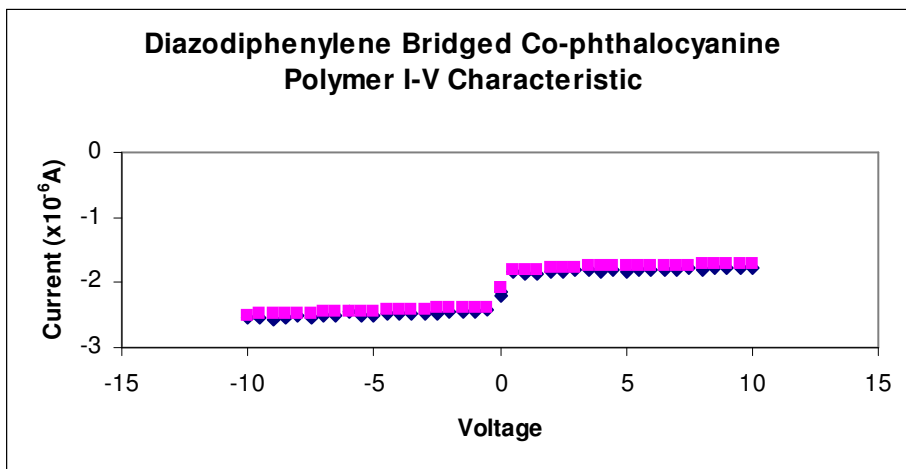


Figure 3.32 I-V characteristic of diazodiphenylene bridged Co-phthalocyanine polymer

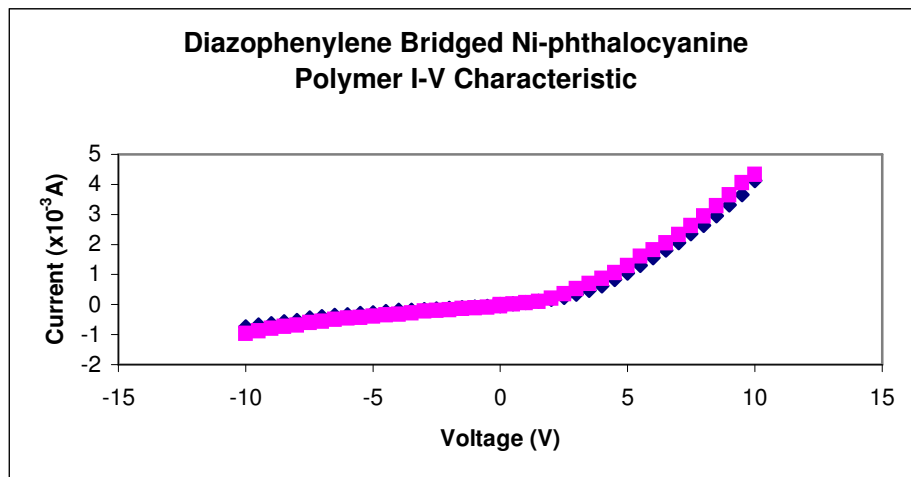


Figure 3.33 I-V characteristic of diazophenylene bridged Ni-phthalocyanine polymer

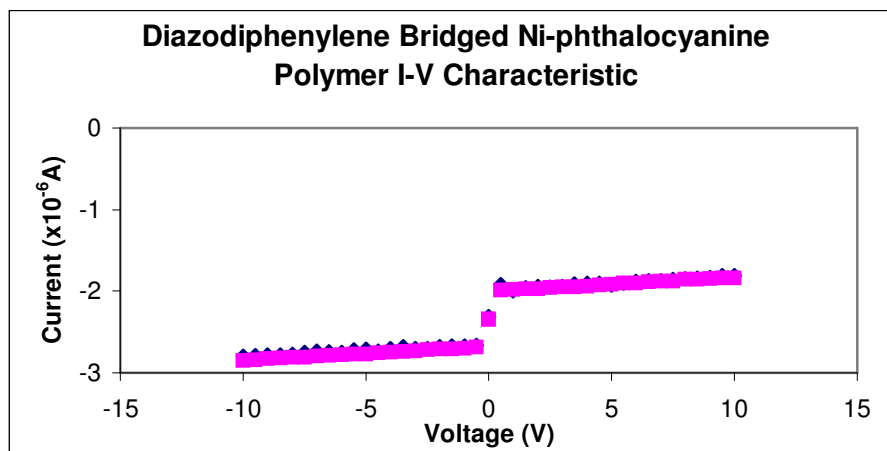


Figure 3.34 I-V characteristic of diazodiphenylene bridged Ni-phthalocyanine polymer

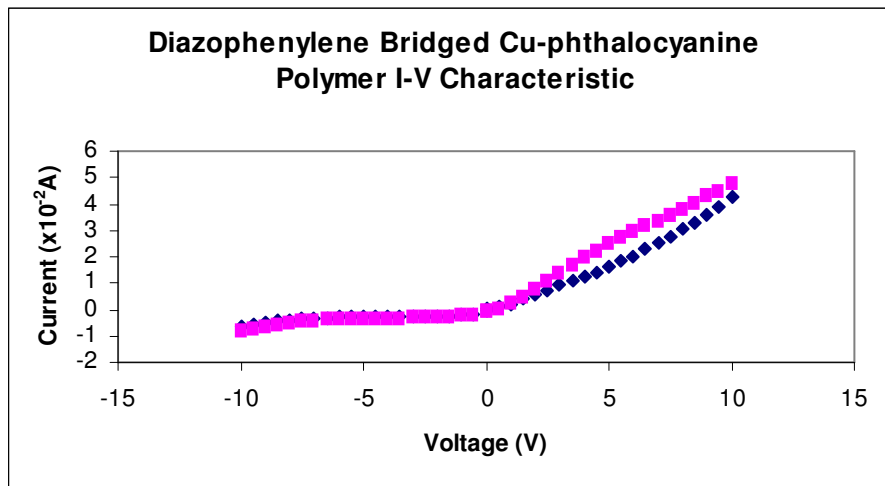


Figure 3.35 I-V characteristic of diazophenylene bridged Cu-phthalocyanine polymer

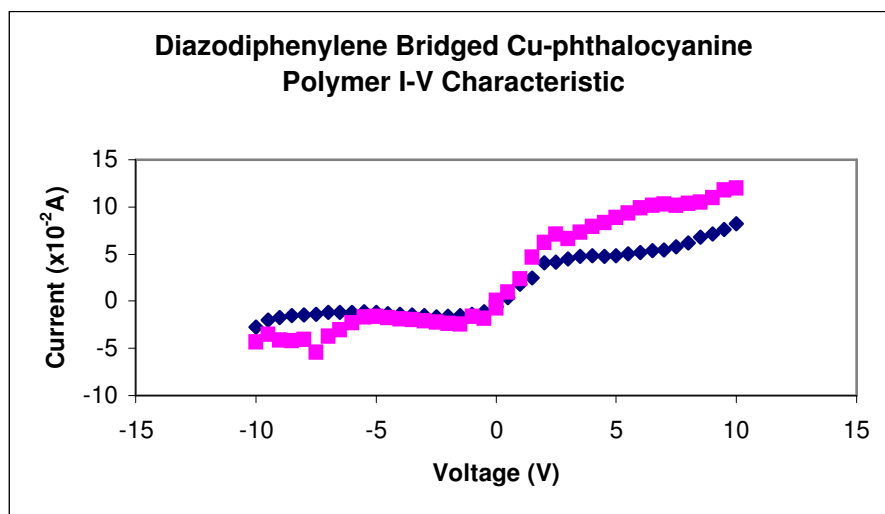


Figure 3.36 I-V characteristic of diazodiphenylene bridged Cu-phthalocyanine polymer

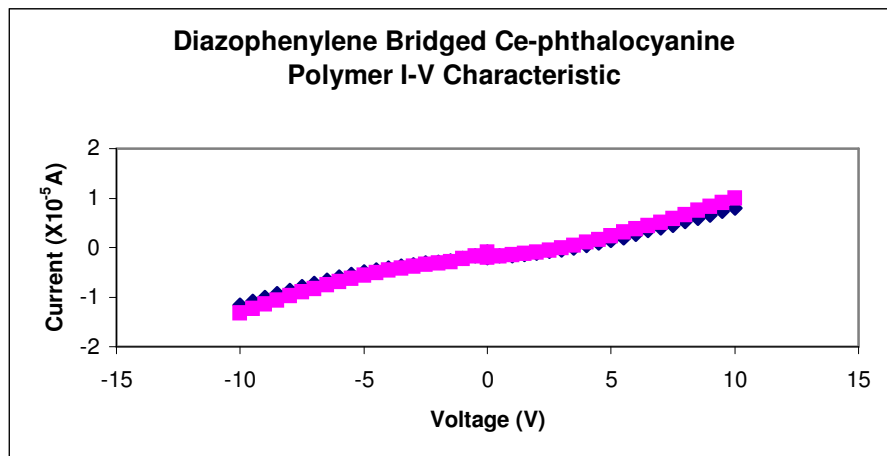


Figure 3.37 I-V characteristic of diazophenylene bridged Ce-phthalocyanine polymer

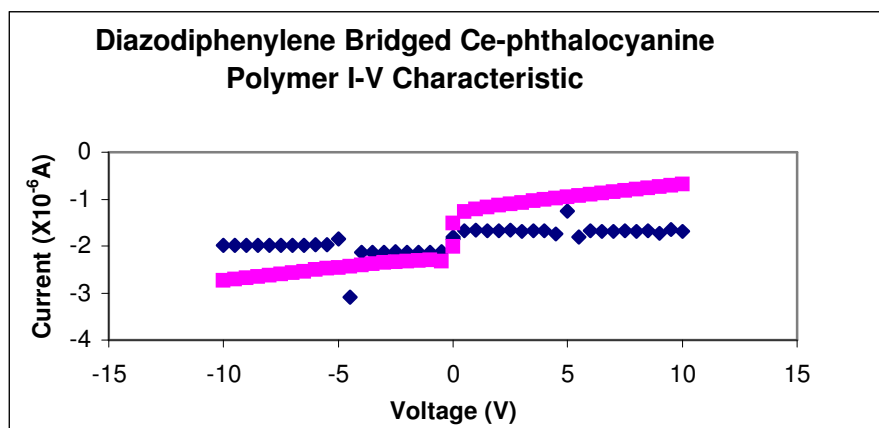


Figure 3.38 I-V characteristic of diazodiphenylene bridged Ce-phthalocyanine polymer

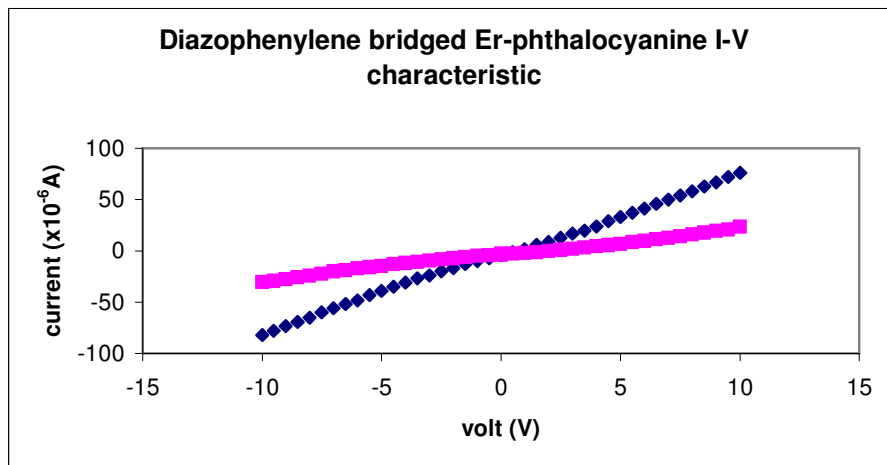


Figure 3.39 I-V characteristic of diazophenylene bridged Er-phthalocyanine polymer

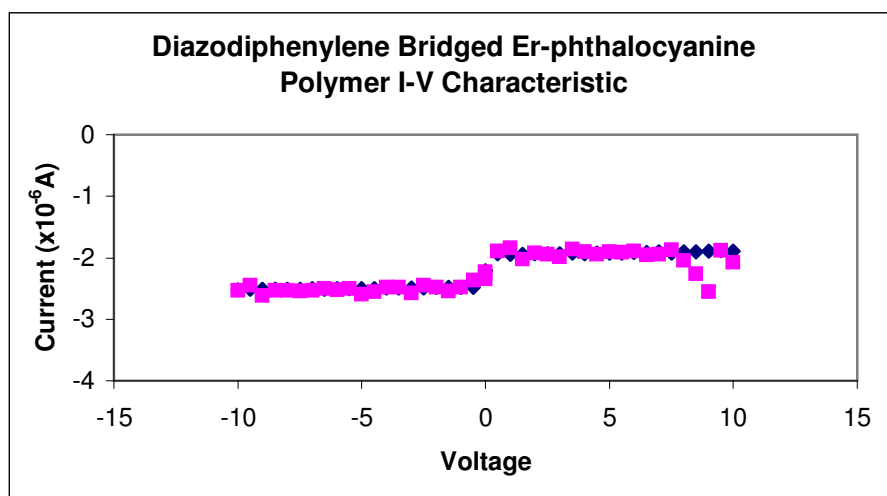


Figure 3.40 I-V characteristic of diazodiphenylene bridged Er-phthalocyanine polymer

CHAPTER 4

CONCLUSION

The combination of phthalocyanines and macromolecules is an excellent example of macromolecular metal complexes and this study contributes greatly on this subject by the novel synthesis of diazophenylene and diazodiphenylene bridged Co/Ni/Cu/Ce/Er phthalocyanine polymers.

Tetranitro Co/Ni/Cu/Ce/Er phthalocyanine complexes were synthesized and reduced to tetraamino Co/Ni/Cu/Ce/Er phthalocyanine complexes according to literature. The FTIR band at 1340 cm^{-1} was characteristic for nitro compounds. The characteristic band for amino compounds was observed at around 3450 cm^{-1} . The transition bands of phthalocyanine complexes were observed at around 650-700 nm region in the UV-Visible spectra. X-ray diffraction spectroscopy measurements showed that tetraamino complexes were crystalline compounds. The tetraamino complexes were highly soluble in common solvents and therefore, they were used for the comparison of molecular weights of soluble parts of diazophenylene and diazodiphenylene bridged phthalocyanine polymers.

Diazophenylene and diazodiphenylene bridged polymers were characterized by FTIR and UV-Visible spectroscopies. The thermoset structure and low solubility of the polymers restricted the spectroscopic characterization to some extent. Short range orientations in the polymer structures were detected by X-Ray diffraction spectroscopy analysis and they were more apparent in diazophenylene bridged Ni-phthalocyanine and diazodiphenylene bridged Ce-phthalocyanine polymers. No phase separation in any of the polymeric substances was observed by the scanning electron micrographs.

The polymers were partially soluble in some solvents such as dichloromethane and tetrahydrofuran and showed a color change when it was pure and when it was in solution. Diazodiphenylene bridged Cu-phthalocyanine polymer was found solvatochromic. Viscometric measurements were done in THF solvent and showed that soluble parts of the polymers had high molecular weights. Also the number average molecular weights of some polymers were determined by ebullioscopic method.

Thermal characterization of the polymers were performed by ash analysis, differential scanning calorimetry, and thermal gravimetric analysis. Ash analysis of the polymers showed that polymers accommodated metals at the core of the phthalocyanine units. The positive deviation from theoretical quantities were due to the aggregating salts of Sn and Na. DSC and TGA measurements were consistent with each other and showed thermal stability of the thermoset polymers.

Conductivity of the polymers were in the order of magnitude of 10^{-8} - 10^{-9} Scm^{-1} . These polymers were extrinsic conductors and their conductivities could be increased up to 10^{-3} Scm^{-1} when doped with iodine.

Conductivities of the polymers were dependent on the central metals and the conductivity increased in the order of Er>Ce>Ni>Co>Cu in both diazophenylene and diazodiphenylene bridged polymers. It was also observed that the conductivity of diazophenylene bridged phthalocyanine polymers was slightly greater than the conductivity of diazodiphenylene bridged phthalocyanine polymers. Conductivities of the diazophenylene and diazodiphenylene bridged Co/Ni/Cu/Ce/Er phthalocyanine polymers were found to obey the power law dependency of metallic conductivities of metals with high precision. There is also a linear relationship between the covalent radius of the metal and conductivity of its polymers except for Ce and Er polymers.

All polymers studied were optically sensitive according to current voltage measurements. Diazophenylene bridged phthalocyanine polymers were more sensitive than diazodiphenylene bridged phthalocyanine polymers. Maximum sensitivity was observed in Er polymers. The character of the polymer samples were similar to semiconductors.

REFERENCES

1. F. H. Moser, A. L. Thomas, *Phthalocyanine Compounds*, Reinhold Publishing Corporation, New York, (1963)
2. A. L. Thomas, *Phthalocyanine Research and Applications*, CRC Press, Florida, (1990)
3. C. C. Leznoff, *Phthalocyanines Properties and Applications* John Wiley & Sons, Inc. New York (1993)
4. P. R. Somani, S. Rakhakrishman, *Mat. Chem. and Phys.*, 77, 117 (2002)
5. Ö. Bekaroğlu, *Appl. Organomet. Chem.*, 10, 605, (1996)
6. N. B. McKeown, *Phthalocyanine Materials, Synthesis, Structure, and Function*, Cambridge University Press (1998)
7. Y. S. Kim and J. C. Jung, *Polym. Bull.* 46, 263, (2001)
8. D. Wöhrle, U. Hündorf, *Macromol. Chem.*, 186, 2177, (1985)
9. M. S. Liao and K. T. Kuo, *Polym. J.*, 25, 947, (1993)
10. B. N. Achar, G. M. Fohlen, and J. A. Parker, *J. Polym. Sci., Polym. Chem. Ed.*, 22, 319, (1984)
11. H. Z. Chen, M. Wang, and S. H. Yang, *J. Polym. Sci., Part A: Polym. Chem.* 35, 91, (1997)
12. H. Z. Chen, M. Wang, and S. L. Yang, *J. Polym. Sci., Part A: Polym. Chem.* 35, 959, (1997)

13. H. Z. Chen, R. S. Xu, and M. Wang, *J. Appl. Polym. Sci.*, 69, 2609, (1998)
14. S. Zhou, W. Qui, W. Hu, Y. Liu, F. Bai, and D. Zhen, *Thin Solid Films*, 375, 263, (2000)
15. H. Chen, M. Wang, L. Feng, and S. Yang, *J. Polym. Sci., Part A: Polym. Chem.* 31, 1165, (1993)
16. H. Z. Chen, M. Wang, L. X. Feng, and S. H. Yang, *J. Appl. Polym. Sci.*, 49, 679, (1993)
17. H. Türk and W. T. Ford, *J. Org. Chem.*, 53, 460, (1988)
18. D. Wöhrle, *Adv. Polym. Sci.*, 50, 45, (1983)
19. D. Wöhrle, O. Hild, N. Trombach, R. Benters, G. Schnurpfeil, and O. Suvorova, *Macromol. Symp.*, 186, 99, (2002)
20. R. Bannehr, G. Meyer, and D. Wöhrle, *Polym. Bull.*, 2, 841, (1980)
21. J. Bellido, J. Cardoso, and T. Akachi, *Macromol. Chem.*, 182, 713, (1981)
22. A. W. Snow, J. R. Griffith, and N. P. Marullo, *Macromolecules*, 17,1614, (1984)
23. A. G. Gürek and Ö. Bekaroğlu, *J. Porphyrines Phthalocyanines.*, 1, 67, (1997)
24. A. G. Gürek and Ö. Bekaroğlu, *J. Porphyrins and Phthalocyanines*, 1, 227, (1997)
25. D. Wöhrle, *Adv. Polym. Sci.*, 50, 45, (1983)
26. B. N. Achar, G. M. Fohlen, and J. A. Parker, *J. Chem. Soc., Polym. Chem. Ed.* 21, 589, (1983)
27. B. N. Achar, G. M. Fohlen, and J. A. Parker, *J. Polym. Sci., Polym. Chem. Ed.* 20, 2773, (1982)
28. B. N. Achar, G. M. Fohlen, and J. A. Parker, *J. Polym. Sci., Polym. Chem. Ed.* 20, 2781, (1982)
29. H. Shirai, S. I. Kondo, K. Nishihata, E. Adachi, M. Suzuki, S. Uchida, M. Kimura, T. Koyoma, and K. Hanabusa, *J. Porphyrines and Phthalocyanines*, 2, 31, (1998)

30. M. Hanach www.uni-tuebingen.de/uni/cob/AKHanack/engtxt/_blau.htm
31. D. Wöhrle, *Macromol. Rap. Commun.* 22,68, (2001)
32. M. Myakov, V. Chudakova, and M. Lopatin, *J. Porphyrins and Phthalocyanines* 5,617, (2001)
33. D. Wöhrle and G. Krawczyk, *Polym. Bull.* 15, 193, (1986)
34. H. R. Allcock and T. X. Neeman, *Macromolecules*, 19,1495, (1986)
35. D. Wöhrle and G. Krawczyk, *Makromol. Chem.* 187, 2535, (1986)
36. D. Wöhrle, *Adv. Polym. Sci.*, 50, 45, (1983)
37. E. Tsuchida and H. Nishide, *Macromolecules*, 22, 2103, (1989)
38. E. Nishide, M. Yuasa, E. Hasegawa, and E. Tsuchida, *Macromolecules*, 20,1913, (1987)
39. A. Kajiwara, M. Kamachi, *Polym. J.*, 21, 593, (1989)
40. H. Shirai, A. Maruyama, M. Konishi, and N. Hojo, *Macromol. Chem.*, 181, 1003, (1980)
41. M. Hassanein and W. T. Ford, *Macromolecules*, 21, 526, (1988)
42. D. Wöhrle, H. Kaune, B. Schumann, and N. I. Yeager, *Macromol. Chem.* 187, 2947, (1986)
38. H. Z. Chen, M. Wang, and S. L. Yang, *J. Appl. Polym. Sci.* 77,2331, (2000)
44. C. C. Leznoff, A. B. P. Lever, Eds., *Phthalocyanines: Properties and Applications*, VCH Publishers, Newyork Vol 3.1, (1993)
45. P. Gregory, *J. Porpyrines and Phthalocyanines*, 4, 432, (2000)
46. N. R. Armstrong, *J. Porpyrines and Phthalocyanines*, 4, 414, (2000)
47. E. A. Lukyanents, *J. Porphyrines and Phthalocyanines*, 3, 424, (1999)
48. C. M. Allen, W. M. Sharman and J. E. Van Lier, *J. Porphyrines and Phthalocyanines* 5, 161, (2001)

49. V. N. Nemykin, V. M. Mytsyk, S. V. Volkov and N. Kobayashi, *J. Porphyrines and Phthalocyanines*, 4,551, (2000)
50. P. R. Somani and S. Radhakrishnan *Mat. Chem. Phys.*, 77,117, (2002)
51. K. Jinno, C. Kohrikawa, Y. Saito, J. Haiginaka, Y. Saito, and M. Mifure, *J. Macrocolum Separations*
52. M. P. Ruiz, B. Behnisch, K. H. Schweikart, M. Hanack, L. Lier and D. Oelkrug, *Chemistry European Journal*, 6, 1294, (2000)
53. Z. Bao, Y. Chen, and L. Yu, *Macromolecules*, 27, 4629, (1994)
54. C. J. Brabec, N. S. Sariçiftçi, and J. M. Hummelen, *Adv. Funct. Mat.* 11, 15, (2001)
55. J. R. Frayer, *J. Porphyrines and Phthalocyanines* 3, 672, (1999)
56. H. Vogel, *Practical Organic Chemistry* 9, 6, 1074, (1969)
57. M. L. Huggins, *J. Am. Chem. Soc.*, 64, 2716, 1942
58. L. Aras, Z. Küçükayavuz, and G. Akovalı, *Physical Chemistry, Laboratory Manual*, METU Press
59. Chemistry Education Web Site from Barns and Noble (2004)
www.sparknotes.com/chemistry/solutions/colligative last accessed date: August 13, 2004
60. Mark Tuckerman Thu. Oct. 28 (1999)
www.nyu.edu/classes/tuckerman/honors.chem/lectures/lecture_13/node5.html last accessed date: August 13, 2004
61. Student Web Site for Chemistry by W. W. Norton & Company
www.wwnorton.com/chemistry/concepts/chapter_5_ch5_5.htm last accessed date: August 13, 2004
62. A. Çırpan, PhD Thesis METU (2004)

63. N. Nugay, PhD Thesis METU (1992)
64. L. J. van Der Pauw, *Philips Technical Review*, 20, 220, (1958)
65. R. Blythe, *Polymer Testing*, 4, 195, (1984)
66. F. M. Smiths, *Bell System Technical Journal*, 37, 711, (1958)
67. Cyclic Voltammetry Preview by Biolpaisley Inc.
www-biolpaisley.ac.uk/macro/Enzyme_Electrode/Chapter1/
cyclic_Voltammetry1.htm, last accessed date: August 13, 2004
68. Epsilon Bioanalytical Systems Inc. (2000) Multichannel CV experiments
www.epsilon-web.net/EC/manual/Techniques/CycVolt/cv.html last accessed date:
August 13, 2004
69. A. Shaabani, *J. Chemical Resolution* 672, (1998)
70. K. Venkataraman, *Synthetic Dyes*, Academic Press, New York, 2, 1118, (1952)
71. H. Vogel, *Practical Organic Chemistry* 9, 6, 837, (1969)
72. J. Piccard, *J. Am. Chem. Soc.* 48, 2878, (1926)
73. D. Wöhrle, U. Marose, and R. Knoop, *Macromol. Chem.*, 186,2209,(1985)
74. C. J. Norrel, H. A. Pohl, M. Thomas, K. D. Berlin, *J. Polym. Sci., Polym. Phys. Ed.*, 12,913,(1974)
75. J. Bellido, J. Cardoso, and T. Akachi, *Macromol. Chem.*, 182,713,(1981)
76. D. Wöhrle, B. Shulte, *Macromol. Chem.*, 189,1167,(1988)
77. D. Wöhrle, B. Shulte, *Macromol. Chem.*, 189,1229,(1988)
78. R. P. Linstead and J. M. Robertson, *J. Chem. Soc.*, 8,1736, (1936)
79. J. M. Robertson, *J. Chem. Soc.*, 21,615, (1935)
80. J. M. Robertson, R. P. Linstead, and C. E. Dent, *Nature*, 135(7),506, (1935)
81. M. A. Abd El-Ghaffar, E. A. M. Youssef, N. R. El-Halawany, M. A. Ahmed, *Die Angewandte Macromolekulare Chemie* 254,1, (1988)

82. S. Venkatachalam, K. V. C. Rao, and P. T. Manoharan, *J. Polym. Sci., Part B: Polym. Phys.*, 32,37, (1994)
83. H. Z. Chen, M. Wang, L. X. Feng, and S.L. Yang, *J. Appl. Polym. Sci.*, 49,679, (1993)
84. T. R. Walton and J. R. Griffith, *J. Polym. Sci., Appl. Polym. Symp.* 26,429, (1975)
85. M. Hanack and G. Paulowski, *Naturwissenschaften* 69, 266, (1982)
86. M. A. Abd El-Ghaffar, M. A. Ahmed, and M. S. Rizk, *J. Indian Chem. Soc.*, 60,550, (1983)
87. A. M. Pharhad Hussain and A. Kumar, *Bull. Mat. Sci.*, 26,329, (2003)
88. E. M. Conwell and M. W. Wu, *Soft Condensed Mater., SPIE Proc.*, 3148,210, (1997)
89. S. K. Saha, Y. K. Su, C. I. Lin, and D. W. Jaw, *Nanotechnology* 15,66, (2004)
90. W. Hu, H. Nakashima, K. Furukawa, Y. Kashimura, K. Ajito, and K. Torimitsu, *Appl. Phys. Lett.*, 85(1),115, (2004)
91. E. Jungyoon, W. Han, K. Lee, S. Cho, and D. Cha, www.kids.or.kr/science/idmc/DATA/DATA/p-13.pdf last accessed date: August 13, 2004
92. P. D. Hooper, M. I. Newton, G. McHale, and M. R. Willis, *Semicond. Sci. Tech.* 12,455, (1997)
93. W. Gao and A. Kahn, *Appl. Phys. Lett.* 79(24),4040, (2001)
94. SRS Annual Report on Organic Semiconductors http://srs.dl.ac.uk/AnnualReports/AnRep01_02/organic-semiconductors.htm last accessed date: August 13, 2004

APPENDIX A

FTIR spectra of tetranitro metal-phthalocyanine complexes, tetraamino metal-phthalocyanine complexes, diazophenylene bridged metal-phthalocyanine polymers and diazodiphenylene bridged metal-phthalocyanine polymers

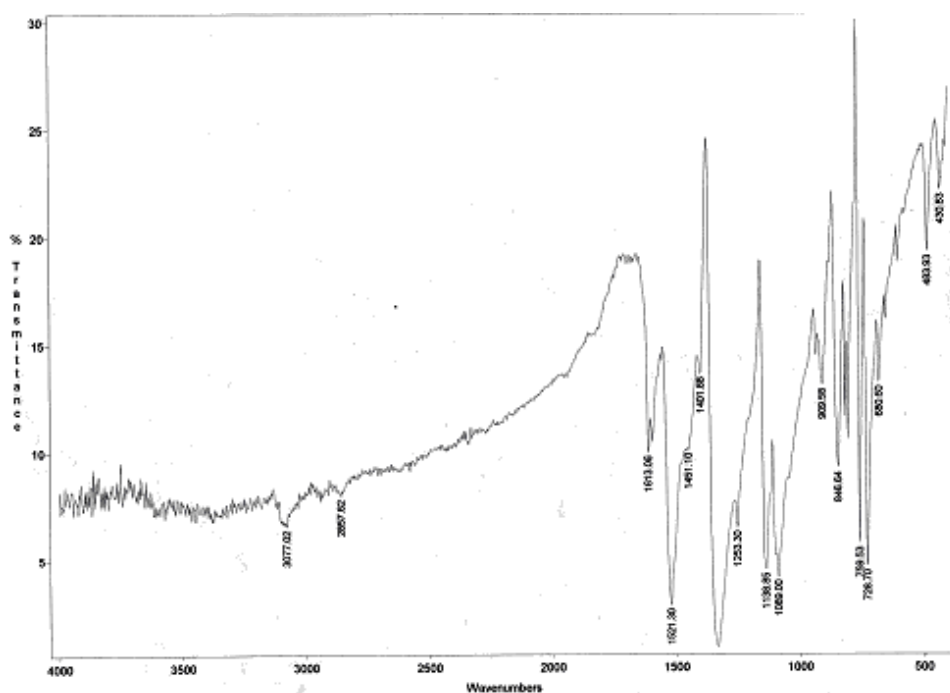


Figure A.1 FTIR spectrum of tetranitro Co-phthalocyanine complex

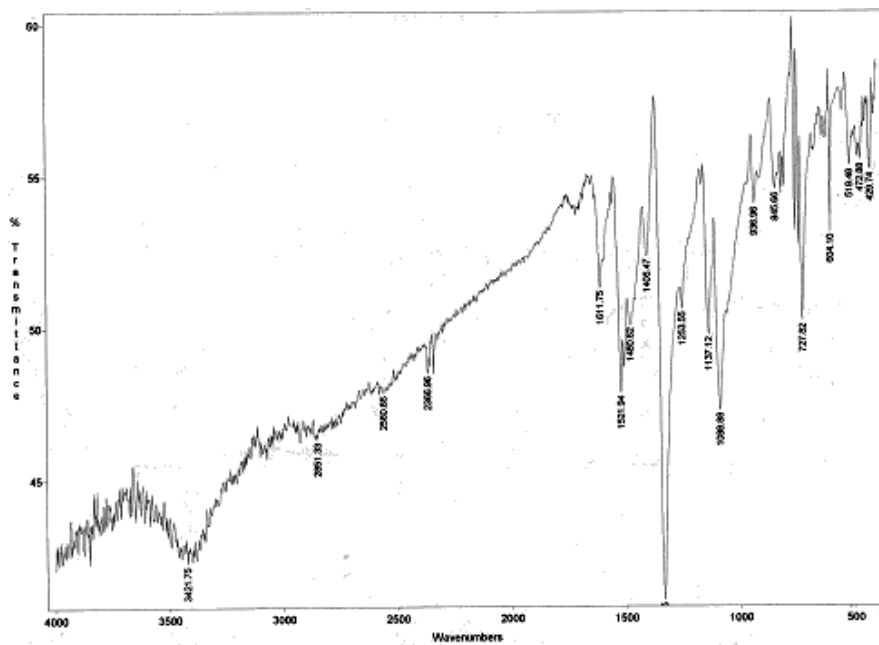


Figure A.2 FTIR spectrum of tetranitro Ni-phthalocyanine complex

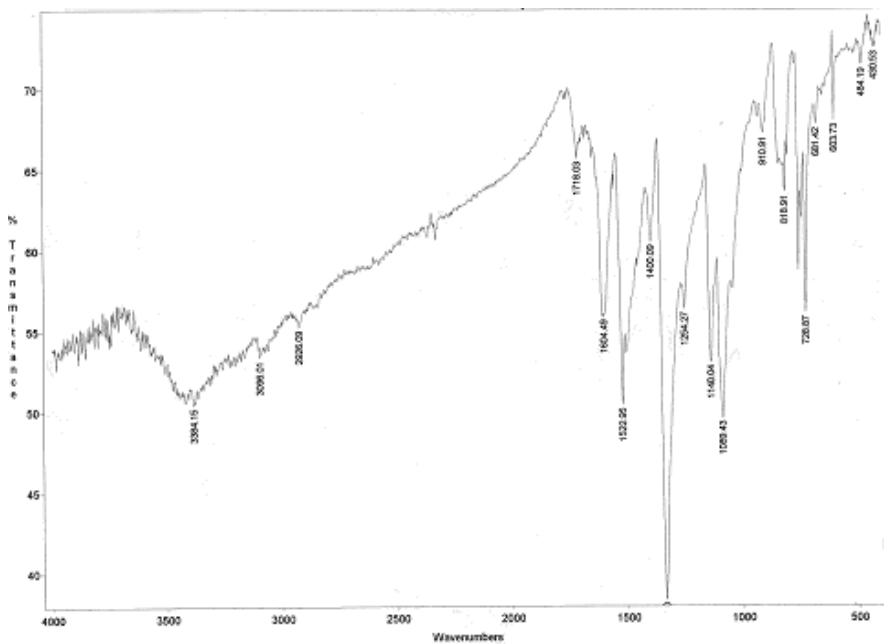


Figure A.3 FTIR spectrum tetranitro Ce-phthalocyanine complex

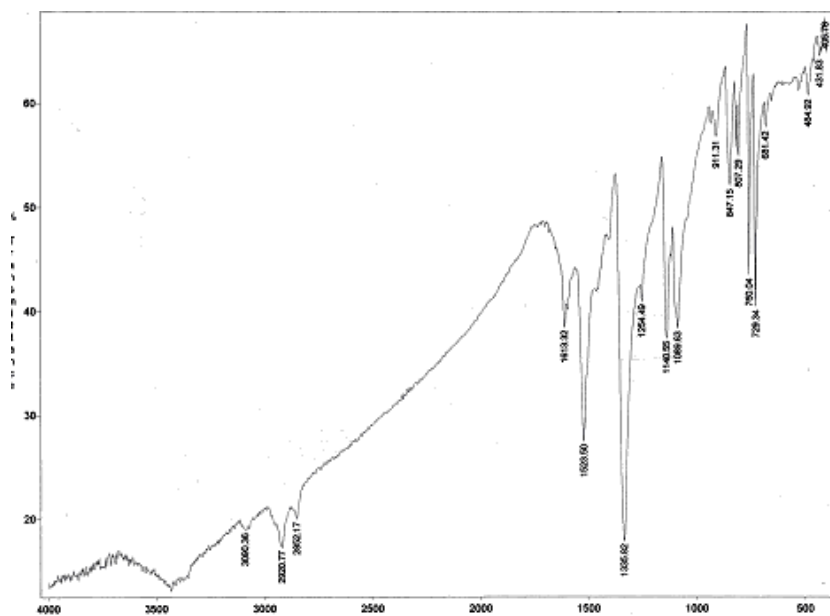


Figure A.4 FTIR spectrum of tetranitro Er-phthalocyanine complex

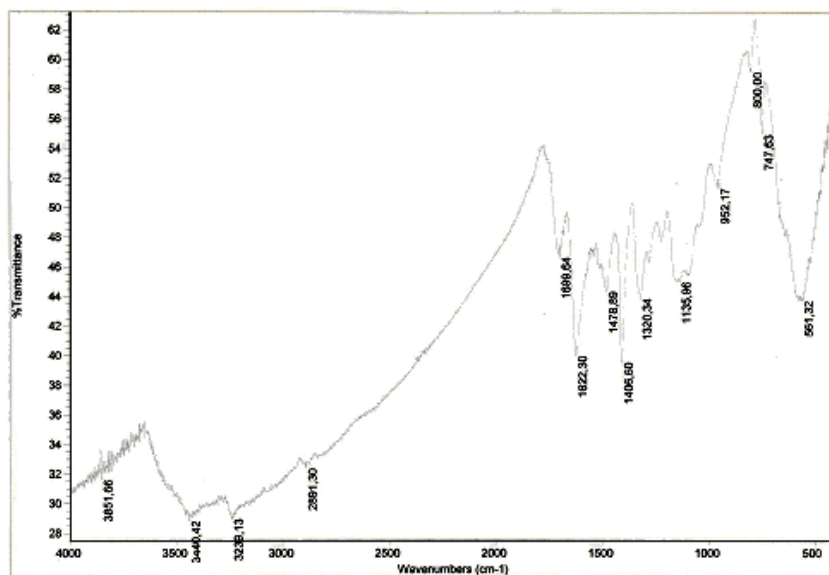


Figure A.5 FTIR spectrum of tetraamino Co-phthalocyanine complex

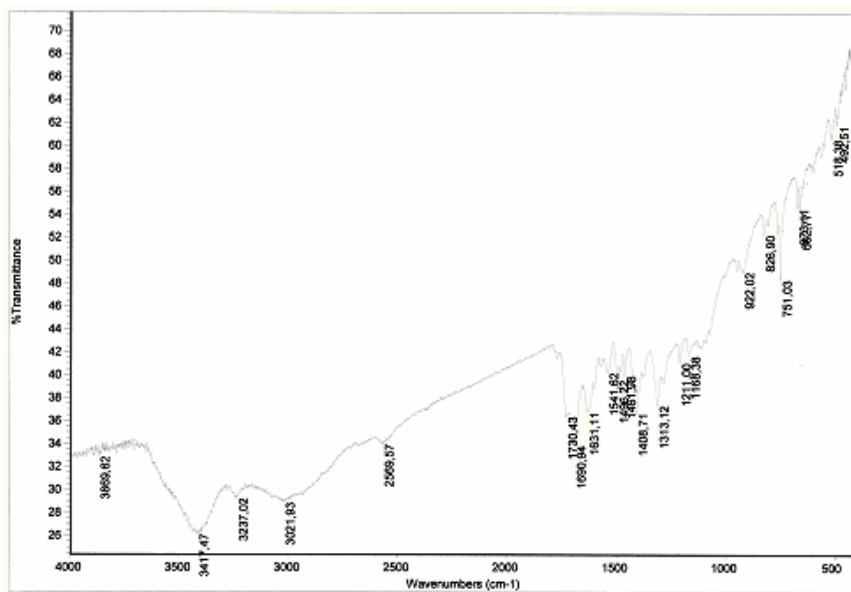


Figure A.6 FTIR spectrum of tetraamino Ni-phthalocyanine complex

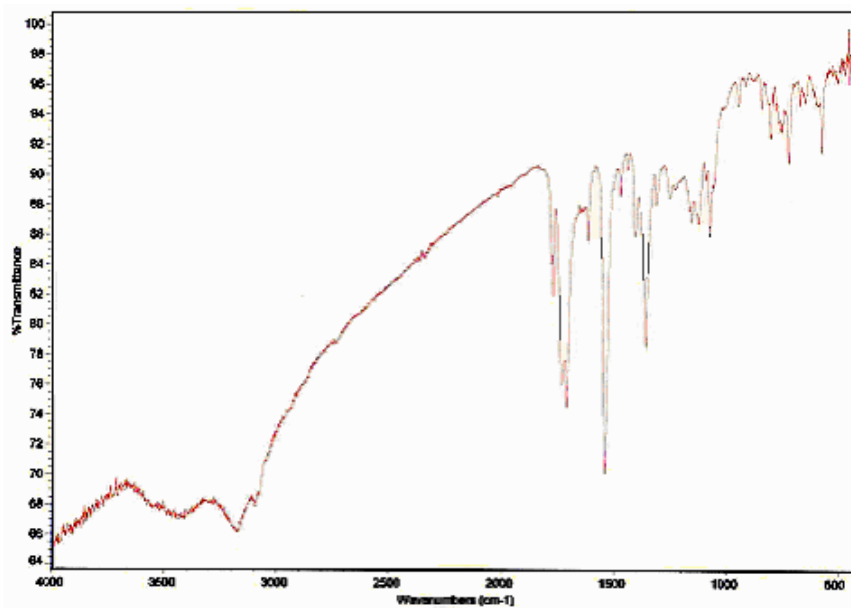


Figure A.7 FTIR spectrum of tetraamino Cu-phthalocyanine complex

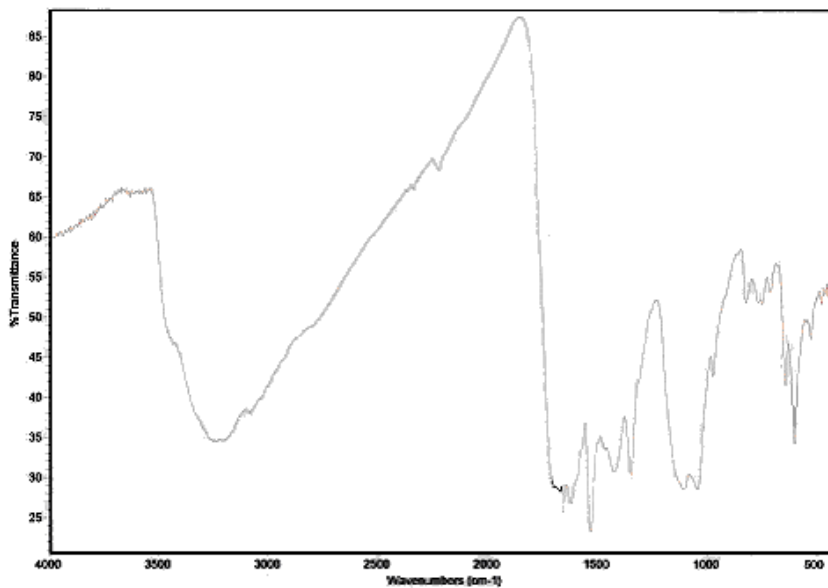


Figure A.8 FTIR spectrum of tetraamino Ce-phthalocyanine complex

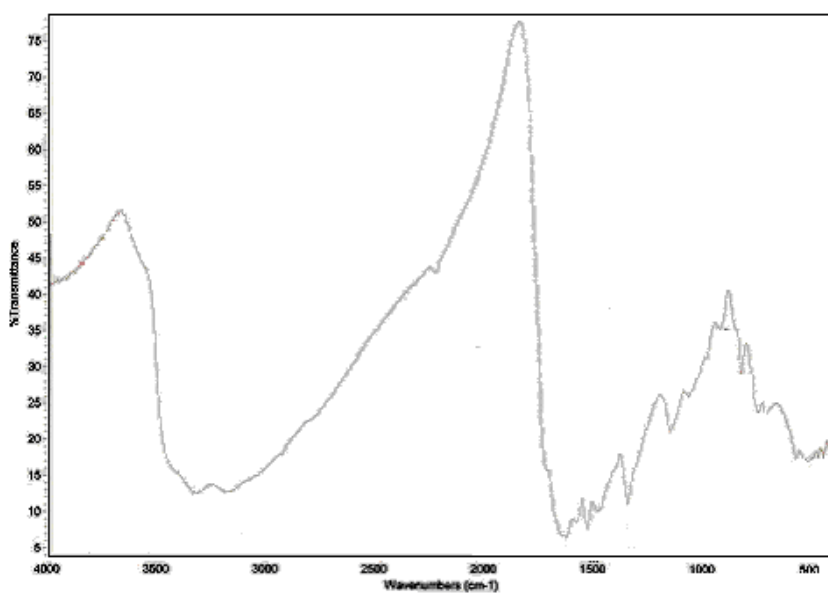


Figure A.9 FTIR spectrum of tetraamino Er-phthalocyanine complex

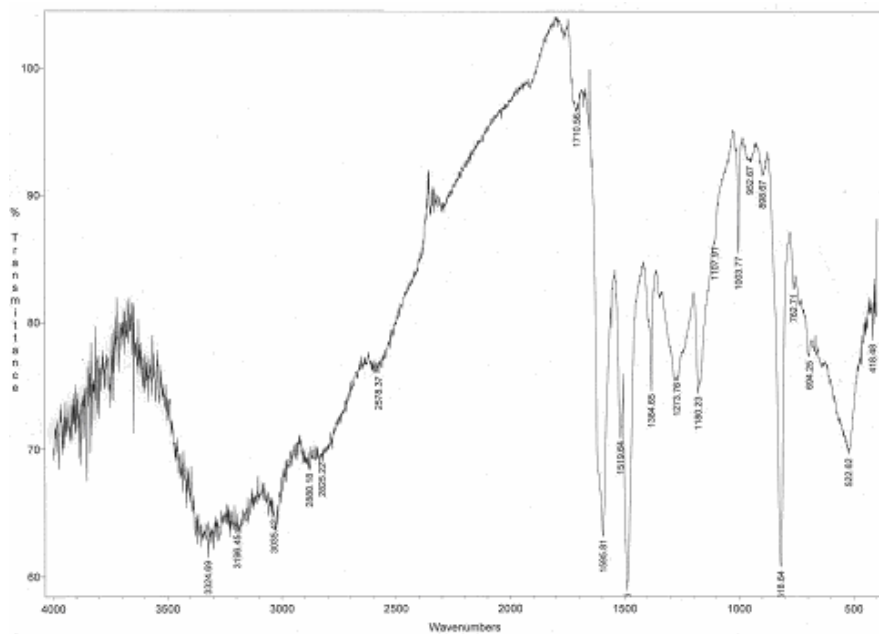


Figure A.10 FTIR spectrum of diazophenylene bridged Co-phthalocyanine polymer

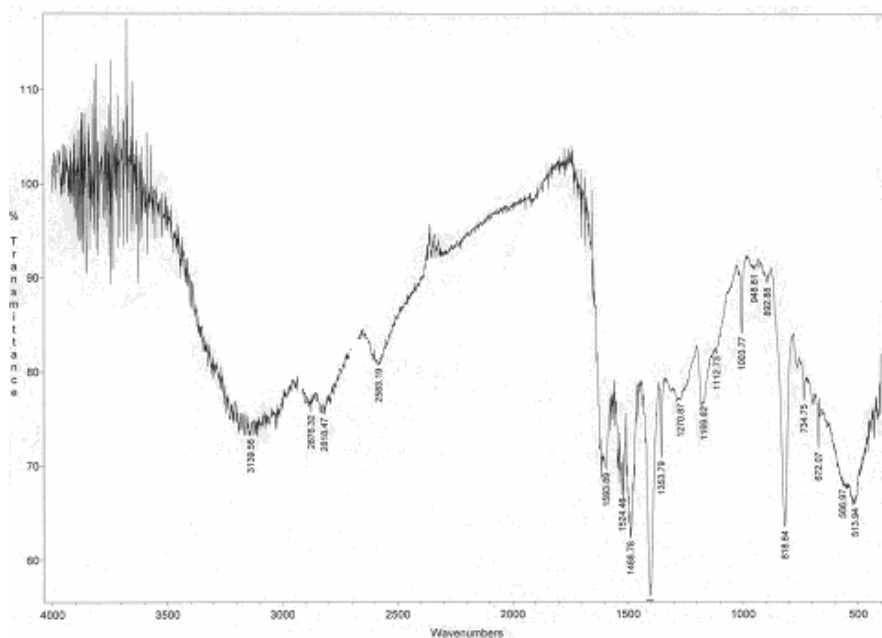


Figure A.11 FTIR spectrum of diazophenylene bridged Ni-phthalocyanine polymer

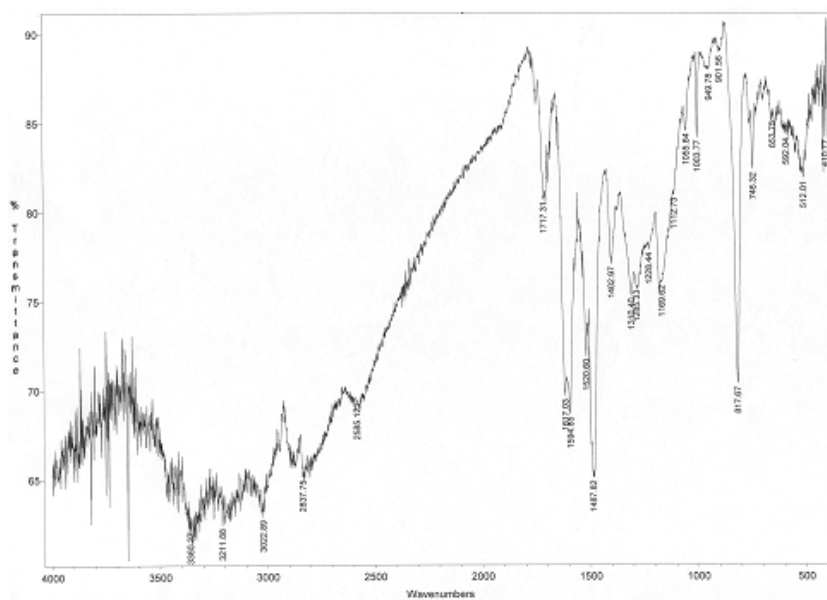


Figure A.12 FTIR spectrum of diazophenylene bridged Ce-phthalocyanine polymer

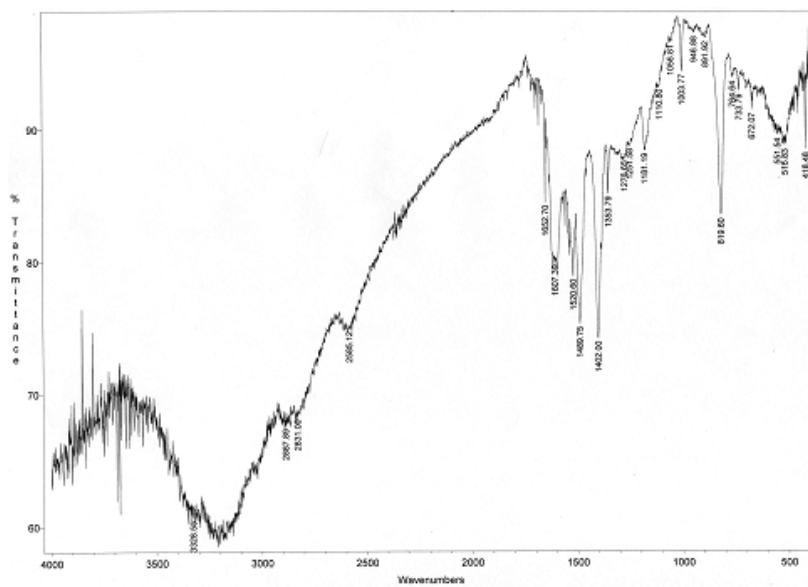


Figure A.13 FTIR spectrum of diazophenylene bridged Er-phthalocyanine polymer

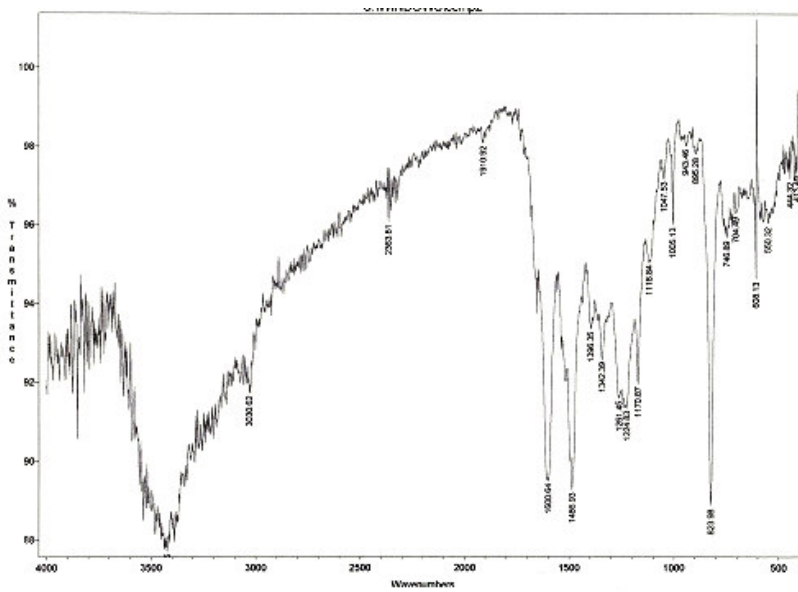


Figure A.14 FTIR spectrum for diazodiphenylene bridged Co-phthalocyanine polymer

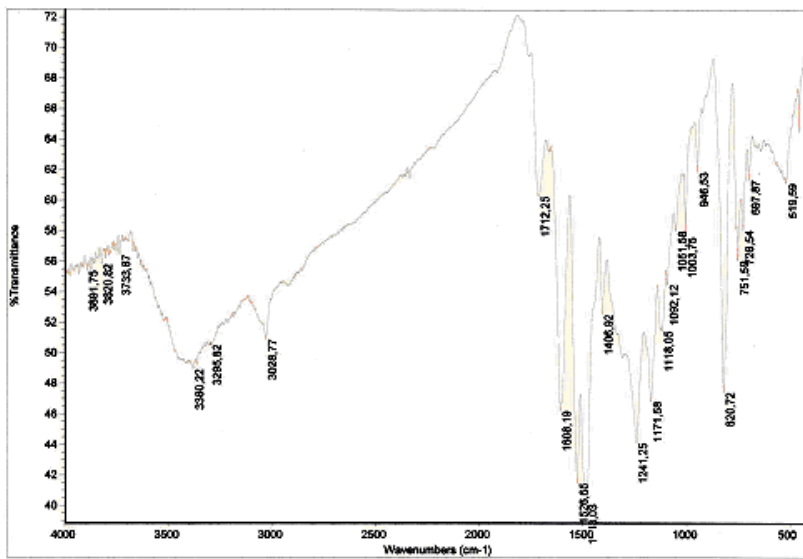


Figure A.15 FTIR spectrum for diazodiphenylene bridged Ni-phthalocyanine polymer

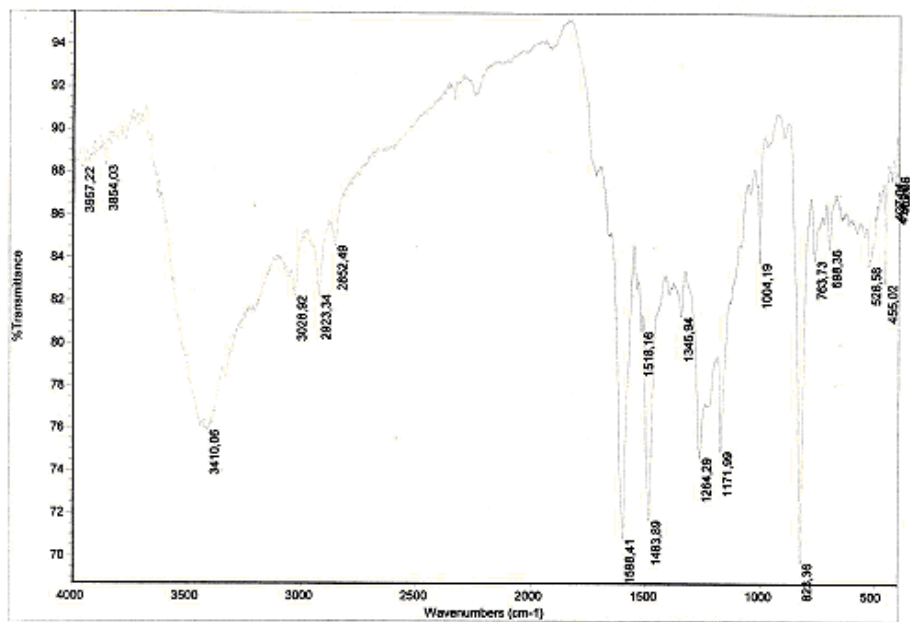


Figure A.16 FTIR spectrum for diazodiphenylene bridged Ce-phthalocyanine polymer

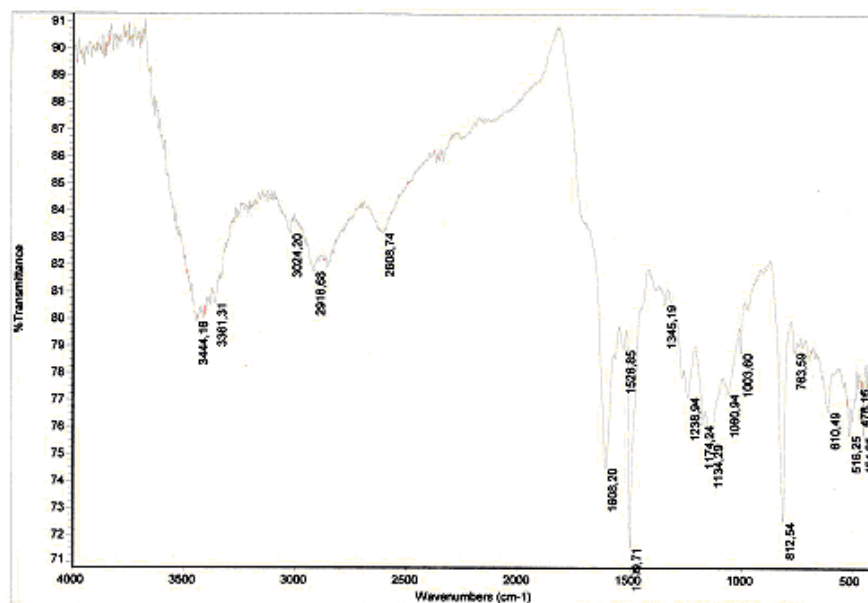


Figure A.17 FTIR spectrum for diazodiphenylene bridged Er-phthalocyanine polymer

APPENDIX B

X-Ray Diffraction spectra of tetraamino metal-phthalocyanine complexes, diazophenylene bridged metal-phthalocyanine polymers and diazodiphenylene bridged metal-phthalocyanine polymers

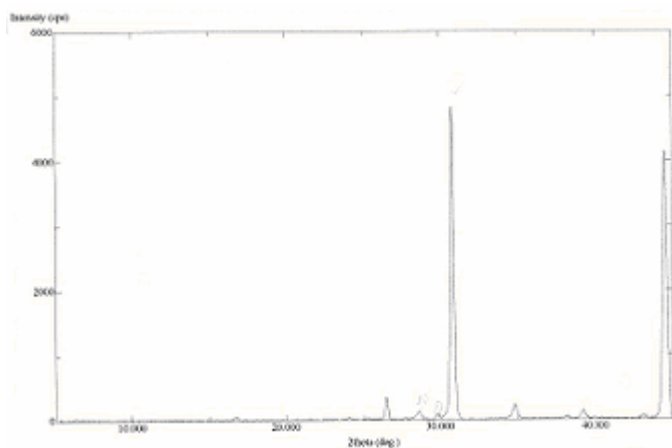


Figure B.1 X-Ray diffraction spectrum of tetraamino Co-phthalocyanine complex

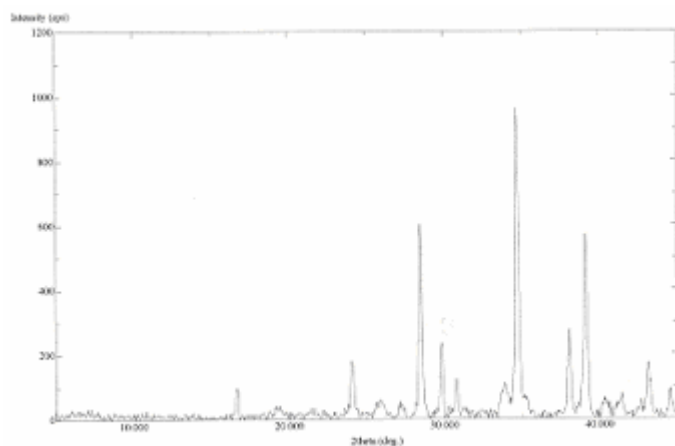


Figure B.2 X-Ray diffraction spectrum of tetraamino Ni-phthalocyanine complex

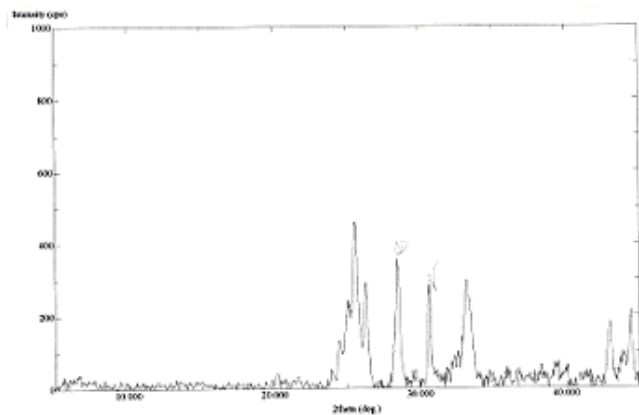


Figure B.3 X-Ray diffraction spectrum of tetraamino Cu-phthalocyanine complex

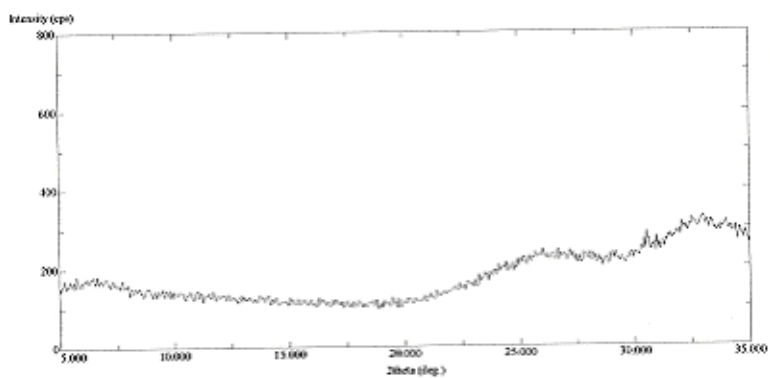


Figure B.4 X-Ray diffraction spectrum of diazophenylene bridged Co-phthalocyanine polymer

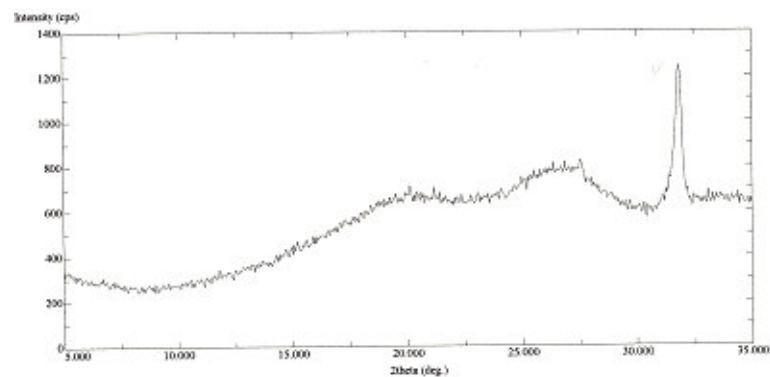


Figure B.5 X-Ray diffraction spectrum of diazophenylene bridged Ni-phthalocyanine polymer

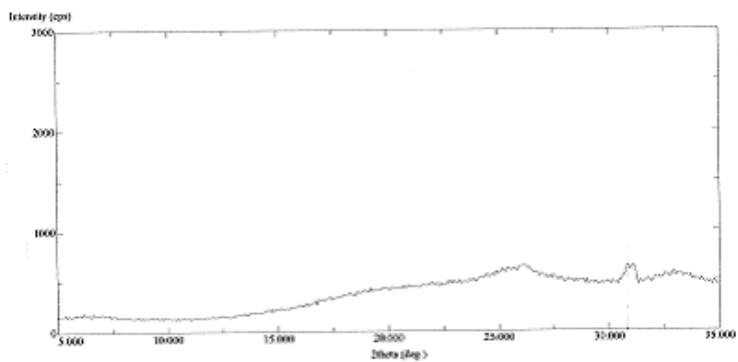


Figure B.6 X-Ray diffraction spectrum of diazophenylene bridged Ce-phthalocyanine polymer

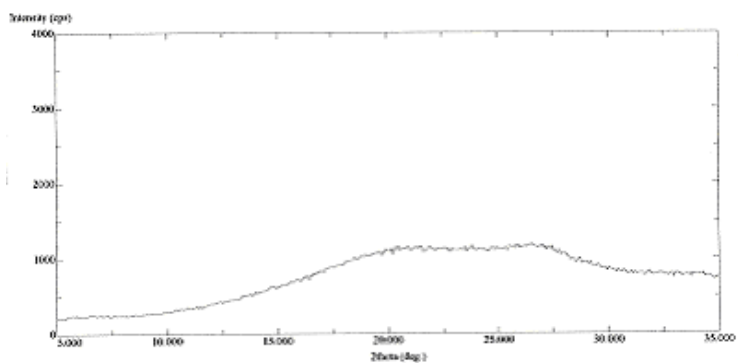


Figure B.7 X-Ray diffraction spectrum of diazophenylene bridged Er-phthalocyanine polymer

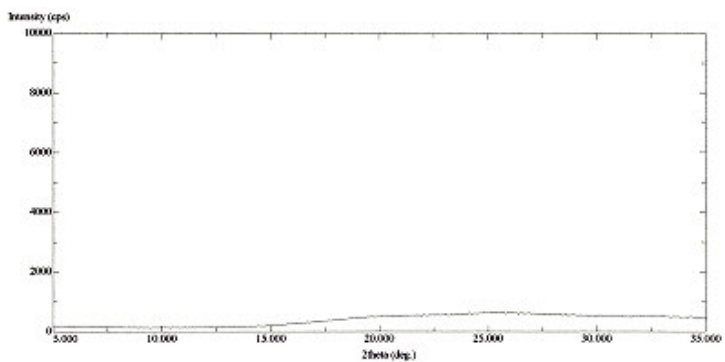


Figure B.8 X-Ray diffraction spectrum of diazodiphenylene bridged Co-phthalocyanine polymer

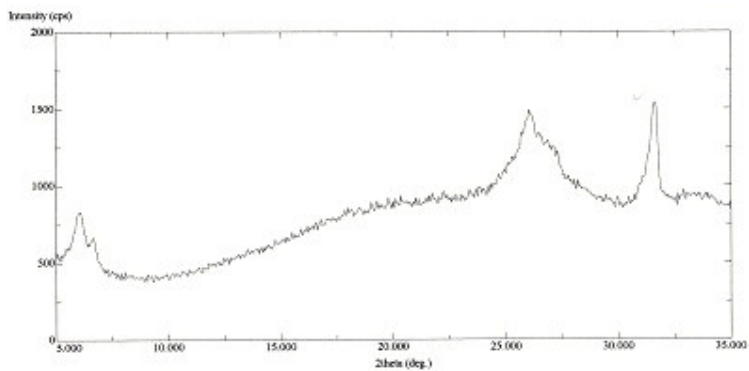


Figure B.9 X-Ray diffraction spectrum of diazodiphenylene bridged Ni-phthalocyanine polymer

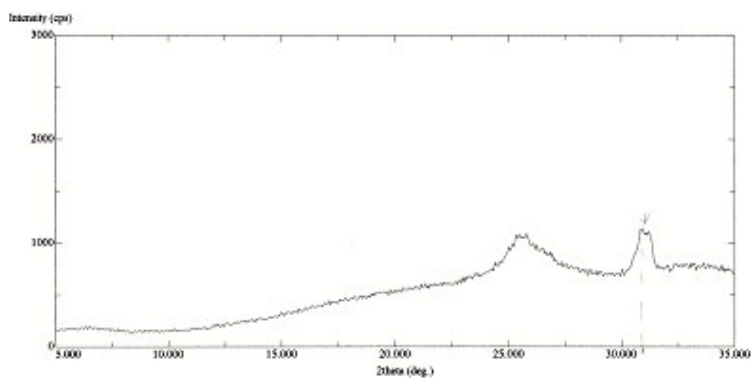


Figure B.10 X-Ray diffraction spectrum of diazodiphenylene bridged Ce-phthalocyanine polymer

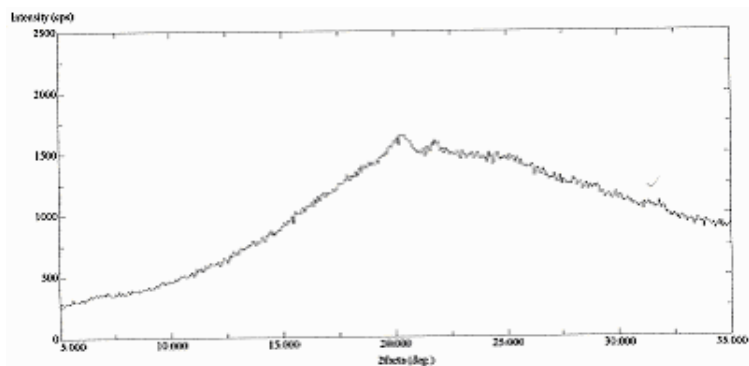


Figure B.11 X-Ray diffraction spectrum of diazodiphenylene bridged Er-phthalocyanine polymer

APPENDIX C

DSC thermograms of tetraamino metal-phthalocyanine complexes, diazophenylene bridged metal-phthalocyanine polymers and diazodiphenylene bridged metal-phthalocyanine polymers

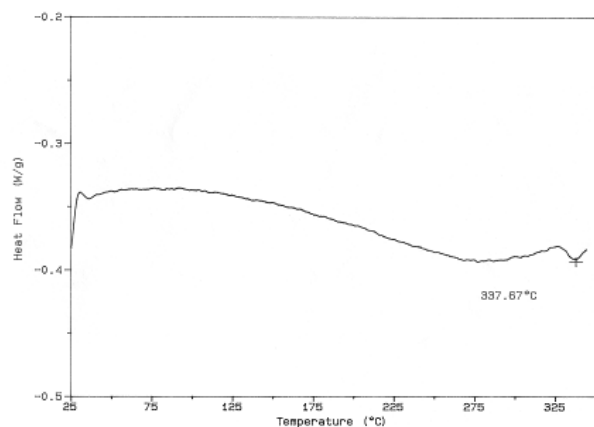


Figure C.1 DSC thermogram of tetranitro Co-phthalocyanine complex

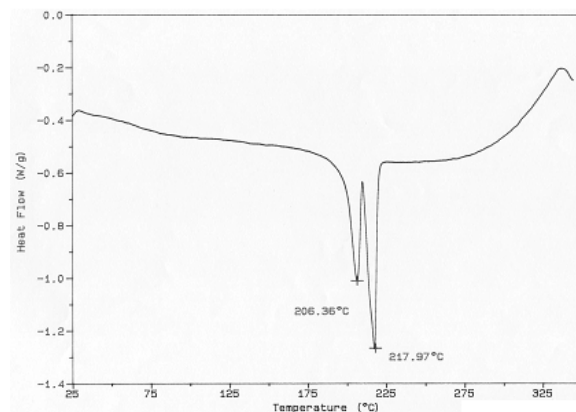


Figure C.2 DSC thermogram of tetranitro Ni-phthalocyanine complex

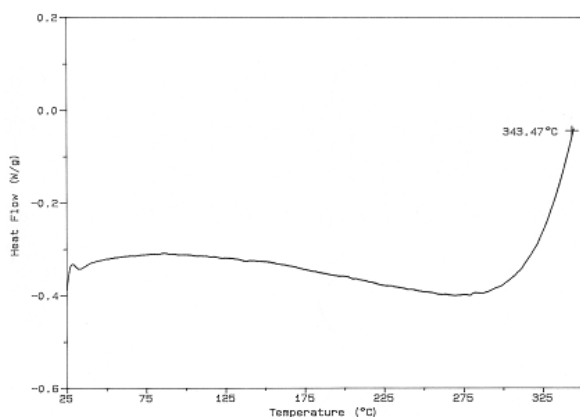


Figure C.3 DSC thermogram of tetranitro Ce-phthalocyanine complex

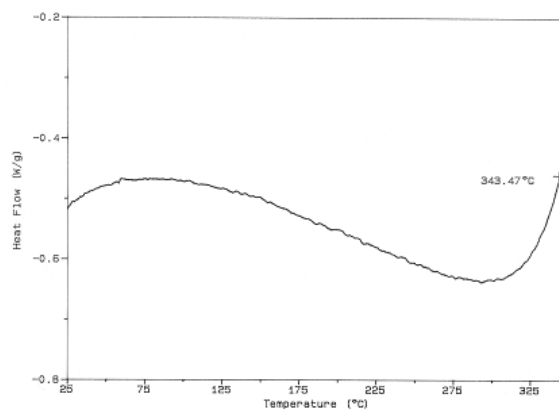


Figure C.4 DSC thermogram of tetranitro Er-phthalocyanine complex

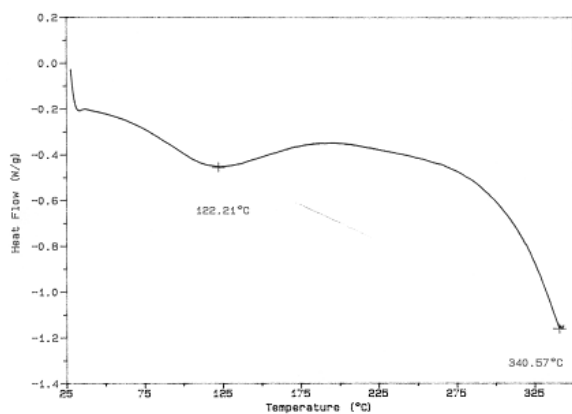


Figure C.5 DSC thermogram of tetraamino Co-phthalocyanine

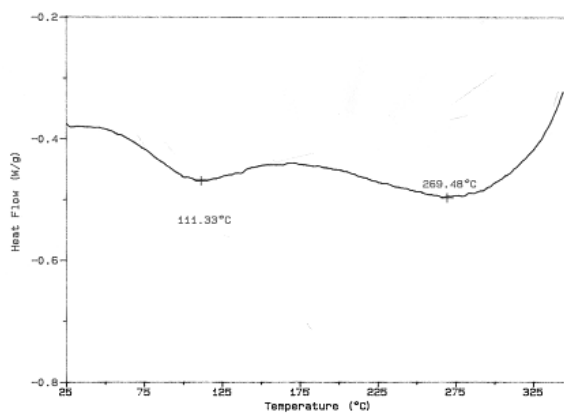


Figure C.6 DSC thermogram of tetraamino Ni-phthalocyanine

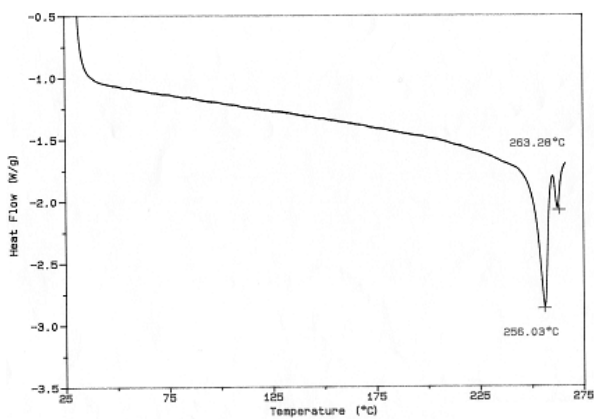


Figure C.7 DSC thermogram of tetraamino Cu-phthalocyanine

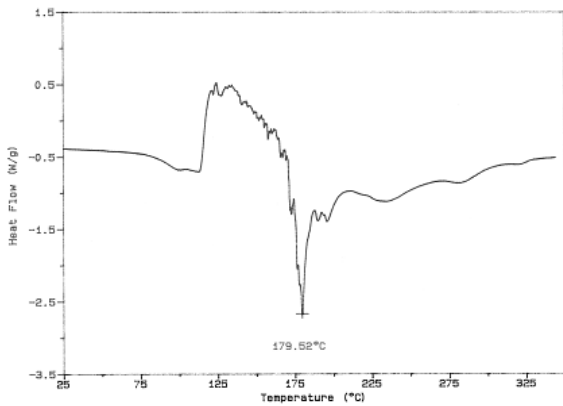


Figure C.8 DSC thermogram of tetraamino Ce-phthalocyanine

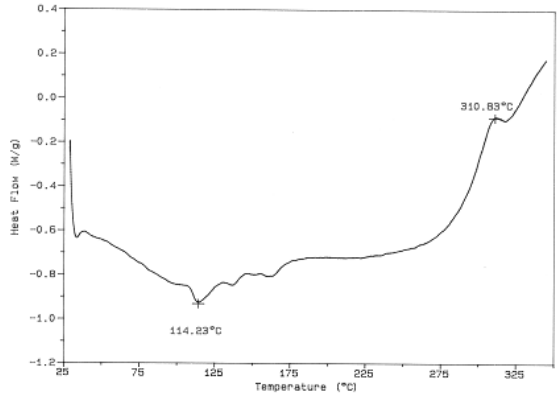


Figure C.9 DSC thermogram of tetraamino Er-phthalocyanine

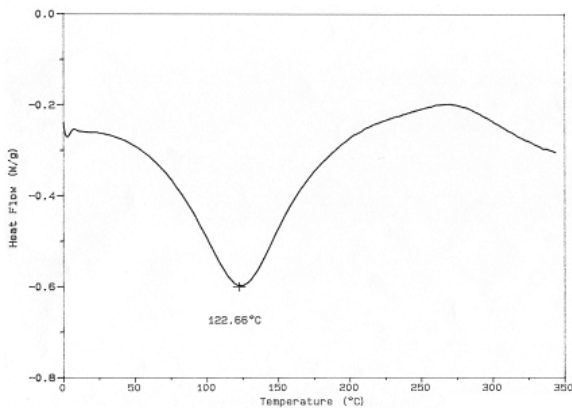


Figure C.10 DSC thermogram of diazophenylene bridged Co-phthalocyanine polymer

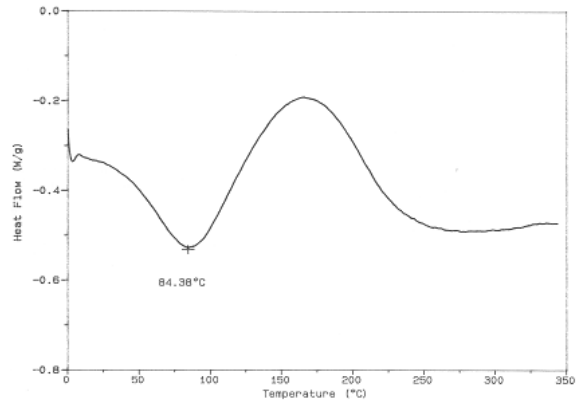


Figure C.11 DSC thermogram of diazodiphenylene bridged Co-phthalocyanine polymer

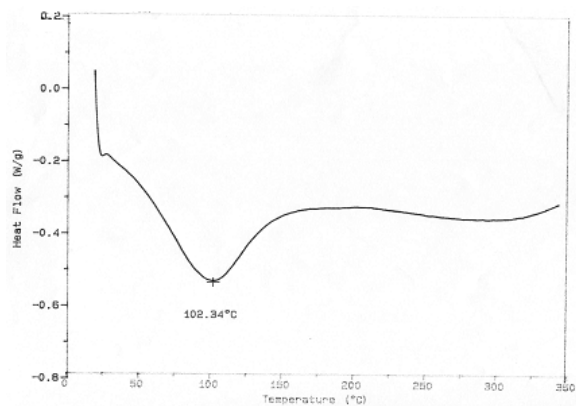


Figure C.12 DSC thermogram of diazophenylene bridged Ni-phthalocyanine polymer

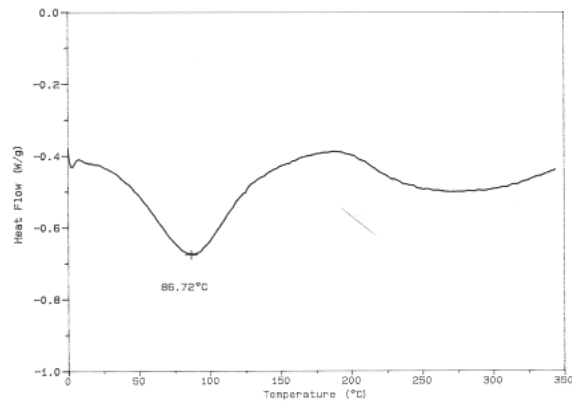


Figure C.13 DSC thermogram of diazodiphenylene bridged Ni-phthalocyanine polymer

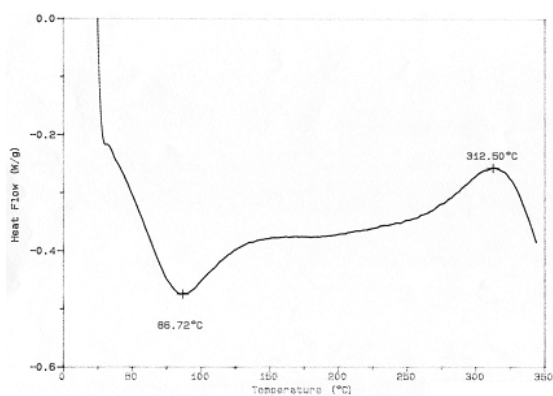


Figure C.14 DSC thermogram of diazophenylene bridged Cu-phthalocyanine polymer

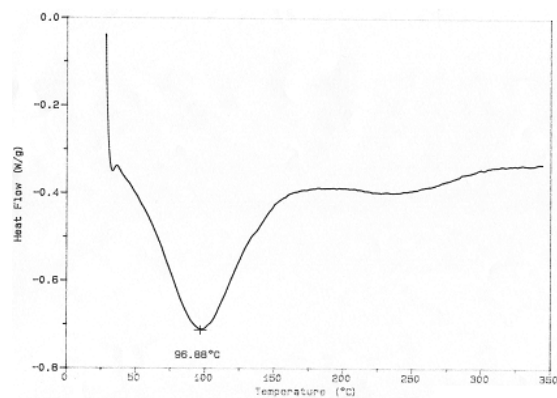


Figure C.15 DSC thermogram of diazodiphenylene bridged Cu-phthalocyanine polymer

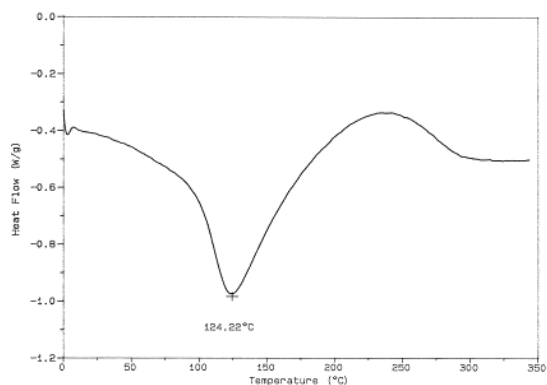


Figure C.16 DSC thermogram of diazophenylene bridged Ce-phthalocyanine polymer

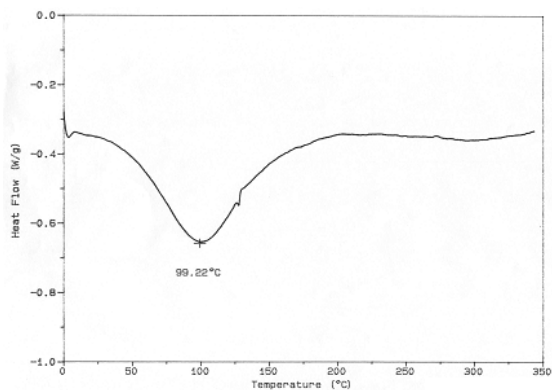


Figure C.17 DSC thermogram of diazodiphenylene bridged Ce-phthalocyanine polymer

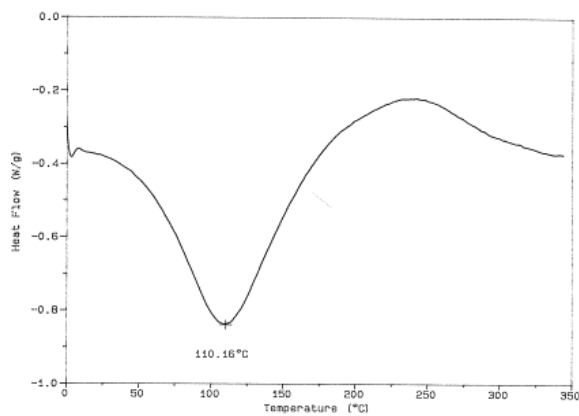


Figure C.18 DSC thermogram of diazophenylene bridged Er-phthalocyanine polymer

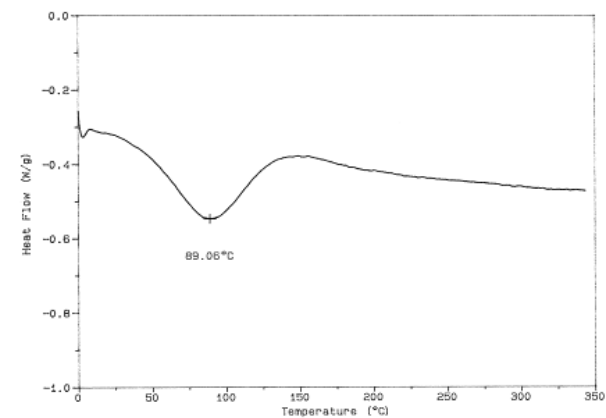


Figure C.19 DSC thermogram of diazodiphenylene bridged Er-phthalocyanine polymer

APPENDIX D

TGA thermograms of tetraamino metal-phthalocyanine complexes, diazophenylene bridged metal-phthalocyanine polymers and diazodiphenylene bridged metal-phthalocyanine polymers

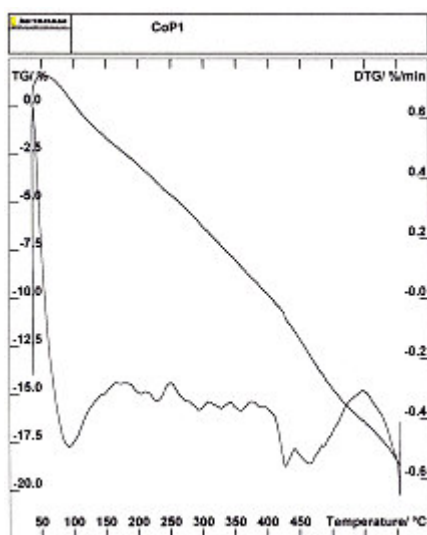


Figure D.1 TGA thermogram of diazophenylene bridged Co-phthalocyanine polymers

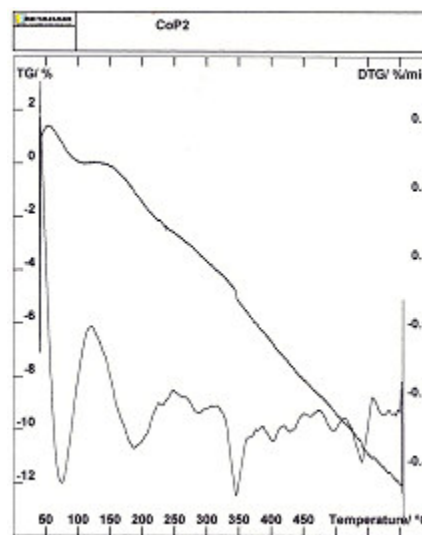


Figure D.2 TGA thermogram of diazodiphenylene bridged Co-phthalocyanine polymers

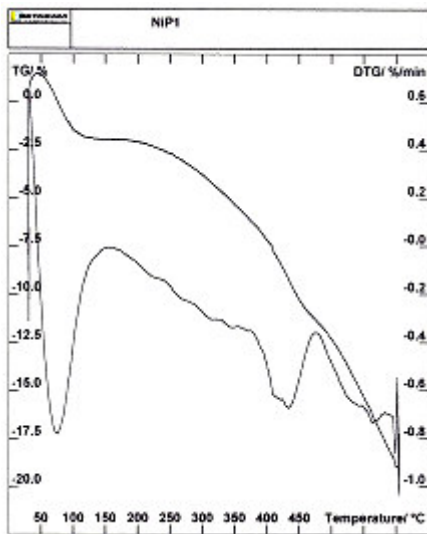


Figure D.3 TGA thermogram of diazophenylene bridged Ni-phthalocyanine polymers

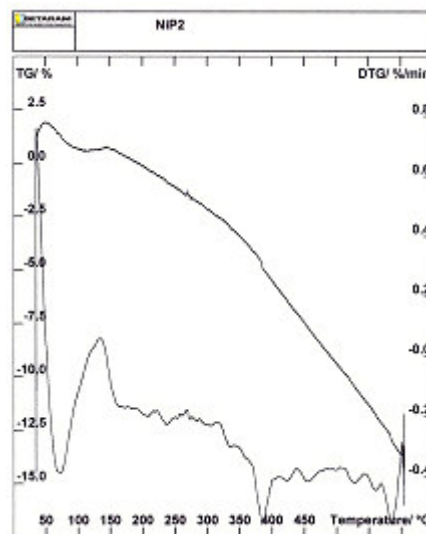


Figure D.4 TGA thermogram of diazodiphenylene bridged Ni-phthalocyanine polymers

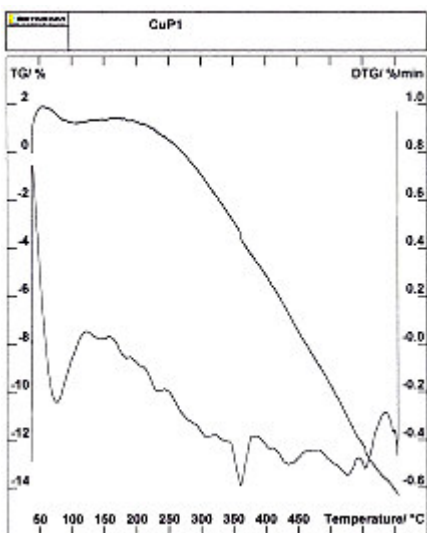


Figure D.5 TGA thermogram of diazophenylene bridged Cu-phthalocyanine polymers

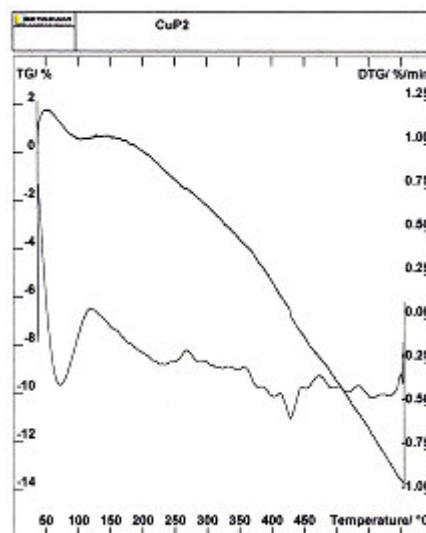


Figure D.6 TGA thermogram of diazodiphenylene bridged Cu-phthalocyanine polymers

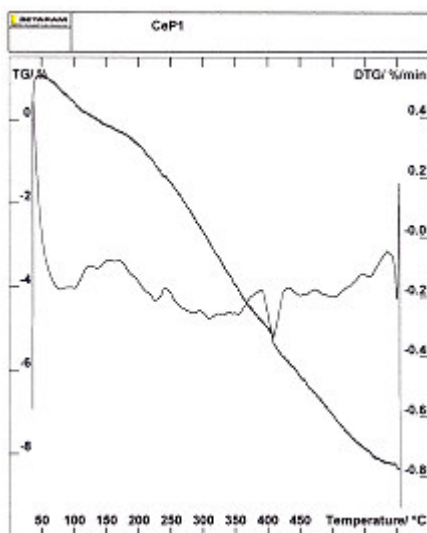


Figure D.7 TGA thermogram of diazophenylene bridged Ce-phthalocyanine polymers

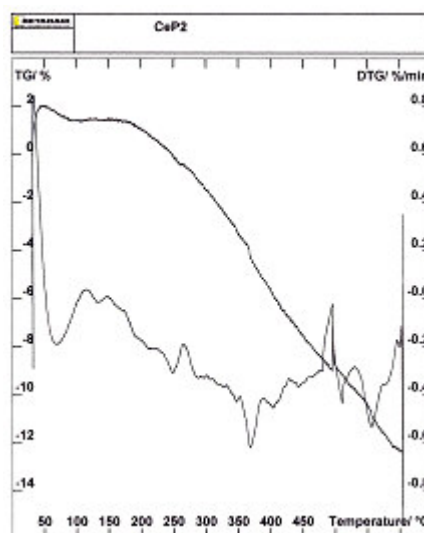


Figure D.8 TGA thermogram of diazodiphenylene bridged Ce-phthalocyanine polymers

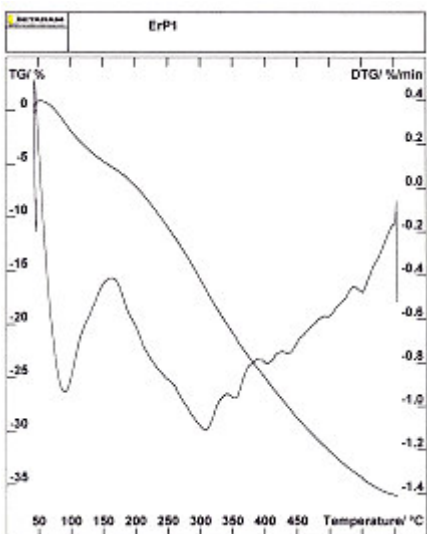


Figure D.9 TGA thermogram of diazophenylene bridged Er-phthalocyanine polymers

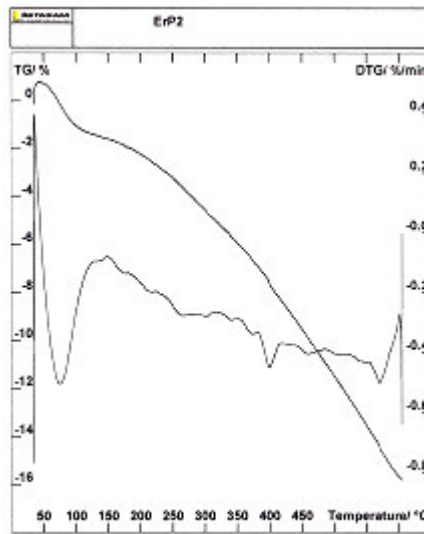


Figure D.10 TGA thermogram of diazodiphenylene bridged Er-phthalocyanine polymers

APPENDIX E

Cyclic Voltammograms of tetraamino metal-phthalocyanine complexes, diazophenylene bridged metal-phthalocyanine polymers and diazodiphenylene bridged metal-phthalocyanine polymers

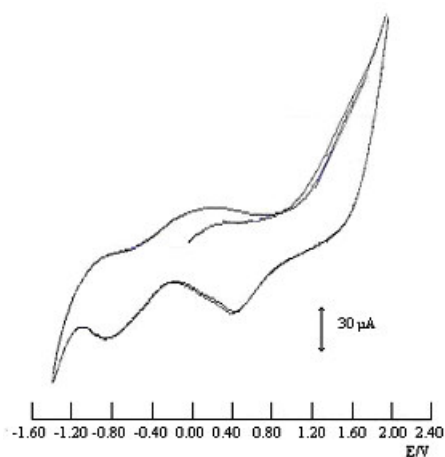


Figure E.1 CV of soluble part of diazophenylene bridged Co-phthalocyanine polymer

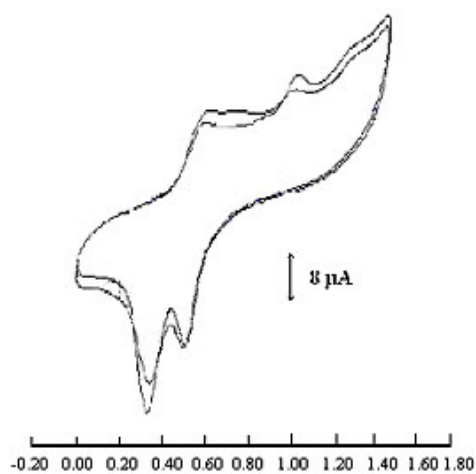


Figure E.2 CV of soluble part of diazodiphenylene bridged Co-phthalocyanine polymer

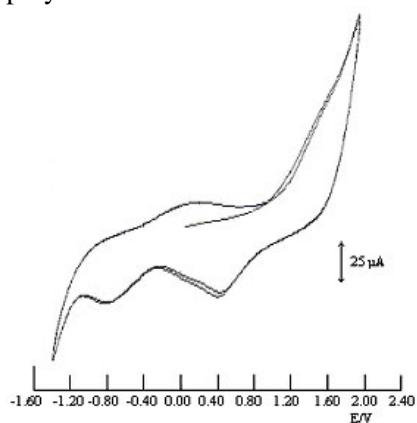


Figure E.3 CV of soluble part of diazophenylene bridged Ni-phthalocyanine polymer

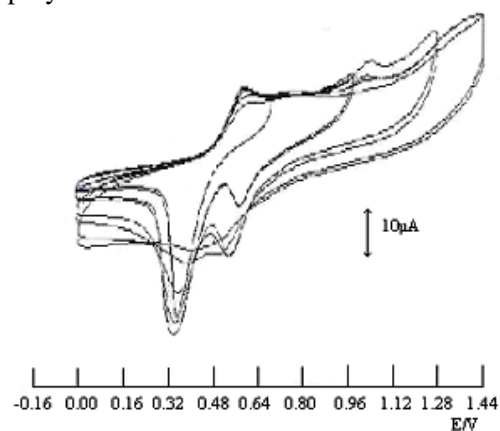


Figure E.4 CV of soluble part of diazodiphenylene bridged Ni-phthalocyanine polymer

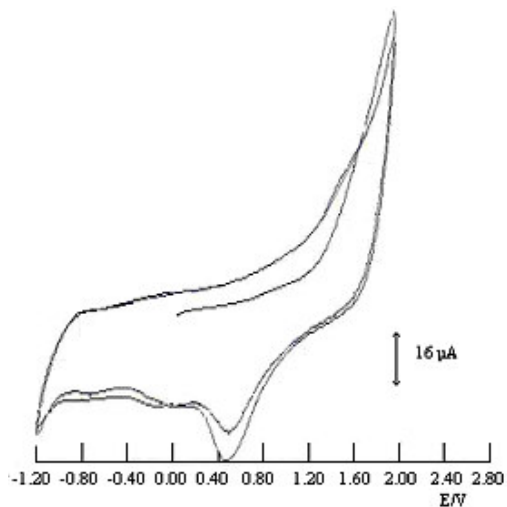


Figure E.5 CV of soluble part of diazophenylene bridged Cu-phthalocyanine polymer

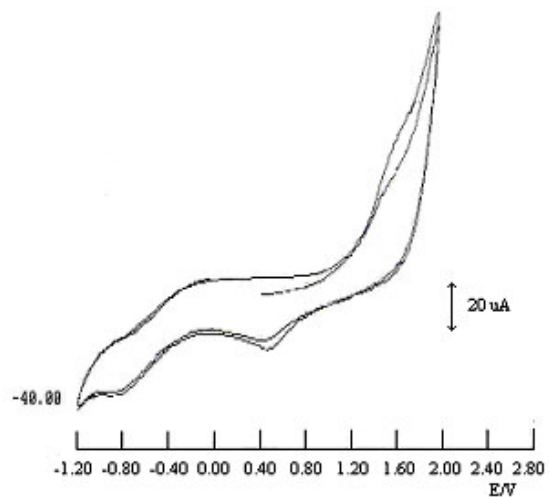


Figure E.6 CV of soluble part of diazodiphenylene bridged Cu-phthalocyanine polymer

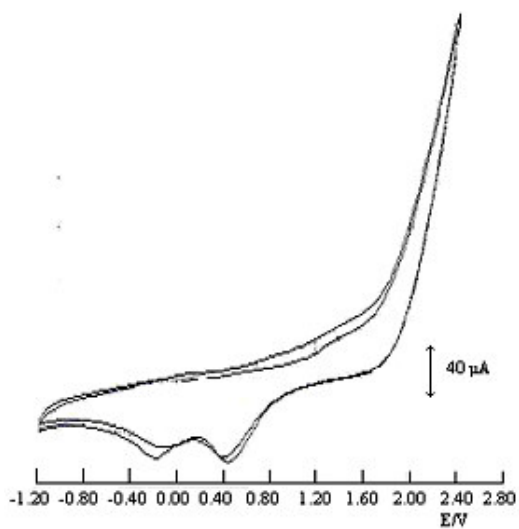


Figure E.7 CV of soluble part of diazophenylene bridged Ce-phthalocyanine polymer

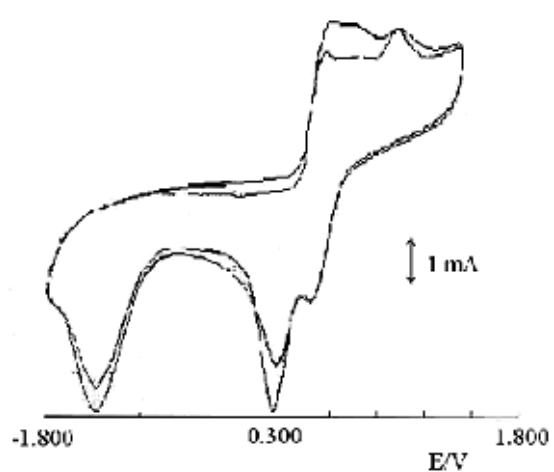


Figure E.8 CV of soluble part of diazodiphenylene bridged Ce-phthalocyanine polymer

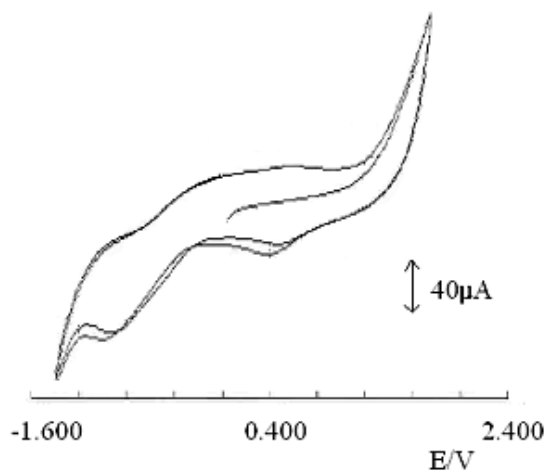


Figure E.9 CV of soluble part of diazophenylene bridged Er-phthalocyanine polymer

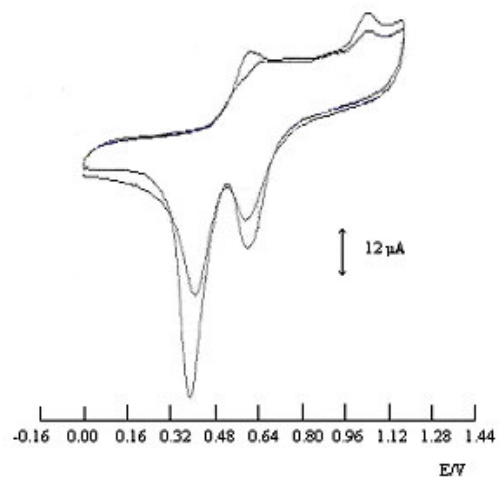


Figure E.10 CV of soluble part of diazodiphenylene bridged Er-phthalocyanine polymer

VITA

Cemil Alkan was born on August 19, 1973 in Kırıkkale. He graduated from Middle East Technical University (METU), Department of Chemistry in 1996. He began his Ms studies at Chemistry department of METU where he became a research assistant. During this time, he worked on miscibility of sulfonated polystyrene ionomers with polyphenylene oxides under the supervision of Prof Dr Leyla Aras. He began PhD studies in 1999 with Prof Dr Leyla Aras and Prof Dr Güngör Gündüz in the area of phthalocyanine polymers. He published two papers and submit another four.

- 1.) C. Alkan, L. Aras “Miscibility of Polystyrene Based Ionomers with Poly(2,6-dibromo-1,4-phenylene oxide)”, J. Appl. Polym. Sci. 82, 3558 (2001).
- 2.) C. Alkan, M. Mih, L. Aras “Compatibilization of Poly(2,6-dimethyl-1,4-phenylene oxide) and Poly(2,6-dichloro-1,4-phenylene oxide) with Sulfonated Polystyrene and its Na and Zn-neutralized Ionomers” Polym. Bull. 50, 191 (2003).
- 3.) C. Alkan, N. Yurtseven, L. Aras "Miscibility of Magnesium, Zinc, and Manganese Sulfonated Polystyrene Ionomers with Methylmethacrylate-co-methacrylic Acid Copolymer” Polym. Bull. (revised manuscript was sent)
- 4.) C. Alkan, L. Aras, G. Gündüz “Synthesis, Characterization and Electrical Properties of 1,4-Diazophenylene Bridged Cu-Phthalocyanine Polymer“e-polymers journal (revised manuscript was sent in the scope of POLYCHAR 12)
- 5.) C. Alkan, L. Aras, G. Gündüz “Synthesis, Characterization and Electrical Properties of 1,4-Diazodiphenylene Bridged Cu-Phthalocyanine Polymer“ J. Appl. Polym. Sci.(submitted 2004)
- 6.) C. Alkan, A. Dumanlı, L. Aras “Sulfonation Degree Determination of Polystyrene Ionomers by Using Adiabatic Bomb Calorimeter” J. Appl. Polym. Sci.(submitted 2004)